

**ACID-BASE, SURFACE ELECTRON DONATING & CATALYTIC  
PROPERTIES OF SOME BINARY MIXED OXIDES CONTAINING  
RARE EARTH ELEMENTS**

THESIS SUBMITTED TO  
THE COCHIN UNIVERSITY OF SCIENCE AND TECHNOLOGY  
IN PARTIAL FULFILMENT OF THE  
REQUIREMENTS FOR THE DEGREE OF

**DOCTOR OF PHILOSOPHY**  
IN  
**CHEMISTRY**  
IN THE FACULTY OF SCIENCE

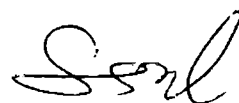
BY  
**BINSY VARGHESE .V**

DEPARTMENT OF APPLIED CHEMISTRY  
COCHIN UNIVERSITY OF SCIENCE AND TECHNOLOGY  
KOCHI-682 022 INDIA

FEBRUARY 1998

## CERTIFICATE

This is to certify that the thesis bound herewith is an authentic record of the research work carried out by Binsy Varghese V, under my guidance, for partial fulfilment of the requirements for the degree of Doctor of philosophy in Chemistry, in the department of Applied Chemistry, Cochin University of Science and Technology, and no part of this has been presented for any other degree.



Dr. S. Sugunan  
(Supervising Teacher)  
Professor in Physical Chemistry,  
Department of Applied Chemistry,  
Cochin University of Science & Technology.

## **DECLARATION**

I hereby declare that the work presented in this thesis is based on the original work done by me under the guidance of Dr. S. Sugunan, Professor, Department of Applied Chemistry, Cochin University of Science & Technology, and has not been included in any other thesis for any degree.



**Binsy Varghese. V**

Kochi 682 022

February 1998

Dedicated

To

My Dear Parents

## ACKNOWLEDGMENT

I express my sincere gratitude and obligation to my supervising guide, Prof. (Dr.). S. Sugunan for his excellent guidance, help and encouragement given to me throughout the course of this work.

I acknowledge my sincere gratitude to Prof. P. Madhavan pillai, Head of Dept. of Applied Chemistry for his timely help and advices. I am very much grateful to all the Faculty members in the department of Applied Chemistry for they have always been a source of inspiration to me.

My sincere thanks are to Dr. Jacob Chacko, Professor and Head, Dept. of Chemical Oceanography, CUBA & Dr. J. Thomas, Associate Professor and Head, Aromatic and Medicinal plants Research Station, Odakkali, Govt. of Kerala, for providing me the facilities for DC analysis. I am thankful to Mr. S. D. Munga and Mr. V. Babu, Research Scholars, Dept. of Chemical Oceanography, for helping me to do the DC Analysis.

I wish to thank Dr. B.Viswanathan, Coordinator, Catalysis Division. IIT Madras for providing the BET data for surface area determination and the authorities of the Regional Sophisticated instrumentation centre, IIT, Madras for providing the EPR spectral data.

I am very happy to record my gratefulness to all my friends, colleagues and well wishers for all their help, cooperation and prayers.

Financial assistance from University Grants Commission, Government of India is gratefully acknowledged.

Finally I wish to express my deep sense of love and gratitude to my loving parents, dear brothers and husband, without whose affectionate encouragement, love and care this work would not have been completed.

Bincy Varghese.V

## CONTENTS

<b>Chapter 1. Introduction &amp; Literature Survey</b>	<b>1</b>
<b>Introduction</b>	<b>2</b>
1.1. Zirconium oxide and Lanthanide oxides as Catalysts	6
1.2. Surface Acid-Base Properties of metal Oxides	11
1.3. Acid-Base Properties & Catalytic Activity	18
1.4. Electron Donor- Acceptor properties.	24
1.5. Surface Site Structures.	30
<b>References</b>	<b>40</b>
<b>Chapter 2. Experimental</b>	<b>55</b>
2.1. Materials Used.	56
2.2. Methods Adopted.	60
<b>References</b>	<b>64</b>
<b>Chapter 3 . Results &amp; Discussion</b>	<b>67</b>
3.1. Introduction	68
3.1.1. Adsorption studies	69
3.1.2. Acid- Base Measurements	73
3.1.3. Catalytic activity	74
3. 2 . Acid- Base, Surface Electron Donating & Catalytic Properties of Cerium -Zirconium mixed oxides	75
3.2.1. Surface area	76

3.2.2. Electron Donating Properties	79
3.2.3. Acid -Base Properties.	81
3.2.4. Catalytic activity Measurements	85
References	104
<b>Chapter 4. Acid- Base, Surface Electron Donating &amp; Catalytic Properties of Praseodymium -Zirconium mixed oxides</b>	<b>107</b>
4.1. Surface area	109
4.2. Electron Donating Properties	110
4.3. Acid -Base Properties.	111
4.4. Catalytic activity Measurements	113
References	121
<b>Chapter 5. Acid- Base, Surface Electron Donating &amp; Catalytic Properties of Neodymium -Zirconium mixed oxides</b>	<b>123</b>
5.1.1. Surface area	126
5.1.2. Electron Donating Properties	126
5.1.3. Acid -Base Properties.	128
5.1.4. Catalytic activity Measurements.	130
5.2. Comparison of the Rare Earths.	133
References	152
<b>CONCLUSIONS</b>	<b>153</b>
<b>LIST OF PUBLICATIONS</b>	<b>154</b>

# **CHAPTER 1**

## **INTRODUCTION & LITERATURE**

### **SURVEY**



## INTRODUCTION

Catalysis research underpins the science of modern chemical processing and fuel technologies. Catalysis is commercially one of the most important technologies in national economies. Solid state heterogeneous catalyst materials such as metal oxides and metal particles on ceramic oxide substrates are most common. They are typically used with commodity gases and liquid reactants. Selective oxidation catalysts of hydrocarbon feedstocks is the dominant process of converting them to key industrial chemicals, polymers and energy sources.[1]

In the absence of a unique successful theory of heterogeneous catalysis, attempts are being made to correlate catalytic activity with some specific properties of the solid surface. Such correlations help to narrow down the search for a good catalyst for a given reaction.

The heterogeneous catalytic performance of material depends on many factors such as [2]

Crystal and surface structure of the catalyst.

Thermodynamic stability of the catalyst and the reactant.

Acid- base properties of the solid surface.

Surface defect properties of the catalyst.

Electronic and semiconducting properties and the band structure.

Co-existence of different types of ions or structures.

Adsorption sites and adsorbed species such as oxygen.

Preparation method of catalyst , surface area and nature of heat treatment.

Molecular structure of the reactants.

Many systematic investigations have been performed to correlate catalytic performances with the above mentioned properties. Many of these investigations remain isolated and further research is needed to bridge the gap in the present knowledge of the field.

In many processes empirical development of catalysts leads to initial high performance but there subsequently be a decline in activity which presents major difficulties in technological applications. Fundamental understanding of the surface structural modifications of the catalysts under working conditions, which directly influence their activity, selectivity and durability is therefore essential. Normally, catalytic activity is expressed as the reaction rate per unit area of the active surface under given conditions. Selectivity is a function of the rate of formation of the desired product with respect to the overall conversion of the initial reactants. The reactant molecules transfer to the catalyst surface where adsorption may occur on an active site with possible rearrangement of their bonds leading to a chemisorption reaction and subsequent desorption of the new species. Thus the nature of the active sites on surfaces, whether they are related to dangling bonds due to co-ordinatively unsaturated surface sites or to defects is important.

Complex oxide catalysts are often inhomogeneous, and extensive local microstructural and compositional variations can occur as a consequence. They belong

to a particular class of heterogeneous catalysts which have active sites distributed throughout the crystal. The loss of structural oxygen ions ( $O^{2-}$ ) results in nonstoichiometry through the formation of anion vacancies; the incorporation of gaseous oxygen (to replenish the catalyst) can occur by electrons freed in the process. Nonstoichiometry results in the generation of a variety of defects during the operation.

The catalytic properties of transition metal oxides are well known [3 to 6]. The properties that are important in the surface chemistry of transition metal oxides are

Presence of cations and anions in stoichiometric ratios and in well defined spatial relationships.

Possibility of covalent and ionic bonding between cations and anions

Presence of strong electric field normal to the surface due to Coulombic nature of the ionic lattice

Presence of charged adsorbed species.

Presence of surface acidity and basicity.

Presence of cationic and anionic vacancies.

Ability of cations to undergo oxidation and reduction.

High mobility of lattice oxygen and the possibility that lattice oxygen are reactants in a reaction.

Interaction of the solid with incident photons that leads to photo-assisted surface chemical processes.

Common to many of the properties listed is the fact that transition metal oxides are made up of metallic cations and oxygen anions. The ionicity of the lattice, which is often less than that predicted by the formal oxidation state, results in the presence of charged adsorbate species, and the common heterolytic dissociative adsorption of molecule (ie. a molecule AB adsorbed as  $A^+$  and  $B^-$ ). Surface exposed cation and anions form acidic and basic sites as well as acid-base pair sites. The fact that the cations often have a number of commonly obtainable oxidation states has resulted in the ability of the oxides to undergo oxidation and reduction and the possibility of the presence of rather high densities of cationic and anionic vacancies.

Transition metal oxides exist in many different crystallographic forms. There does not appear to be a simple generalisation that relates the structure to the stoichiometry or to the position in the periodic table. It is not uncommon to find a certain oxide in more than one crystal structure at ordinary temperature as a result of the high activation energy in the process of transforming from a less thermodynamic stable to a more stable structure. There is one generalisation, which is the fact that ionic radii of transition metals are smaller than that of  $O^{2-}$ . Thus the oxygen ions are usually close packed with the smaller metal ions located in the octahedral or tetrahedral holes among the oxygen ions.

Oxides commonly studied as catalytic materials belong to the structural classes of corundum, rock salt, wurtzite, spinel, perovskite, rutile and layer structures.

The definition of the surface microstructure and composition in the act of catalysis therefore requires extremely careful fundamental studies. One step is to systematically develop experimentally and theoretically, our understanding of the nature of defect structures of simpler well defined oxides; and extend it to the more complex commercially relevant mixed metal oxide systems.

## **1.1 Zirconium oxide and Lanthanide oxides as Catalysts.**

ZrO<sub>2</sub> is an excellent catalyst support [7-10]. There is also abundant catalysis literature in the area of strong zirconia based solid acids [11-16]

Hydrous zirconia is an excellent catalyst for the reduction of aldehydes and ketones with 2-propanol[17,18]. The effect of calcination temperature on the catalytic activity of ZrO<sub>2</sub> for reduction of aldehydes and ketones were studied. The catalytic activity was found to be maximum at 300°C and decrease with increase in activation temperature [19].

XRD studies revealed that ZrO<sub>2</sub> pre-treated below 973K is mainly amorphous. Small amounts of metastable tetragonal and monoclinic phase being contained. While ZrO<sub>2</sub> pretreated above 973K is monoclinic. Thus the lattice constant of ZrO<sub>2</sub> at 873K will be considerably different from that of ZrO<sub>2</sub> at 1073K. The fluorite phase of ZrO<sub>2</sub> appears only at 2370°C. By doping with lower valent ions such as Ca<sup>2+</sup>, Y<sup>3+</sup> [20] ,

$Mg^{2+}$  ,  $Mn^{2+}$  [21 ] and  $Cu^{2+}$  , the cubic structure will be stabilized and remains viable down to room temperature, it is metastable at that temperature [2].

In homogeneous precipitation (urea hydrolysis) method of preparing zirconia, the presence of anions do not influence the formation of acid sites rather some anions favourably contributed to the creation of more number of basic sites [22]. Mesoporous zirconia powders with high surface areas can be prepared by surfactant assisted synthesis with lauryl sulphate [23] and tetradecylphosphate [24] as the surfactants. Zirconia prepared by this method was found to be superior to the conventional zirconia catalyst in n-butane isomerisation reaction. Knowles and Hudson recently showed that alkylammonium salts can be used to prepare zirconia in the mesoporous range [25]. Aerogels with high surface areas can also be prepared [26, 27], but they are synthesised from moisture sensitive precursors, and low pressure separation of organic solvents from the precipitation media are also necessary.

Zirconia is a good support material for reduction reactions due to its reducing properties which seems to play an important role in the support effects [28]. It shows both acidic and basic properties. It is reported that addition of basic oxides (La) suppress the acidic behaviour whereas addition of an acidic oxide promotes acidic property [29]. Several Zirconia supported catalysts were prepared by using metals like Pd, Cu [30] ,Mg,  $SiO_2$  and  $CrO_3$  [31].

Surface acidity and basicity of Sm-Zr [32], La-Zr-Al [33] were studied and correlated with catalytic activity for cyclohexanone reduction. Catalytic

properties of  $\text{SiO}_2\text{-ZrO}_2$  for skeletal isomerisation and hydrogen transfer have been studied. Effect of sulfation of these catalysts are also studied [34]. Sulfated zirconia is known as a super acid and it is shown to be a better acid catalyst than Amberlyst-15.[35]

Experimental studies revealed that rare earth oxides, with appropriate pretreatment can act as effective catalysts for a number of reactions [36]. Their thermal stability enables them to act as catalysts for a number of reactions. The catalytic activity of rare earth oxides have been the subject of many recent research papers.

Some of the properties of Lanthanum and succeeding 14 Lanthanide elements have been explained on the basis of electronic configuration. The normal valence of the Lanthanide ions are tripositive. The trivalent ion of Lanthanum has the electronic configuration of the closed Xe shell, and the succeeding elements successively add 14 electron to the inner 4f subshell. The electronic configuration of the outer subshell is  $5s^2 5p^6$  for all the ions. The outer subshell of the tetra- and divalent ions remains  $5s^2 5p^6$ .

Taylor and Diamond [37] have shown that the paramagnetic oxides  $\text{Gd}_2\text{O}_3$  and  $\text{Nd}_2\text{O}_3$  are more active in catalysing the ortho-para hydrogen conversion than the non paramagnetic  $\text{La}_2\text{O}_3$ . The magnetic properties of the Lanthanide ions depend on the electron structure of the 4f subshell, and therefore, differs from each other. The catalytic activity differs from each other in such a reaction as the para

hydrogen conversion which proceeds by the para magnetic mechanism. On the other hand the difference in the activity is rather small in the reaction where the chemical bond is formed between the reactant and the catalyst surface.

The chemical properties of rare earth compounds are quite similar to each other, because the 4f orbital does not contribute significantly to the chemical bond of the Lanthanide compound. It has been said that the same is true for the catalytic property of the Lanthanide oxides. The activity patterns of rare earth oxides in heterogeneous reactions were investigated for simple catalytic reactions. The activity patterns are found to resemble each other [38]. A decrease in the catalytic activity of Lanthanide oxides from lanthanum to lutetium in the low temperature hydrogenation of ethylene was correlated with their decrease in basicity [39].

The effect of electronic configuration on catalytic activity of Lanthanide oxides in the oxidation of butane was studied [40]. A good correlation was obtained between catalytic activity and the fourth ionisation potential of the Lanthanide. It has been found in a series of catalytic oxidations that the catalytic activity of the Lanthanide oxide significantly differs from each other. Comparing the activation energies of the isotopic exchange of oxygen and of the desorption of carbon dioxide in the oxidation of carbon monoxide, it is found that the dependence of the activation energies on the atomic number were similar to that of the magnetic moment. Minachev compared the catalytic activity in the oxidation of hydrogen and propylene with that in the isotopic



exchange of oxygen, and suggested that the catalytic activity depends on the binding energy of the oxygen with the surface and on the valence of the Lanthanide ions.

Lanthanum oxide was found to be a promoter for magnesium oxide catalyst in oxidative coupling of methane (OCM) [41]. The promotion effect of  $\text{Dy}_2\text{O}_3$ ,  $\text{Nd}_2\text{O}_3$ ,  $\text{Yb}_2\text{O}_3$ ,  $\text{La}_2\text{O}_3$ ,  $\text{Gd}_2\text{O}_3$ , to the Rhodium - Alumina catalyst for OCM reaction had also been investigated [42]. A linear relationship was obtained between the carbon skeleton propagation of the hydrocarbon formed and the basicity of the Lanthanide oxide.

Crystal structure, support and valence state were found to have no effect on the catalytic activity of lanthanide oxides in the dehydrogenation of cyclohexane [43]. Carbon monoxide hydrogenation was done over mixed oxide catalysts of Lanthanide and yttrium. The addition of Lanthanide oxide to yttrium oxide was found to enhance the formation of light alkenes [44].

The hydrogen-oxygen reaction on  $\text{Dy}_2\text{O}_3$  was studied and a mechanism involving a competitive adsorption of hydrogen and oxygen on the catalyst, as the rate determining step was proposed [45].

The catalytic activity of rare earth oxides in low temperature ethylene hydrogenation had been studied as a function of temperature of pretreatment. Associatively adsorbed ethylene was involved in the reaction, and hydrogen activation

was likely to be the rate determining step [39]. The reaction of alkene/lanthana system with hydrogen and deuterium had been studied [46]

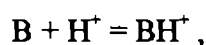
Catalytic activity in the butene isomerisation over Lanthanum oxide was studied as a function of pretreatment temperature. Activity increased with pretreatment temperature attained a maximum at 650°C and then decreased due to surface anion disorder [47]. Tanaka *et. al* made an attempt to correlate catalytic activity of the oxides in the decomposition of formic acid and polymerisation of isobutylene to the heat of formation of the oxide [48].

In general the catalytic activity depends on a number of factors, and therefore, it is difficult to clarify the exact nature of the catalytic activity. Using a series of catalysts with similar chemical properties such as the lanthanide oxides, more exact conclusions can be expected

## 1.2 Surface Acid Base Properties of Metal oxides

The **acid strength** of a solid is the ability of the surface to convert an adsorbed neutral base into its conjugate acid [49]. The acid strength of a solid can be expressed as the Hammett acidity function  $H_0$ .

If the acid base interaction involves the equilibrium of the type

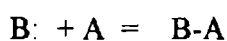


the acidity function due to Hammett and Deyrup [50] is given by

$$H_o = -\log k - \log[BH^+]/[B] = -\log a_{H^+} f_B/f_{BH^+}$$

Where  $a_{H^+}$  is the proton activity,  $[B]$  and  $[BH^+]$  are the concentrations,  $f_B$  and  $f_{BH^+}$  represent the activity coefficients of base and its conjugate acid respectively.

If the acid base interaction involve an electron pair transfer from adsorbate to the surface,



$$H_o = pK_a + \log [B]/[AB] = -\log a_A f_B/f_{AB} ,$$

Where  $a_A$  is the activity of the Lewis acid or electron pair acceptor. The base strength of solid base can be expressed as the  $H_o$  of its conjugate acid.

The **acidity** (acid amount) at an  $H_o$  value shows the number of acid sites whose acid strength is equal to or less than the  $H_o$  value. The **basicity** (base amount) at an  $H_o$  value shows the number of basic sites whose conjugate acid have acid strength equal to or greater than the  $H_o$  value [51]. Thus it is possible to measure the acid and base strength of a solid on a common scale.

Tanabe proposed a representative parameter  $H_{o,max}$  for the surface.  $H_{o,max}$  can be defined as the  $H_o$  value at the point of intersection where acidity = basicity = 0, which expresses the equal strongest  $H_o$  value of both acidic and basic sites [52].

Many methods are found in the literature to measure the acid base strength of solid surfaces.

Relative strengths of some common solid acids in terms of equivalent sulphuric acid concentrations were established. The red shifts of the spectra from the adsorbed neutral forms of 4- nitrotoluene and 4-nitrofluorobenzene were used to deduce the equivalent sulphuric acid concentration. These acidity measurements correlated well with their catalytic activity [53].

Acidity and basicity of  $\text{La}_2\text{O}_3$ ,  $\text{CeO}_2$ ,  $\text{Sm}_2\text{O}_3$ ,  $\text{Eu}_2\text{O}_3$  and  $\text{Y}_2\text{O}_3$  had been compared by step wise thermal decomposition of adsorbed carbon dioxide and thermally programmed desorption of adsorbed ammonia respectively [54]. When gaseous bases are adsorbed on acid sites, a base adsorbed on a strong acid site is more stable than one adsorbed on a weak acid site, and is more difficult to desorb. As elevated temperatures stimulate the evacuation of adsorbed bases from acid sites, those at weaker sites will be evacuated preferentially. The differential thermal analysis of solid acids or solid bases after adsorption of gaseous bases or acids respectively could give a measure of acid or base strength respectively [51].

The cooperation of acid sites with basic sites is surprisingly powerful for particular reactions and causes highly selective reactions. This kind of reaction is often seen in enzyme catalysis. Thus, it becomes sometimes necessary to know not only the strengths of the acidic and basic sites but also the orientation of acid-base pair site (distance between acidic and basic sites, sizes of acidic and basic sites, etc.). To

characterise the nature of an acid-base pair site the TPD method using phenol is useful. Phenol is known to adsorb on both acidic  $\text{SiO}_2 - \text{Al}_2\text{O}_3$  and basic MgO. It was found recently that phenol also adsorbs on  $\text{ZrO}_2$  and the desorption temperature of phenol adsorbed on  $\text{ZrO}_2$  is higher than those of phenol adsorbed on MgO and  $\text{SiO}_2 - \text{Al}_2\text{O}_3$ . Phenol adsorption is strongest on  $\text{ZrO}_2$  and weakest on  $\text{SiO}_2 - \text{Al}_2\text{O}_3$ . This supports a characteristic acid-basic bifunctional catalysis of  $\text{ZrO}_2$ . It was also found that  $\text{ZrO}_2$  showed higher activity and selectivity than  $\text{SiO}_2 - \text{Al}_2\text{O}_3$  and MgO for formation of nitriles from alkylamines, which can be interpreted by the bifunctional catalysis of  $\text{ZrO}_2$  [55].

From ammonia adsorption isotherm, cation exchange capacities and IR spectral studies of adsorbed probes, a schematic study of acid sites on silica - alumina [56], and silica-titania [57] were done.

The  $H_0$  values of silica supported heteropoly compounds (HPC) have been determined spectrophotometrically utilising adsorbed dicinnamaldehyde acetone as a probe molecule [58]. A linear relationship was obtained between the amount of HPC supported and its  $H_0$ .

UV spectroscopy of adsorbed Hammett indicators were used to find out the acidity of some heteropoly acids containing W, and their acid strength were found to increase as the valency of the central atom increases. UV spectra of Dicinnamaldehyde acetone indicator in acetonitrile gave a broad peak at 362 nm which is due to the neutral form of the indicator. When the heteropoly acids is added the

absorbance at 362nm is decreased and a new band appeared at 540nm due to its protonated form. The ratios of the extinction coefficients of the two forms were found to be 1.3. By using this ratio,  $[BH^+]/[B]$  of heteropoly acid solutions were calculated from the Hammett relationship. The catalytic activity for the decomposition of isobutyl propionate in a homogeneous system was correlated well with the acid strength [59].

The acid-base properties of MgO, SiO<sub>2</sub>, silica - alumina, chemically treated alumina etc. have been studied by IR spectroscopy of adsorbed probes like benzene, pyridine, nitrile and pyrrole [60]. An IR study of adsorbed carbon dioxide on lanthanum oxide surface has also been carried out [61]. The acid base properties of ZnO- TiO<sub>2</sub> was investigated by IR study of adsorbed pyridine [62]. The chemisorption of pyridine and trimethylamine on silica - alumina surface was studied by IR spectroscopy [63].

IR spectroscopy of adsorbed molecules could differentiate between Lewis and Bronsted acid sites. n-Butyl amine ( $pK_b=3.38$ ) is a stronger base than ammonia ( $pK_b=4.75$ ) and pyridine ( $pK_b=8.75$ ). So it will react with weaker acid sites. IR spectra of n-butyl amine adsorbed on silica- alumina were measured to investigate the character and properties of the acid sites on the surface.[64]

Lewis basic sites on ZrO<sub>2</sub> -TiO<sub>2</sub> system estimated by electron acceptor adsorption was affected considerably by change in composition [65].

The heat of adsorption of various bases or acids is also clearly a measure of the acid or base strength on the solid surface [51].

Take *et al* determined the base strength distribution on alkaline earth oxides by titration of the solid suspended in cyclohexane with benzoic acid [66]. The catalytic activity and selectivity of alkaline earth oxides in the elimination of HCl from 1,2-dichloroethane was quantitatively interpreted using the base strength obtained. Nakashima *et al* determined the base strength distribution on  $\text{Sm}_2\text{O}_3$  by benzoic acid titration method [67].

Miki Niwa *et al* used benzaldehyde - ammonia titration method for studying the acid base properties of metal oxide surfaces [68,69].

Amine titration method for the determination of acid strength of solids was first reported by Tamele [70]. It was based on Johnson's experiment [71]. It consists of titration of the solid suspended in benzene with n-butyl amine in benzene using p-dimethylaminoazobenzene ( $\text{pK}_a = 3.3$ ) as the indicator. The yellow basic form of the indicator changes to its red acidic form when adsorbed on the solid acid. The titres of n-butyl amine required to restore the yellow colour gave a measure of the number of acid sites on the surfaces. The use of various indicators with different  $\text{pK}_a$  values enabled the determination of the amount of acid at various acid strengths. This method gave the sum of Bronsted and Lewis acid sites. Johnson [71] showed that carbon tetrachloride and isooctane could also be used as solvents and benzyl amine as the titrating base. He also showed that it was necessary to take two or three days for

the titration of silica- alumina in order to minimise the adsorption of amine on the non acidic portions of the surface.

This difficulty led Benesi to modify the technique, so that the indicators could be added to portions of the catalyst in suspension, after the catalyst sample had reached equilibrium with n-butyl amine . The end point being determined by a series of approximations [72, 73]. Deeba and Hall tested Benesi's assumption that both n-butyl amine titrant and the indicators were in adsorption equilibrium with the acid sites on the surface, and found it to be invalid [74]. They suggested strong irreversible chemisorption of bases with varying  $pK_a$  values as a more reasonable method.

Take *et. al* also questioned Benesi's assumption of the establishment of equilibrium between the acid sites, n-butyl amine titrant and the indicator, as no evidence had been given by Benesi to strengthen his assumption [75]. Take et al proposed a new spectrophotometric method for measuring the acid base distribution of acid sites beyond  $H_0 = -8.2$  [76], which cannot be obtained by usual visual titration method. Murrell and Dizpenziere combined modified Benesi procedure and dry box techniques. Addition of an excess of sterically hindered pyridine and subsequent titration with n-butyl amine using dry box techniques allowed the Lewis acid sites to be assessed accurately [77]. By combination of this procedure with modified Benesi procedure, the number of Bronsted sites could also be determined.

Drushel and Sommers [78] proposed the use of fluorescent indicators for evaluating the acid strength of cracking catalysts.



A method involving the titration of a solid acid with the indicator itself in a non polar solvent was suggested [79]. It determines the number of acid sites from the amount of indicator chemisorbed at saturation.

Yamanaka and Tanabe proposed the titration of solid bases in benzene with trichloroacetic acid in benzene using Hammett indicators for measuring its basicity [80]. Base strength could also be expressed as a Hammett acidity function as in the case of acidity.

Sugiyama *et al* proposed a new procedure for determining the acid base properties of coloured oxides by indicator method [81].

Titration of dark coloured solids can be carried out by adding a small known amount of a white solid acid. Using this method acid strength and acid amount have been measured for chromic oxide employing alumina as the standard material [82].

Basicity of  $ZrO_2 - TiO_2$ ,  $Al_2O_3$  and  $TiO_2$  were studied by titration and electron acceptor adsorption [65].

### **1.3 Acid- Base Properties & Catalytic Activity.**

Bezouhanoca *et al* proposed cyclohexanol conversion as a test for the acid base properties of metal oxide catalysts [83].

Activities of ZnO-SnO<sub>2</sub> mixed oxide in the isomerisation of cyclopropane and dehydration of 2-butanol were correlated with acidic properties. Basicity was well correlated with the activities for isomerisation of 1-butene and decomposition of diacetone alcohol [84].

The catalytic activities of TiO<sub>2</sub>- SiO<sub>2</sub>- Al<sub>2</sub>O<sub>3</sub> ternary oxide system and its component oxides in the alkylation of toluene with 2-propanol and in the dehydration of 2-propanol were well correlated with the acidity obtained from butyl amine titration [85]. The catalytic activity of TiO<sub>2</sub> - SiO<sub>2</sub> mixed oxide was studied for the amination of phenol, hydration of ethylene and isomerisation of butene. The activities of the catalyst for the three reactions were well correlated with the acidity obtained from butyl amine titration and gaseous adsorption of basic gases [86].

Double bond migration of 2-propenyl ethers have been studied over metal oxide catalysts [87]. La<sub>2</sub>O<sub>3</sub> is found to be highly active. A mechanism is suggested in which the reaction is assumed to be initiated by the abstraction of H<sup>+</sup> from allyl ether, by the basic site on the catalyst to form the cis- allylic anion as an intermediate. Double bond migration of allyl amine to enamine over basic oxides (MgO, CaO ) was attempted [88]. The double bond migration of allyl amine proceeds via anionic intermediates.

Isomerisation of 1-butene over ZrO<sub>2</sub> catalyst with varying pre-treatment was studied. Though the active sites consist of both basic and acidic sites, activity was best correlated with basicity [89].

Change in the isomerisation activity of  $\text{La}_2\text{O}_3$  for the decomposition of 4-hydroxy,4-methyl,2-pentanone with pre-treatment temperature was well correlated with the change in basicity [90].

The acid base property of  $\text{MgO-TiO}_2$  binary oxides was studied. The catalytic activity for the decomposition of diacetone alcohol was investigated and correlated with catalyst basicity, while the dehydration activity of 4-methyl,2-pentanol was correlated with the acidity. The catalytic activity of the alkylation was observed at the maximum at the composition of 1:1 where acidity and basicity have a considerable value [91]. Catalytic activity and selectivity in OCM reaction on  $\text{La}_2\text{O}_3$ ,  $\text{CeO}_2$ ,  $\text{Sm}_2\text{O}_3$ ,  $\text{Eu}_2\text{O}_3$  and  $\text{Y}_2\text{O}_3$  to form  $\text{C}_2$  hydrocarbons depend both on acidity and basicity in a complex manner. Stronger acid sites are found to be harmful for  $\text{C}_2$  selectivity. Possibility of the involvement an acid base pair  $\text{M}_{\text{LC}}^{\text{n}+} \text{O}_{\text{LC}}^{2-}$  was proposed, LC denotes low coordination state [54].

The catalytic activity of silica supported heteropoly compounds for tertiary butyl alcohol dehydration in the liquid phase or gaseous phase depends on the  $\text{H}_0$  value [58].

The dehydration of isopropanol on silica -alumina gels was found to be independent of the amount of acid or basic sites but depends on the ratio of the former to the latter [92].

The alkylation of toluene with 2-propanol was attempted on MoO<sub>3</sub> - SiO<sub>2</sub> - Al<sub>2</sub>O<sub>3</sub> ternary oxide system [93]. Read attempted the decomposition of nitrous oxide on Nd<sub>2</sub>O<sub>3</sub>, Dy<sub>2</sub>O<sub>3</sub> and Er<sub>2</sub>O<sub>3</sub> [94].

S.T. King *et al* carried out a mechanistic study of methyl benzoate and benzoic acid reduction on a Y<sub>2</sub>O<sub>3</sub> [95]. Experimental evidence indicated that reduction to benzaldehyde is via surface benzoate.

Yuzo Imizu *et al* carried out a mechanistic study of hydrogenation of conjugated diene over lanthanum oxide catalyst [96]. The kinetics of the isomerisation of butene over lanthana and ZnO were studied [97]. The mechanisms were found to be similar.

The oxidation of carbon monoxide has been investigated on catalysts obtained by thermal activation of granular tin (+4) oxide gel in the temperature range of 200-500 °C. These are found to be active for this reaction at moderately low temperatures. Thermogravimetry and nitrogen adsorption have been used to investigate the water content and specific surface area of the activated catalysts, and these parameters have been related to the initial catalytic activities. The partial deactivation during CO oxidation at low temperatures which apparently accompanied by partial reduction of catalyst surface, has been studied as a function of both activation and reaction temperatures. The kinetics of the steady state reaction have been investigated at 180-210°C on the 450°C activated catalyst and the postulated mechanism involves adsorption of CO, desorption of CO<sub>2</sub> and oxygen regeneration of

the catalyst. The kinetics can be represented by the Langmuir type rate equation, similar to that derived for the same reaction on both  $V_2O_5$  and  $Fe_2O_3$ , and this permits the evaluation of experimental activation energies for the adsorption and desorption steps.[98]

The interpretation of the kinetic data demands that the catalyst undergoes successive reduction and reoxidation during the carbon monoxide oxidation and since the reaction on the steady state catalyst is independent of oxygen concentration, the reoxidation step at equilibrium must be considerably faster than the other two steps. The darkening of the colour of the catalyst during partial deactivation to a steady state condition at low temperatures, however is indicative of an overall partial reduction of the catalyst. Yoneda and Makishima [99] also observed this darkening and attributed it to a partial reduction. For this catalyst the reduction can be accounted for by a mechanism of surface oxygen abstraction, and does not necessarily demand participation of bulk oxygen. The X-ray powder diffraction pattern and the transmission IR spectrum of the partially reduced  $SnO_2$  were identical with the original material.

X-ray photoelectron spectroscopy of  $La_2O_3$  based OCM reaction provided strong evidence for the presence of surface super oxide ions ( $O^{2-}$ ) or peroxy carbonate ions ( $CO_4^{-2}$ ) [100].

From FTIR study of methane adsorption on  $\text{CeO}_2$  [101,102] and  $\text{MgO}$  [103], Li et. al reported that two types of adsorbed methane were formed on them, one interacts with the normal surface oxygen anion and the other interacts with the O-species, the structure of the latter was notably distorted. The two types can be successfully distinguished by coadsorption with  $\text{CO}$ .

Ceria can be depleted easily of oxygen by annealing at elevated temperatures at reduced oxygen pressure. Lower valent dopants such as yttrium, several rare earth elements, magnesium and calcium can also introduce free oxygen vacancies in ceria. The structure of oxygen vacancy complexes in ceria was studied by  $^{111}\text{In}$  Time Differential perturbed angular correlation Spectroscopy and four defect complexes with indium tracer atoms in undoped and lightly doped ceria have been observed [104].

EPR studies of unsupported  $\text{V}_2\text{O}_5\text{-Fe}_2\text{O}_3$  [105] catalysts revealed that by doping with cesium sulfate a new phase is formed in the solids which apparently increases their selectivity in the catalytic oxidation of polycyclic hydrocarbons. The percentage of this phase rises with increasing iron content. The new phase is amorphous. Its composition is nonstoichiometric and varies slightly depending on the iron content. A number of EPR measurements at different conditions indicated that the active centers probably consists of oxygen lattice vacancies in the coordination spheres of  $\text{Fe}^{3+}$  ion which are occupied by an electron.

The acid- base properties of  $\text{MoO}_3\text{-Bi}_2\text{O}_3\text{-P}_2\text{O}_5$  were studied by gaseous adsorption method. The oxidation and isomerization activity of olefins are proportional to the acidity of the catalyst, and the oxidation activity for an acidic compound and hydrogen is connected with the basicity. The selectivity was also interpreted in connection with the acid- base properties [106].

#### 1.4 Electron Donor - Acceptor Properties

When electron acceptors or donors are adsorbed on metal oxides, the corresponding radicals are formed as a result of electron transfer between the adsorbate and the metal oxide surface. The **electron donor strength** of a metal oxide can be defined as its conversion power for an electron acceptor adsorbed on the surface to its anion radical. The formation of anion radicals on the surfaces of various oxides were reported. For a strong electron acceptor its anion radical will be formed on every donor site of the oxide surface. For moderately strong electron acceptors anion radicals can be formed on strong donor sites only. Weak acceptors fail to form anion radicals even on strong donor sites. Electron accepting strength of an acceptor is expressed as the limiting electron affinity value at which free anion radical formation is not observed at the oxide surface [107].

The adsorbed water on hydroxylated silica surfaces act as specific adsorption sites for other molecules [108]. Some of the lattice oxygen ions on oxide surface may act as electron donors in the adsorption of nitro compounds [109].

ESR spectral studies of adsorption of naphthalene, anthracene, phenanthrene and biphenyl on porous silica gel made it possible to detect and identify radical cation which become stabilised on the gel surface[110].

Surface electron donating properties of silica - alumina, silica - titania and alumina -titania systems were studied by TCNQ adsorption [111].

Effect of silica surface dehydroxylation on adsorption of aromatic hydrocarbons in solutions of n-alkanes were investigated. Since the molecules of aromatic hydrocarbons on hydroxylated silica are oriented parallel to the surface, the influence of the size of the molecule at same orientation on the adsorption was investigated and the distribution function for several systems were determined [112].

Surface heterocycles undergo electron transfer at the oxide surface in an analogous manner as aromatic hydrocarbons [113].

The electron donor property of  $\text{TiO}_2$  and  $\text{MgO}$  have been investigated by TCNE (tetracyanoethylene) and TNB (trinitrobenzene) adsorption. Adsorption sites are  $\text{OH}^-$  and weakly co-ordinated  $\text{O}^{2-}$  ions, the latter increasing at higher activation temperatures. ESR spectral studies revealed that charge transfer complexes are weakly adsorbed on  $\text{OH}^-$  ions at the surface. The unpaired spin is then delocalised



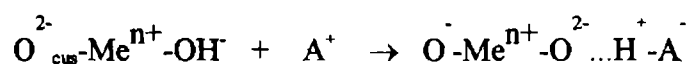
over the adsorbate molecule as a whole. On weakly co-ordinated  $O^{2-}$  ions the negative radicals are more strongly adsorbed, the electron is then localised at one site on the molecule ie. on the nitrogen atom [114].

The active sites on  $TiO_2$  surface for dehydration of formic acid were found to be EDS (electron donor sites). Electron donor sites were estimated by TCNE or TNB adsorption. These centers are  $Ti^{3+}$  and O-Ti-OH (formed by partial dehydration for high and low pre-treatment temperatures respectively) [115].

Adsorption of argon, nitrogen and water vapour on  $ZrO_2$  were studied. Surface properties were found to depend on the amount of irreversibly adsorbed water retained by the sample, far in excess required for a classical mono-layer [116].

Adsorption of TCNQ on various oxides from solvents of different ionisation potentials was attempted. Two types of dependence on ionisation potentials were observed [117]. The electron transfer reaction on pigmentary samples of  $TiO_2$  was also discussed [118].

The electron donor properties of several oxides like CaO, MgO, ZnO,  $Al_2O_3$ , silica - alumina were investigated using ESR spectral studies of adsorbed nitrobenzene. A correlation between electron donor sites and Lewis base strength was established. A model for the surface was proposed. The active sites were described as an acid-base pair, and the interaction of EDS to an acceptor is as follows.



$\text{Me}^{\text{n}+}$  is the surface cation and  $\text{O}_{\text{cus}}^{2-}$  is a surface oxygen ion in a low coordinate state. The radical is bound to the surface by static interaction [119].

Electron donor and acceptor properties of alumina, silica supported palladium oxide have been studied. The complex formed on adsorption,  $\text{Al}_2\text{O}_3\text{-PdO}_2\text{-C}_2\text{H}_2$  is radically different from  $\text{SiO}_2\text{-PdO}_2\text{-C}_2\text{H}_2$  [120]

Adsorption of electron acceptors with electron affinities from 1.26eV to 2.84eV on the surface of alumina was studied by adsorption isotherm, ESR and electronic spectra. Limiting amount adsorbed was found to decrease with decreasing electron affinity. Electron transfer from alumina surface ranged between 1.77 and 1.26eV in terms of the electron affinity of the acceptor [121]. The limit of electron transfer on titania surface lies between 1.77 and 1.26eV in terms of the electron affinity of the acceptor [122].

TCNQ adsorption was studied on zirconia-titania system[123] and alumina [124] in acetonitrile medium. TCNQ adsorption was carried out on some metal oxides and their radical forming activity is found to be in the order  $\text{MgO} > \text{ZnO} > \text{Al}_2\text{O}_3 > \text{TiO}_2 > \text{SiO}_2 > \text{NiO}$  [125].

The strength and distribution of electron donor sites on  $\text{Al}_2\text{O}_3$ ,  $\text{TiO}_2$  and  $\text{ZrO}_2\text{-TiO}_2$  were investigated with different electron acceptors [110].

TCNQ adsorption on zirconia system was investigated. The electron donor property of zirconia was found to decrease with increase in calcining temperature, reached a minimum at 200°C and then increased [126].

Lewis basic sites on zirconia - titania system was estimated by electron acceptor adsorption. It was found to be affected considerably by change in composition of the catalyst [84].

Adsorption of TCNQ on titania and alumina were carried out with solvents differing in acidity and basicity. Amount of TCNQ adsorbed decreased with increase in basicity of the solvent, but changed little with acidity [127, 128].

Adsorption of chloranil from various solvents on alumina and titania were studied. The amount of chloranil adsorbed was successfully correlated with the acid base interaction at the interface [129]. Change of zeta potentials of metal oxides caused by adsorption of TCNQ on alumina and titania from organic solvents were discussed on the stand point of electron transfer mechanism [130].

The acid-base and electron donor properties of  $\text{Pr}_6\text{O}_{11}$  [131],  $\text{CeO}_2$  [132],  $\text{Dy}_2\text{O}_3$  [133],  $\text{Y}_2\text{O}_3$  [134, 135],  $\text{Sm}_2\text{O}_3$  [136],  $\text{La}_2\text{O}_3$  [137] and  $\text{Nd}_2\text{O}_3$  [138, 139] and their mixed oxide oxides with alumina were investigated as a function of composition and activation temperature. The extent of electron transfer were characterised by magnetic measurement. Ceria and lanthana were found to enhance the electron donating ability of alumina without changing the limit of electron transfer. The

solvent effect on the extent of electron transfer was also studied. The decrease in the limiting amount of electron acceptor adsorbed with increase in basicity of solvent was explained using the Drago equation, connecting the heat of mixing of substances with acid base interaction.

$$-\Delta H_{AB} = C_A C_B + E_A E_B$$

where C and E are the Drago constants for the acidic compound A and basic compound B.

The catalytic activity for Dy<sub>2</sub>O<sub>3</sub> [140], Sm<sub>2</sub>O<sub>3</sub> [141], CeO<sub>2</sub> and its mixed oxides with alumina [142] for MPV (Meerwein-Pondorff-Verley) type reduction were investigated as a function of activation temperature. The activity was correlated with the electron donating properties of the respective oxides.

The electron donor properties of Perovskite type mixed oxides (LaFeO<sub>3</sub>, PrFeO<sub>3</sub>, SmFeO<sub>3</sub>, LaCoO<sub>3</sub>, PrCoO<sub>3</sub>, SmCoO<sub>3</sub>, LaNiO<sub>3</sub>, PrNiO<sub>3</sub>, SmNiO<sub>3</sub>) were determined using electron acceptor adsorption. The acid-base properties were studied using titration method using Hammett indicators, and well correlated with catalytic activity for MPV type reduction [143] and oxidation of cyclohexanol with benzophenone [144].

Surface electron donor property and acid-base properties of lanthana doped strontium oxide were investigated as a function of dopant concentration and activation temperature and the data well correlated with the catalytic activity for MPV

type reduction [145]. The catalytic activity of La-Zn [146], Al-Ce-Dy [147] mixed oxides for MPV type reduction were studied and correlated with their acid-base properties.

## 1.5 Surface site structures

In most transition metal oxides, the oxygen ions in the bulk form closed pack layers and the metal cation occupy holes among the anions. Since the bulk oxide ion are densely packed as possible, the oxide ion ligands around a metal cation are thought to have saturated the coordination sphere of the bulk cation, that is the bulk cation is coordinatively saturated. But the surface anions and the cations have fewer numbers of nearest neighbours than the corresponding ions in the bulk. These surface anions and cations are coordinatively unsaturated. In most instances, coordinative unsaturation results in ions that are active in bonding with adsorbates, however, all coordinatively unsaturated sites (cus) may not be necessarily active.

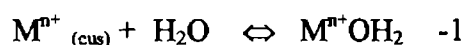
An oxide or hydrous oxide sample prepared by precipitation from an aqueous solution is formed by condensation and polymerisation of hydroxylated metal ion. For example, a M (III) metal ion existing as a monomeric unit possess a saturated coordination of three hydroxyls and three water ligands. Condensation of hydroxyl groups from two different monomeric units links the monomers with a bridging oxygen

to form a dimer. Dimer formation with more than one bridging oxygen or bridging through hydroxyl groups are also possible.

When condensation occurs between many different monomeric units, by drying at elevated temperatures, a three dimensional net work will be formed, which can be amorphous, semi-crystalline or crystalline, depending on the nature of the metal and the drying conditions. The surface metal ions as well as the surface oxide ions will have lower coordination numbers than that in the bulk. Often  $M^{n+}$  (cus) sites behaves as a Lewis acid and  $O^{2-}$  (cus) as a Lewis base. More extensive coordinative unsaturation is possible if more dehydroxylation take place, or if surface lattice oxygen is removed by reduction [148].

The presence of (cus) sites explain a variety of phenomena including poisoning of a surface, competitive adsorption and the common requirement of heating an oxide to activate it for chemisorption and catalysis.

Activation of an oxide by heating is needed because of the strong adsorption of water on oxides. An oxide surface becomes fully covered with adsorbed water and hydroxyl groups once it is exposed to moisture in the atmosphere.



In the first scheme, water is adsorbed molecularly to satisfy the coordinative unsaturation of the metal ion. In the second scheme, the (cus) action and

anion pair adsorbs a water molecule dissociatively as OH<sup>-</sup> and H<sup>+</sup>. So then the surface ions become coordinatively saturated and unable to adsorb other molecules. Heating causes the reverse processes, removal of water and formation of surface coordinative unsaturation. The extent of dehydroxylation depends on the temperature [148, 149]. Weakly adsorbed water are removed first (reverse of scheme 1). A rapid loss of water occurs around 200 to 350°C (reverse of scheme 2). Further dehydroxylation of the remaining hydroxyl groups beyond 400°C is slow, difficult and they are found to be isolated.

Removal of weakly adsorbed water (hydrogen bond) do not necessarily activate the surface. The chemisorptive capacity and catalytic activity increase rapidly as the degree of dehydroxylation increases. The manner in which these quantities increase depends on the molecules and the reaction because different requirements of surface sites may be involved. There can also be a directional character of (cus) sites as observed in the case of C≡O adsorption on ZnO [150].

In general molecules may interact with an oxide surface in different ways.

1. Molecular (nondissociative) adsorption in which the interaction is mainly by  $\sigma$  donation and/or  $\Pi$  bonding interaction. This can takes place on a single cus ion.

2. Dissociative adsorption in which a molecule dissociates upon adsorption

Dissociation of H<sub>2</sub>O into H<sup>+</sup> and OH<sup>-</sup> upon adsorption is an example of heterolytic dissociative adsorption in which the molecule is dissociated into charged species. This

type of adsorption usually required an anion-cation coordinatively unsaturated pair site. Homolytic dissociative adsorption in which neutral species are formed may also occur but less frequently.

3. Abstractive adsorption in which the adsorbate abstracts a species from the surface (often a proton). This commonly occurs on acidic oxides. If a proton is abstracted from the surface and the adsorbed species become cationic, the adsorbate could be held to the surface by electrostatic forces and coordinatively unsaturated sites might not be involved.

4. Reductive adsorption in which an adsorbed molecule is oxidised and while the surface is reduced. It may also be abstractive as in the case when a hydrocarbon molecule is oxidised on adsorption to a carboxylate utilising the lattice oxygen while reducing the cation. In addition to adsorption a surface may catalyse reactions of adsorbates.

In a general view the origin of acidic properties are surface (OH-) groups (Bronsted) and over exposed metal cations (Lewis acidity). The temperature range of their existence can be different depending on the solid, but after evacuation at 673K most of the Bronsted acidity has disappeared from the surface.

The acidic activity of electron deficient defects on metal oxide surfaces depend on the position of the particular metal in the periodic system of elements, i.e.



on the electronegativity of the metal cation. The larger the electronegativity the stronger the electron accepting power.

The electronegativity of the metal ion would be expected to change linearly with its charge;  $X_i = (1 + 2z) X_0$ , where  $X_0$  is the electronegativity of the neutral atom ( $z=0$ ) and  $z$  is the charge of the metal ion. This parameter  $X_i$  can be regarded as a semiempirical acidity parameter of the metal ion.[151]

The greater the covalency of the oxide, i.e. the higher the value of the charge/ radius ratio, the more likely acidity is to be found. On the other hand, an oxide with a low value of the ratio is more ionic in nature and will present more basic sites.[152]

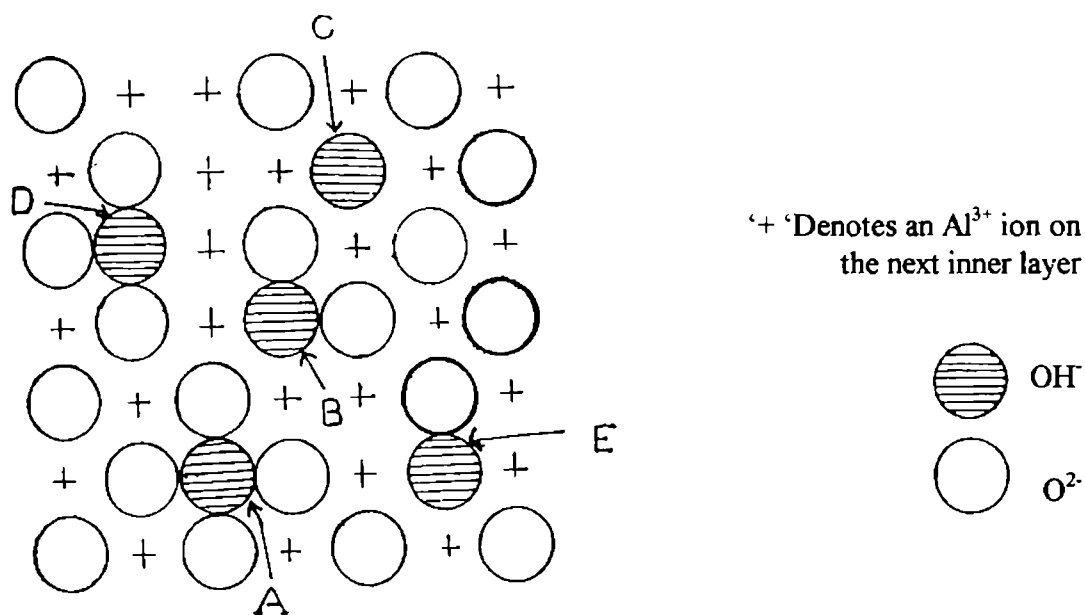
Surface hydration of  $\gamma$ - alumina has been studied by IR spectra and gravimetry. The extent of surface hydration is governed primarily by the drying temperature. Results show that hydroxyl groups although apparently mobile, persist as such on the surface at high temperatures on distinct type of sites rather than in a completely random state [153].

If dehydroxylation occurs randomly between pairs of hydroxyl groups, it would be difficult to achieve complete removal of surface hydroxyl groups. Even at high temperature evacuation, isolated surface hydroxyl groups are often present on anatase [154], that show IR absorption bands at about  $3700 \text{ cm}^{-1}$ . The intensities of

These bands decrease with increasing evacuation temperature, the rate of decrease is fastest for the lowest frequency band.

Peri carried out a systematic study and modelling of alumina surface by studying the IR spectra of ammonia adsorbed on it. Adsorption of ammonia was analogous to the adsorption of water. Sites which chemisorb to form  $\text{NH}_2^- + \text{OH}^-$  were considered as ion pair or acid-base sites [155].

Recently Peri has proposed a detailed scheme for the surface of  $\gamma$ -alumina prepared by heating aluminium hydroxide. The scheme for alumina heat treated at  $800^\circ\text{C}$  is shown in Figure, where five types of isolated hydroxyl groups labeled A to E are identifiable.



Suggested Scheme for acidic and basic sites on  $\gamma$ -Alumina

Each of them has a different nearest neighbour configuration. The five absorption maxima in IR spectrum (at 3800, 3750, 3744, 3733, 3700  $\text{cm}^{-1}$ ) are associated with sites A, D, B, E and C respectively. Each site has a different local charge density; type A with four  $\text{O}^{2-}$  ions as neighbours, is the most negative (a basic site) and type C which is lacking nearest neighbours is the most positive [156].

Acid sites on an alumina surface at high activation temperatures may be formed by lattice distortions. As the temperature of pretreatment is increased a water molecule is removed from two hydroxyl groups attached to aluminium atoms to form an Al-O-Al link. The distance between aluminium atoms becomes progressively greater with further dehydration. The distortion of Al-O-Al link becomes larger [157]. Lewis acid centres of silica-alumina was also investigated. Results lead to the conclusion that, the vacant 3p orbital of aluminium atom on the surface accepts one electron from the higher occupied  $\text{O}$  orbital of p-phenylenediamine molecule adsorbed, and it acts as a Lewis acid centre [158].

Electron transfer mechanism at alumina surface is investigated by Flockhart et al. Different types of surface sites are responsible for TCNE anion radical formation. Unsolvated hydroxyl ions at low temperature pre-treatment and defect sites involving  $\text{O}^{2-}$  ions at high temperature pretreatments respectively. Above 500°C dehydration of the surface results in the formation of two types of defects. At one of these, the presence of two or more adjoining vacancies in the surface layer results in an abnormally exposed aluminium ion. The resultant positive charge makes this sites an

electron acceptor and gives it an oxidising character. At the second type of active centre, two or more oxide ions occupy adjoining surface sites and a potential electron donor site is created, the number of such sites increases with increase in temperature [159].

Properties of acid sites formed on mixing oxides are demonstrated with titania - silica and silica -alumina as examples. The generation of strong and new acid sites on mixing oxides is attributed to a charge imbalance localised on  $M_1$  -O-  $M_2$  bonds formed in the mixed oxide, where  $M_1$  is the host metal ion and  $M_2$  is the mixed metal ion [160].

Tanabe *et.al* [161] extended Pauling's electrostatic valence rules [162] to account for the generation of acidity in binary oxides. They make two postulates.

1. The coordination number (and valence) of each metal ion in its own oxide is retained in the binary oxide.
2. The coordination number (and valence) for the oxygen ion in the oxide of the major metal component is retained for all oxygen ions in the binary oxide.

If these postulates hold, excess electrostatic charges will be created in most cases when metal oxides form chemical bonds with one another. Excess negative charges would produce Bronsted acids; positive charges would produce Lewis acids. The hypothesis is applicable to chemically mixed binary oxides and not to mechanically mixed oxides. This hypothesis predicts which combinations of oxides in the periodic table will

generate acidity and at what compositions the Bronsted or Lewis acidity will appear, but it does not predict the acid strength. Experimental evidence for this model was provided by Shibata *et.al* [163], in which a fairly good correlation was obtained between the highest acid strength observed and the average electronegativities of two metal ions in each oxide system.

Another model proposed by Kung [164] takes a rather different approach. In Tanabe's model, charge compensation at the substituting ion by neighbouring oxygen ions is important. In Kung's model, changes in electrostatic potential experienced by the substituting cation due to all the ions present in the matrix oxide is important. Thus Tanabe's model is a localized model and Kung's model is a delocalized model.

The ESR spectral data and diffuse reflectance of the polyacenes adsorbed on the surfaces of silica gel, alumina, and silica - alumina were studied. The amount of cation radicals generated on the surface was enhanced upon irradiation with UV light. This was interpreted in terms of photoionisation accomplished via a charge transfer state, which was expected to vary with the strength of the Lewis acid site [165].

IR spectral study of titania surface suggested the formation of incompletely co-ordinated titanium atoms on the surface, which was confirmed by the ionisation of perylene [166]. Relationship between surface acidity and particle size of titania was discussed [167]. The highest acid strength apparently increased with a

decrease in particle size. The oxygen vacancies generate a considerable number of dangling bonds whose energy levels are located in the band gap region between the valence and the conduction bands. Electrons trapped in these levels probably cause the local charge imbalance and hence the generation of new and strong acid sites over the surface of finely divided titania particles.

Lattice oxygen atoms in praseodymium oxide plays an important role in the catalytic oxidation of carbon monoxide [168]. Rosynek *et al* attempted a study on the thermal dehydration - rehydration behaviour of the  $\text{La}(\text{OH})_3 / \text{La}_2\text{O}_3$  system, for characterisation of catalytic lanthanum oxide. The dehydration of hydroxide is through an intermediate oxyhydroxide  $\text{LaOOH}$  [169].

Ji-Xuang Wang *et al* used EPR spectroscopy to detect  $\text{O}^{2-}$  ions on the surface of  $\text{La}_2\text{O}_3$  following quenching of the sample in oxygen from  $650^\circ\text{C}$ . These  $\text{O}^{2-}$  ions are believed to be formed by the reaction of oxygen either with thermally generated electron - hole pairs or the surface peroxide ions [170].

## REFERENCES

1. Pratibha .L. Gai-boyos, Catal. Rev.-Sci. Eng., 34 1&2, 1-54 (1992).
2. P. J. Gellings and H. J. M. Boumeester : Catalysis Today ,12, 1 (1992)
3. K. Takahashi, M. Shibagaki, H. Kuno and H. Matsushita : Chem. Lett.,1141 (1989)
4. K. Arata and K. Tanabe : Bull. Chem. Soc. Jpn., 11, 245 (1991)
5. M. Misono, K. Sakato, F. Ueda and Y. Yoneda : Bull. Chem. Soc. Jpn., 53, 648 (1980)
6. Z. Chen, T. Llzuka and K. Tanabe : Chem. Lett., 1085 (1984)
7. P. E. Marti, M. Maciejewski and A. J. Baiker : J. Catal., 139, 494 (1993)
8. Y. Amenomiya. : Appl. Catal., 30, 347 (1987)
9. R. A. Dalla Betta, A. G. Piken and M. J. Shelef : J. Catal., 40, 173 (1975)
- 10 L. A Bruce and J. F. Mathews: Appl. catal., 4,353 (1982)

11. V. Adeeva, J. W. de Hann, J. Janchen, G. D Lei, V. Schunemann, L. J. M. van de Ven, W. M.H. Sachtler and R.A. van Santen : J. Catal., 151, 364 (1995)
12. T. K. Cheung, J. L. d'Itri, B. C. Gates: J. Catal., 151, 464 (1995)
13. K.Ebitani, H. Konno, T. Tanaka and H. Hattori: J. Catal., 135, 60 (1992)
14. E. Iglesia, S. L. Soled and G. M. Kramer : J. Catal., 144, 238 (1993)
15. H. Hino, : Chem. Lett., 971 (1989)
16. M. Hino and K. Arata : Catal. Lett., 30, 25 (1995)
17. M. Shibagaki, K. Takahashi and H. Matsushita : Bull. Chem. Soc. Jpn, 61, 3283 (1988)
18. M. Shibagaki, H. Kuno K. Takahashi and H. Matsushita : Bull. Chem. Soc. Jpn., 61, 4153 (1988)
19. M. Shibagaki, K. Takahashi and H. Kuno and H. Matsushita : Bull. Chem. Soc. Jpn., 63, 258 (1990)
20. M. Shibagaki, K. Takahashi and H. Kuno and H. Matsushita ; Journal of physical Society of Japan, 8, 61, 2848 (1992)
21. A. Keshavaraja and A. V. Ramaswamy : J. Mater. Res., 9, 837 (1994)



22. K.M.Parida, P.Patnaik, J.Das and T.Misra : *Catalysis Modern Trends*, Edited by N.M.Gupta and D.K .Chakraborty, (1995)
23. G.Larsen, E.Lotero , M.Nabity, L.M.Petkovic and D.S.Shobe : *Journal of Catalysis*, 164, 246 (1996).
24. F.Schuth, U. Ciesla and S. Schacht: *Angew. Chem.*, 35, 541 (1996)
25. J. A. Knowles and M. J. Hudson : *J. Chem. Soc. Chem. Commun.*, 2083 (1995)
26. D. M. Ward and E. I. Ko : *J. Catal.*, 150, 18 (1994)
27. S. J. Teichner, G.A . Nicolaon, M. A. Vicarini and G. E. E. Gardes : *Adv. Colloid Inerf. Sci.*, 5, 245 (1976)
28. T. Lizuaka, M. Itoh, H. Hattori and K.Tanabe : *J. Chem. Soc. Faraday Trans.*, 1, 78, 501 (1982)
29. R. Franklin, P. Goulding, J. Haviland, R.W.Joyner, I. McAlpine, P. Moles, C. Norman and T. Nowell : *Catalysis Today*, 10, 405 (1991)
30. P. S. Saiprasad, B. David Raja, K.S. RamaRao, N. Lingaih, G. S. Salvapathyand P. Kantarao : *Catalysis Modern Trends*, Edited by N. M. Gupta and D. K . Chakraborty, (1995)

31. Anitha Raichel, V. Durga Kumari, and P. Kanta Rao : Catalysis Modern Trends, Edited by N.M.Gupta and D.K .Chakraborty, (1995)
32. S.Sugunan , Sunitha Kurur and Anto Paul : Indian Journal of Chemistry, 33A,1096 (1994)
33. S.Sugunan and Anto Paul : Indian Journal of Chemistry, 36A, 300 (1997)
34. G. Yadav and T. S. Thorat : Catalysis Modern Trends, Edited by N.M.Gupta and D.K .Chakraborty Narosa Publishing house ,NewDelhi (1995)
35. J.A.Navio, G.Colon, M.Macias, J.M.Campelo, A.A.Romero and J.M.Marinas : J. Catal. , 161, 605 (1996)
36. Y. Sakata, M.Yoshino, H. Imamura and S.Tsuchiya : Chem. Soc.Faraday Trans. , 86, 3489 (1990)
37. H.S Taylor and H. Diamond : J. Amer. Chem. Soc.,: 57, 1251 (1935)
38. P. Pomonis : React. Kinetics Catal. Lett., 18, 247 (1981)
39. K. M. Minachev, Y. S. Khodakov and V.S. Nakshunov : J. Catal., 49, 207 (1977)
40. T. Hattori, J. Inoko and Y. Murakami : J. Catal., 42, 60 (1976)
41. V. R. Choudhary, S. T. Choudhary, A. M. Rajput and V. H. Rane : Chem. Commun., 555 (1989)

42. Y.Takita, T.Yokoo, N.Egashira and F.Hori : Bull. Chem. Soc. Jpn., 55, 2653 (1982)
43. C.B.McGough and G.Houghton : J. Phy. Chem., 65, 1887 (1961)
44. T. Arai, K. Maruya, K. Domen and T.Onishi : Bull. Chem. Soc. Jpn., 62, 349 (1989)
45. J. F. Read, E.W.Perkins : J. Catal., 42, 443 (1976)
46. R. Bird, C.Kemball and H. Frankleach : J. Catal., 105, 199 (1987)
47. M. P. Rosynek, J. S. Fox and J. L. Jenesen : J. Catal., 71, 64 (1981)
48. K. Tanaka and K.Tamaru : Bull. Chem. Soc. Jpn., 37, 1862 (1964)
49. Cheves Walling : J. Am. Chem. Soc., 72, 1164 (1950)
50. L. P. Hammett and A. J. Deyrup : J. Am. Chem. Soc., 54, 2721 (1932)
51. K. Tanabe : "Solid acids and bases", Academic Press, New York, (1970)
52. Tohr Yamanaka and Kozo Tanabe : J. Phy. Chem., 80, 1723 (1976)
53. Benjamine Umansky, J.E. Hardt and W.Keith Hall : J. Catal.,127, 128 (1991)
54. V. R.Choudhary and V.H.Rane : J. Catal., 130, 411 (1991)
55. B. Xu, T.Yamaguchi and K. Tanabe : Chem. Lett., 281, (1988) )

56. J. J. Fripiat, A. Leonard and J. B. Vytterhouven : *J. Phy. Chem.*, 69, 10 (1965)
57. C. U. Ingemar Odenbrand, Jan J. M. Brandin and Guido Buska: *J. Catal.*, 135, 505 (1992)
58. R. Obtusuka, Yoshio Morioka and Junchi Kobayashi : *Bull. Chem. Soc. Jpn.*, 63, 2071 (1990)
59. T. okuhara, C. Hu , M. Hashimoto and M. Misono :*Bull. Chem. Soc. Jpn.*, 67, 1186 (1994)
60. P. O. Scokart and P. G. Rouxhet : *J. Colloid and Interface Sci.*, 86, 1 (1982)
61. M. P. Rosynek and D.T. Magnuson : *J. Catal.*, 48, 417 (1977)
62. K. Tanabe, C. Ishiya, I. Matzuzaki, I. Ichikawa and H. Hattori : *Bull. Chem. Soc. Jpn.*, 45, 47 (1972)
63. M. R. Basila, T. R. Kanter and Kee. H. Rhee : *J. Phy. Chem.*, 68, 11 (1964)
64. T. Morimoto, J. imai and M. Nagao: *J. Phy. Chem.*, 78(7), 704 (1974).
65. K. Esumi and K. Meguro : *J. Jpn. Soc. Colour Materials*, 58, 9 (1985)
66. J. I. Take, N. Kikuchi and Y. Yoneda : *J. Catal.* 21, 164 (1971)
67. Y. Nakashima, Y. Takata, H. Imamura and S. Tsuchiya : *Bull. Chem. Soc. Jpn.*, 63, 3313 (1990)

68. M. Niwa, K. Susuki, M. Kishida and Y. Murakami : *Applied Catalysis*, 67, 297 (1991)
69. M. Niwa, S. Inagaki and Y. Murakami : *J. Phy. Chem.*, 89, 2550 (1985)
70. M. W. Tamele : *Disc. Faraday Soc.*, 8, 270 (1950)
71. O. Johnson : *J. Phy. Chem.*, 59, 827 (1955)
72. H. A. Benesi : *J. Phy. Chem.*, 61, 970 (1957)
73. H. A. Benesi : *J. Am. Chem. Soc.*, 78, 5490 (1956)
74. M. Deeba and W. Keith hall : *J. Catal.*, 60, 417 (1979)
75. J. I. Take, Y. Nomizo and Y. Yoneda : *Bull. Chem. Soc. Jpn.*, 46, 3568 (1973)
76. J. I. Take, T. Tsuruya, T. Sato Y. Yomeda : *Bull. Chem. Soc. Jpn.*, 45, 3409 (1972)
77. L. L. Murrell and N.C. Dispenziere Jr : *J. Catal.*, 117,275 (1989)
78. H.V.Drushel and A.L. Sommers : *Anal . Chem.*, 38, 1732 (1966)
79. J. I. Take, H. Kawai and Y.Yoneda : *Bull. Chem. Soc. Jpn.*, 50, 2428 (1977)
80. Tohr Yamanaka and K. Tanabe : *J. Phy. Chem.*, 79, 2407 (1975)

81. K. Sugiyama, Y. Nakano, H. Miura and T. Matsuda : *Bull. Chem. Soc. Jpn.*, 58, 1825 (1985)
82. S. E. Voltz, A. E. Hirsthler and A. Smith : *J. Phy. Chem.*, 64, 1594, (1960)
83. C. P. Bezoubanoca and M.A. Alzihari : *Catal. Lett.*, 11, 245 (1991)
84. G. W. Wang, H. Hattori and K. Tanabe : *Bull. Chem. Soc. Jpn.*, 56, 2407 (1983)
85. K. R. Sabu, K. V. C. Rao and C.G.R Nair : *Bull. Chem. Soc. Jpn.*, 64, 1426 (1991)
86. M. Itoh, H. Hattori and K. Tanabe : *J. Catal.*, 35, 225 (1974)
87. H. Matsushashi and H. Hattori : *J. Catal.*, 85, 457 (1984)
88. A. Hattori, H. Hattori and K. Tanabe : *J. Catal.*, 65, 245 (1980)
89. Y. Nakano, T. Lizuaka , H. Hattori and K. Tanabe : *J. Catal.*, 57, 1 (1979)
90. Y. Fukuda H. Hattori and K. Tanabe : *Bull. Chem. Soc. Jpn.*, 51, 3150 (1978)
91. K. Tanabe, H. Hattori, T. Sumiyoshi, K. Tamaru and T. Kondo : *J. Catal.*, 53, 1 (1978)

92. E. Fedorynska, T. Woznieski, S. Malinowski, I. Ahamed and Anna Madura : *J. Colloid and Interface Sci.*, 69, (1979)
93. K. R. sabu, K.V.C.Rao and C.G.R. Nair : *Bull. Chem. Soc. Jpn.*, 64, 1920 (1991)
94. J. F. Read : *J. Catal.*, 28, 428 (1973)
95. S. T. King and E. J. Strojny : *J. Catal.*, 274 (1982)
96. Y. Imizu, K. Sato and H. Hattori : *J. Catal.*, 76, 53 (1982)
97. J. Goldwasser and W. Keith hall : *J. Catal.*, 71, 53 (1981)
98. M. J.Fuller and M.E. Warwick *J. Catal.*, 29, 441, (1973)
99. Yoneda .Y and Makishima .Sactes. Congr. Int. Catal. 2e, paris 2103 (1960.)
100. J. L. Dubois, M. Bisiaux, H.Mimoon and C. J. Cameron : *Chem. Lett.*, 967 (1990)
101. C. Li and Q. J. Xin : *Chem. Soc. Chem. Commun.*, 782 (1992)
102. C. Li and Q. J. Xin: *J. Phys.Chem.*, 96, 7714 (1992)
103. C. Li, G. Li and Q. J. Xin : *J. Phys.Chem.*, 98, 1933 (1994)
104. R. Wang, J. A. Gardner, W. E. Evenson and J. A. Sommers: *Physical review.*, 47, 638 (1993)

105. A. Bruckner, G.U. Wolf, M. Meisel, R. Slooser and H. Mehner: *J. Chem. Soc. Faraday Trans.*, 90 (20), 3159 (1994)
106. M. Ai and T. Ikawa: *J. Catal.*, 40, 203 (1975)
107. K. Esumi and K. Meguro : *J. Colloid and Interface Sci.*, 66, 1 (1978)
108. M. L. Hair and W. Hertl : *J. Phy. Chem.*, 73, 4269 (1969)
109. A.L. Tench and R. L. Nelson : *J. Chem. Physics*, 40, 2763 (1964)
110. A. Lund and A. Shimazu : *J. Phy. Chem.*, 75, 12 (1969)
111. H. Hosaka, N. Kawashima and K. Meguro : *Bull. Chem. Soc. Jpn.*, 45, 3371 (1972)
112. Yu. A. Elterkov, V. V. Khopina and A.V. Kiselev : *J. Chem. Soc. Faraday Trans.*, 68, 889 (1972)
113. L. Petrakis and K. S. Seshadri : *J. Phy. Chem.*, 76, 10 (1972)
114. M. Che, C. Naccasche and B. Imelic : *J. Catal.*, 24, 328 (1972)
115. M. A. Enriquexz and J. P. Fraissand : *J. Catal.*, 74, 77 (1982)
116. H. F. Holmes, E. L. Fuller and R. A. Beh : *J. Colloid and Interface Sci.*, 47, 2 (1974)
117. H. Hosaka and K. Meguro : *Colloid and polymer sci.*, 252, 322 (1974)



118. S. Davidson and R. M. Slater : Bull. Chem. Soc. Jpn., 48, 2416 (1975)
119. D.Gordishi and V. Indovino : Bull. Chem. Soc. Jpn., 49, 2341 (1976)
120. I.Bodrikov, K.G. Khulbe and R.S.Mann : J. Catal., 43, 339 (1976)
121. K. Meguro and K.Esumi : J. Colloid and Interface Sci., 59, 93 (1977)
122. K. Esumi and K. Meguro : Bull. Chem. Soc. Jpn., 55, 1647 (1982)
123. K. Esumi, H. Shimada and K. Meguro : Bull. Chem. Soc. Jpn., 50, 2797 (1977)
124. K. Esumi and K. Meguro : J. Colloid and Interface Sci., 61, 191 (1977)
125. H.Hosaka, T.Fugiwara and K. Meguro : Bull. Chem. Soc. Jpn., 44, 2616 (1971)
126. K.Esumi and K.Meguro : Bull. Chem. Soc. Jpn., 55, 315 (1982)
127. K.Esumi, K.Miyato, F.Waki and K.Meguro : Collids and surfaces, 20, 8 (1986)
128. K.Esumi, K.Miyata and K.Meguro : Bull. Chem. Soc. Jpn., 58, 3524 (1985)
129. K.Esumi, K.Miyata, F.Waki and K.Meguro : Bull. Chem. Soc. Jpn., 59, 3363 (1986)

130. K.Esumi, K.Magura and K.Meguro : J. Colloid and Interface Sci., 141, 578 (1991)
131. S.Sugunan ,G.D.Devika Rani and P.A.Unni Krishnan :J. Mater. Sci. Technol., 10,425,(1994)
132. S.Sugunan and J.M.Jalaja : Collect. Czech. Chem. Commun., 59, 2605, (1994)
133. S.Sugunan and K.B.Sherly and G.D.Devika Rani : React. Kinet. Catal. Lett., 51(2), 525 (1993)
134. S.Sugunan ,G.D.Devika Rani : Journal of Material Science Letters , 10, 887 (1991)
135. S.Sugunan ,G.D.Devika Rani and P.A.Unni Krishnan :Indian Journal of Engineering and Material Sciences, 12, 245 (1995)
136. S. Sugunan and J.J. Malayan :J.Adhesion Sci. Technol., 9(1), 73 (1995).
137. S. Sugunan and K.B. Sherly : Indian Journal of Chemistry, 32(A), 689 (1993)
138. S. Sugunan ,G.D. Devika Rani : Indian Journal of Chemistry, 32(A), 993 (1993)
139. S. Sugunan ,G.D. Devika Rani : Journal of Material Science, 29, 4811 (1993)
140. S. Sugunan and K.B. Sherly :React. Kinet. Catal. Lett., 51(2) 533 (1993)

141. S. Sugunan and J.M. Jalaja :React. Kinet. Catal. Lett., 55(2), 399 (1995)
142. S. Sugunan and V. Meera : Collect. Czech. Chem. Commun., 60, 977 (1995)
143. S.Sugunan and V. Meera : Indian Journal of Chemistry, 34(A), 984 (1995)
144. S. Sugunan and J. M. Jalaja : Indian Journal of Chemistry, 34(A), 216 (1995)
145. S. Sugunan and Binsy Varghese :React. Kinet. Catal. Lett., 57(1), 87 (1996)
146. S. Sugunan and Binsy Varghese :React. Kinet. Catal. Lett., 62(1), 157 (1997)
147. S. Sugunan and Bindhu Jacob : Indian Journal of Engineering and Material Sciences, 4, 120 (1997)
148. R.L. Burwell., Jr.,G.I.Haller, K. C. Taylor and J. F. Read: Adv. Catal., 29,1 (1969).
149. M.Nagao and T.Morimoto : J.Phys.Chem., 84, 2054 (1984)
150. R.R. Gay, M.H.Nodine, V.E. Henrich , H.J.Zieger and E.I.Solomon :J. Amer.Chem.Soc., 102, 6752 (1980).
151. Sanderson R.T, Chemical periodicity; Reinhold; Newyork, (1960)
152. Aline Auroux and Antonella Gervasini: J.Phys. Chem., 94,6371 (1990).
153. J.B.Peri : J. Phy. Chem., 69, 231 (1965)

154. N. D. Parkyn, P. 150 in Chemisorption and catalysis ed by P. Hepple, Elsevier Publ. Co, Amsterdam, Netherlands, (1971)
155. J.B Peri : J. Phy. Chem., 69, 220 (1965)
156. J. B. Peri : J. Phy. Chem., 69, 211 (1965)
157. E. B. Cornelius, T. H. Milliken, G.A. Mills and A.G. Oblad : J. Phy. Chem., 59, 809 (1955)
158. M. Okuda and T. Tachibana : Bull. Chem. Soc. Jpn., 33, 863 (1960)
159. B. D . Flockhart, I. R. Leith and R. C. Pink : Trans. Faraday society, 65, 542 (1969)
160. H. Nakabayashi : Bull. Chem. Soc. Jpn., 65, 914 (1992)
161. K. Tanabe, T. Sumiyoshi, K. Sibata, T. kiyoyura and J. Kitagawa : Bull. Chem. Soc. Jpn., 47, 1064 (1974)
162. L. Pauling.: "The nature of the Chemical Bond" p.547. Cornell Univ. Press. Ithaca NewYork (1960)
163. K. Shibata, T. Kiyoura, J. kitagawa, T. Sumiyoshi and K. Tanabe : Bull. Chem. Soc. Jpn., 46, 2985 (1973)
164. H. Kung : J. Silid State Chem., 52, 191 (1984)

165. K. Takimoto and Masaji Miura : Bull. Chem. Soc. Jpn., 44, 1534 (1971)
166. M. Primet, Pierre Pichat and M. V. Mathiew : J. Phy. Chem., 75, 9 (1971)
167. K. Mishiwaki, N. Kakuta and Aki fumi Ueno : J. Catal., 118, 498 (1989)
168. Y. Takasu, M. Matsui and Y. Matsuda : J. Catal., 76, 61 (1982)
169. M. P. Rosynek and D. T. Magnuson : J. Catal., 46, 402 (1977)
170. Ji-Xiuan Wang and J. K. Lunsford : J. Phy. Chem., 90, 3890 (1986)

**CHAPTER 2.**

**EXPERIMENTAL**

## **2.1 Materials Used**

Cerium nitrate (99.9% pure) ,

Praseodymium nitrate (99.9% pure) ,and

Neodymium nitrate (99.9% pure) were obtained from Indian Rare Earths

Ltd. Udyogamandal, Kerala.

Zirconyl nitrate was obtained from Romali.

### **Reagents for Adsorption studies .**

#### **Electron Acceptors**

Electron acceptors used in the study were

7,7,8,8- Tetracyanoquinodimethane (TCNQ),

2,3,5,6-tetrachloro-p- benzoquinone (chloranil),

p-dinitrobenzene (PDNB) and

m- dinitrobenzene (MDNB).

TCNQ was obtained from Merck-Schuchardt and was purified by repeated recrystallisation from acetonitrile [1].

Chloranil was obtained from Sisco Research Laboratories Pvt Ltd and was purified by recrystallisation from benzene [2].

p-Dinitrobenzene was supplied by Koch Light Laboratories Ltd and was purified by recrystallisation from chloroform [3].

m-Dinitrobenzene was obtained from Loba-Chemie Indoaustral company and was purified by recrystallisation from carbon tetrachloride [4].

**Solvents:-**

Acetonitrile :SQ grade acetonitrile obtained from Qualigens Fine Chemicals was first dried by passing through a column filled with silica gel 60-120 mesh size activated at 110°C for two hours. It was then distilled with anhydrous phosphorous pentoxide and the fraction between 79-82°C was collected [5].

**Reagents for Acidity Basicity Measurements**

**Benzene:** Benzene used for acidity and basicity measurements was purified by the following procedure [6]. Pure Benzene obtained from Qualigens Fine Chemicals was shaken repeatedly with about 15% of its volume of concentrated sulphuric acid in a stoppered separating funnel until the acid layer was colourless on standing. After shaking, the mixture was allowed to settle and the lower layer was drawn off. It was then washed with water and 10% sodium carbonate solution and was finally dried with anhydrous Calcium Chloride. It was filtered, distilled and the distillate was kept over sodium wire for one day and again distilled and the fraction boiling at 80°C was collected.

**Hammett Indicators:**

Hammett indicators used for the study are the following.

1. Methyl red (E.Merck India Pvt Ltd)
2. Dimethyl yellow (Loba-Chemie Industrial Company)
3. Bromo thymol blue (Qualigens Fine Chemicals)
5. Crystal violet (Romali)



6. Neutral red (Romali)

7. Thymol blue (Qualigens Fine Chemicals)

Trichloro acetic acid (SQ grade), obtained from Qualigens Fine Chemicals and n-butyl amine (Cemphasol Pure) were used without further purification.

### **Reagents for catalytic activity measurements**

#### **Reagents for Reduction reaction**

Cyclohexanone: Cyclohexanone (LR grade) obtained from BDH was purified through bisulphite method [7]. A saturated solution of Sodium bisulphite was prepared from 40 gramme of finely powdered Sodium bisulphite. The volume of the resulting solution was measured and it was treated with 70 % of its volume of rectified spirit. Sufficient water were added to dissolve the precipitate which separated. 20 g of commercial cyclohexanone was introduced into the aqueous alcoholic bisulphite solution with stirring and the mixture was allowed to stand for 30 minutes. The crystalline bisulphite compound was filtered off at the pump and washed it with a little rectified spirit.

The bisulphite compound was transferred to a separating funnel and decomposed with 10 % NaOH solution. The liberated cyclohexanone was removed, saturated the aqueous layer with salt and extracted it with 30 ml of ether. The ether extract was combined with the ketone layer and dried with 5 g of anhydrous magnesium sulphate. The dried etherial solution was filtered into a 50 ml distilling

flask, attached with a reflux condenser and distilled off the ether using a water bath. The residual cyclohexanone was distilled and the fraction at 153°C was collected.

2-Propanol: (LR grade) reagent obtained from E.Merck was further purified by adding about 200g of quicklime to one litre of 2-propanol. it was kept for 3-4 days and then refluxed for 4 hours. It was then distilled and the fraction distilling at 82°C was collected [8].

### **Reagents for Oxidation reaction**

Toluene : (SQ grade) toluene obtained from Qualigens Fine Chemicals was shaken twice with cold Conc.  $H_2SO_4$  ( 100 ml of the acid with 1 litre of toluene), then with water, 15% aq. $NaHCO_3$  and again with water. Then it was dried successively with  $CaSO_4$  and  $P_2O_5$ , distilled and the fraction disilling at 110°C was collected [9].

Cyclohexanol : Cyclohexanol obtained from Merck was refluxed with freshly ignited  $CaO$  and then fractionally distilled. The fraction distilling at 161°C was collected [10].

Benzophenone : The reagent was supplied by Sisco Research Laboratories Pvt. Ltd. and was purified by recrystallisation from ethanol [11].

### **Reagents for Esterification Reaction**

1-Butanol : (LR grade) reagent obtained from Merck was further purified by drying with anhydrous potassium carbonate and fractionally distilled. The fraction distilling at 116.5°C was collected [12].

Acetic acid : (LR grade) reagent obtained from Merck was purified by adding some acetic anhydride to react with the water present. It was then heated for one hour just below boiling in the presence of 2g CrO<sub>3</sub> per 100 ml and then fractionally distilled. The fraction at 116 -118°C was collected [13].

n-Decane : (LR grade) reagent obtained from Sd. Fine Chemicals Pvt.Ltd was further purified by shaking with Conc. H<sub>2</sub>SO<sub>4</sub>. It was washed with water and aq.NaHCO<sub>3</sub>. Finally it was washed with more water, then dried with MgSO<sub>4</sub>, refluxed with sodium and distilled. The fraction distilling at 174°C was collected [14].

## **2.2 Methods adopted**

### **Catalyst preparation:-**

The mixed oxides were prepared by the decomposition of their mixed hydroxides. The mixed hydroxides were prepared by co precipitation method. To the boiling solution containing calculated quantities of zirconyl nitrate and nitrates of Lanthanides, 1:1 ammonia solution was added slowly with constant stirring, allowed to boil again for 5 minutes and allowed to stand overnight. The precipitate was filtered through a whatman No : 1 filter paper and washed with distilled water containing a little ammonia till the precipitate is free from nitrate ions. It was dried at 120° C [15] overnight and ignited at 300° C for 2 hours. The mixed oxides was then sieved to get 100-200 mesh size. Mixed oxides of the following compositions were prepared ( 20, 40, 60 and 80 weight % of Lanthanide oxide). Samples were activated at 300, 500 or

800° C were studied. Pure oxides prepared under identical conditions were also studied.

#### **Adsorption studies[16] :-**

The oxides were activated at a particular temperature for two hours prior to each experiment. 0.5g of the catalyst was placed in a 25ml test tube and outgassed at 10 torr for one hour. into the test tube which was fitted with a mercury sealed stirrer, 10ml of a solution of an electron acceptor in an organic solvent was then poured in. After the solution had sufficiently been stirred for 4 hours at 28°C in a thermostated bath, the oxide was collected by centrifuging the solution. The amount of electron acceptor adsorbed was determined from the difference in concentration of electron acceptor before and after adsorption. The absorbances of electron acceptors was measured by means of a UV-VIS-Spectro photometer (Hitachi 200-20) at the  $\lambda_{max}$  of the electron acceptor in the solvent. The  $\lambda_{max}$  of TCNQ, Chloranil, PDNB and MDNB were 393.5nm, 288nm, 262nm, and 237nm respectively. The reflectance spectra of the adsorbed samples were measured with a Hitachi 200-20 uv-visible spectrophotometer with a 200 - 0531 reflectance attachment. The radical concentration of the electron acceptors adsorbed on the oxides were determined from the ESR spectra measured at room temperature using a Varian E-112 X/Q band ESR spectrometer. Radical concentrations were calculated by comparison of peak area obtained by double integration of the first derivative curve for the sample and standard

solution of 1,1-diphenyl-2-picryl-hydrazyl in benzene. Surface areas of oxides were determined by BET method using Carlo Erba Strumentazione sorptomatic series 1800

#### **Acidity Basicity Measurements:**

The oxides were activated at a particular temperature for 2 hours prior to each experiment. The acidity at various acid strength of a solid was measured by titrating 0.1g of solid suspended in 5ml benzene, with a 0.1N solution of n-butyl amine in benzene. At the end point the basic colour of the indicator appeared [17]. The basicity was measured by titrating 0.1g of solid suspended in 5ml of benzene with 0.1N solution of trichloroacetic acid in benzene using the same indicators. At the end point the colour of the indicator on the surface were the same as the colours which appeared by adsorption of respective indicators on the acid sites. The colour of the benzene solution was the basic colour at the end point, and it turned to the acidic colour by adding an excess of acid[18]. As the result of the titration lasting for 20 hours were the same as those for 2 hours, 2 hours was taken for each titration.

Since the dark coloured oxides mask the indicator colour on the surface the indicator colour change is not visible and the titration is not possible in the normal fashion. So the titration was carried out by adding a known amount of white solid material (alumina) in the titration mixture [19]. The end point of the titration was taken by noting the colour change on the white standard material. A convenient colour change was observed when 0.1g of the coloured oxide and 1g of the white

standard solid were taken. By comparing the acidity/ basicity of the white solid and the combination, the acidity/ basicity of the coloured oxide was determined.

### **Catalytic activity measurements**

#### **Reduction Reaction :**

0.5g of the catalyst after activation at a particular temperature was placed in a 50ml R.B flask equipped with a reflux condenser. 5 mmol of cyclohexanone, 20 ml of isopropanol were added. The contents were heated under reflux for 8 hours . The progress of the reaction was followed by measuring cyclohexanone concentration before and after the reaction. The concentration of cyclohexanone were found by absorbance measurements at the  $\lambda_{\max}$  of 287nm using a UV-VIS-Spectrophotometer[20].

#### **Oxidation Reaction:**

In an RB flask placed 0.5 g of the activated catalyst, 10cc of toluene solution of cyclohexanol (0.25 mmol ), Benzophenone (14.6 m mol) and n-decane (0.2 mmol) as an internal standard were placed. The contents were heated under gentle reflux at 110°C for two hours [21]. The amount of cyclohexanone formed was determined by a Perkin-Elmer 1022 Capillary Column GC with an FID detector.

#### **Esterification Reaction:**

The esterification was carried out in a RB flask attached with a reflux condenser in which the catalyst (1g), acetic acid (2 m mol), n- butanol (32 m mol) and 2 drops of n-decane as an internal standard were added. The contents of the flask

were maintained at 98 °C and stirred continuously on a magnetic stirrer for 4 hours [22]. The progress of the reaction was studied by gas chromatographic analysis on a Chemito 8510 GC with an FID detector. The progress of the reaction was followed by comparing the peak area of the product and the internal standard.

## References

1. D. S. Acker and W. R. Hertler : J. Am. Chem. Soc. 84, 3370 (1962)
2. L. F. Fiesser and M. Fiesser : "Reagents for organic Synthesis", John Wiley , New York p.125 (1967)
3. B. S. Furness, A. J. Hannaford, V. Rogers, P. W. G. Smith and A. R. Tatchell : "Vogel's text book of Practical organic chemistry", 4th edn, ELBS, London (1978), p.708.
4. B.S. Furness, A.J. Hannaford, V. Rogers, P.W.G. Smith and A. R. Tatchell, : "Vogel's text book of Practical organic chemistry", 4th edn, ELBS, London (1978), p.626
5. A.I.Vogel "A Text book of Practical organic chemistry" 3rd edn ELBS London p. 407 (1973)

6. A.I. Vogel "A Text book of Practical organic chemistry" 3rd edn ELBS  
London p. 177 (1973)
7. A.I.Vogel "A Text book of Practical organic chemistry" 3rd edn ELBS  
London p. 342 (1973)
8. A.I.Vogel "A Text book of Practical organic chemistry" 3rd edn ELBS London  
p. 886 (1973)
9. A.I.Vogel "A Text book of Practical organic chemistry" 3rd edn ELBS  
London  
p. 487 (1973)
10. A.I.Vogel "A Text book of Practical organic chemistry" 3rd edn ELBS  
London  
p. 185 (1973)
11. D. D. Perrin, W.L. F. Armarego and D.R. Perrin : "Purification of Laboratory  
Chemicals". 2nd edn., Pergamon Press, p.123 (1983)
12. A.I.Vogel "A Text book of practical organic chemistry" 3rd edn ELBS London  
p. 170 (1973)
13. D.D. Perrin, W.L.F. Armarego and D.R.Perrin : "Purification of Laboratory  
Chemicals". 2nd ed., Pergamon Press, p.77 (1983)
14. A.I.Vogel "A Text book of Practical organic chemistry" 3rd edn ELBS  
London p. 190 (1973)



15. Snell-Ettre Encyclopedia of Industrial Chemical Analysis., Inter Science Publications, p.510 Vol.17 (1973)
16. K. Esumi, K. Miyata, F.Waki and K.Meguro : Bull. Chem. Soc. Jpn. 59, 3363 (1986)
17. O. Johnson : J. Phy. Chem. 59, 827 (1955)
18. Tohr Yamanaka and K.Tanabe : J. Phy. Chem. 79, 2407 (1975)
19. K. Tanabe and Y. Watanabe : J. Res. Inst. Catalysis, Hokkaido Univ. 11, 65 (1963).
20. M. Shibagaki, K. Takahashi, H. Kuno and H. Matsushita : Bull.Chem. Soc. Jpn. 63,258 (1990)
21. H.Kuno,K.Takahashi, M.Shibagaki and H.Matsushita : Bull.Chem. Soc.Jpn.,63,1943 (1990).
22. K.Takahashi, M.Shibagaki and H.Matsushita : Bull.Chem. Soc.Jpn.,63,2353 (1989).

**RESULTS & DISCUSSION**  
**CHAPTER 3**

## INTRODUCTION

The thermochemistry of rare earth metal doped Zirconia indicates that the addition of rare earth metal increases the thermal stability of the host oxide and stabilised it in a high surface area form [1]. The catalytic property of metal oxides depend on many factors. Attempts are now being done to establish valid correlations between the catalytic activity and other surface properties

A detailed review of the literature revealed that no attempts were made to study the surface electron donating property and catalytic activity of mixed oxides of zirconium with rare earth metals. Zirconium is a transition element and zirconia is unique in exhibiting acid, base, oxidising and reducing properties. Further zirconia based materials are now attracting much attention because of their promising potential as catalysts for use in combustion and hydrogenation [2], Piezo electric ceramics and thermal barriers.

In this work we have attempted to study the surface properties of the mixed oxides of zirconia with the first three lanthanides. Based on BET surface area, chemisorption, temperature programmed reduction (TPR) and oxidation (TPO), X-ray diffraction (XRD) and X-ray photoemission (XPS) characterisation rare earth oxides have been classified [3] into three classes according to their ability to create anion vacancies

1. Oxides of the types  $Re_2O_3$  which are unreducible,

2.  $\text{CeO}_2$  where anion vacancy can be created extrinsically by the reduction process and
3.  $\text{Pr}_6\text{O}_{11}$  and  $\text{Tb}_4\text{O}_7$  where anion vacancy exists due to the non stoichiometric nature of these oxides

$\text{CeO}_2$  have Cerium in  $+4$  oxidation state.  $\text{Pr}_6\text{O}_{11}$  contains Praseodymium in  $+3$  and  $+4$  oxidation states in the ratio 2:4 and  $\text{Nd}_2\text{O}_3$  is the normal sesquioxide of neodymium with the oxidation state of  $+3$ .  $\text{CeO}_2$  and  $\text{Pr}_6\text{O}_{11}$  are nonstoichiometric oxides.

The studies made are (1) The strength and distribution of electron donor sites on the oxide surface. (2) The strength and distribution of acid and base sites on the oxide surface (3) The catalytic activity of the oxide surface (4) Their surface areas and the variation in the above properties with (a) Activation temperature (b) Composition of the mixed oxides and (c) The rare earth element present.

### **3.1.1. Adsorption studies**

The strength and distribution of electron donor sites on the oxide surface were studied by adsorption of various electron acceptors with a range of electron affinities. The electron donor properties of some of the oxides as a function of the basic nature of the medium were reported by many authors [4]. It was found that the amount of electron acceptor adsorbed decreases with the increase in the basicity of the medium, due to the competition between the solid base and the solvent base for electron acceptor interaction. In this study the electron acceptor adsorption on the oxide surfaces were done from acetonitrile, which is a very weak base [5].

On the surface of the oxides there will be a distribution of electron donor sites of various strength. The electron donor strength of a metal oxide is the limiting electron affinity value of the electron acceptor for which free anion radical formation is not expected on the oxide surface. The distribution or the amount of electron donor sites of a particular strength is estimated by the amount of electron acceptor adsorbed on the oxide surface. To study the strength and distribution of electron donor sites on the catalysts, electron acceptors of various electron affinity were used. They are listed in Table 1 with their respective electron affinities.

Table 1 Electron Acceptors used

Electron Acceptor	Electron Affinity
7,7,8,8 Tetracyanoquinodimethane (TCNQ)	2.84 eV
2,3,5,6 Tetrachloro-p-benzoquinone (Chloranil)	2.40 eV
1,4 Dinitrobenzene (PDNB)	1.77 eV
1,3 Dinitrobenzene (MDNB)	1.26eV

For all the oxides studied the amount of PDNB and MDNB adsorbed was so negligible that the amount adsorbed could not be estimated by spectrophotometric method. For most of the oxides chloranil and TCNQ were adsorbed on the oxide surface. The adsorption isotherms are of Langmuir type, suggesting a chemical monolayer adsorption. It is verified by the linear plot of

$C_{eq}/C_{ad}$  against  $C_{eq}$ , where  $C_{eq}$  is the equilibrium concentration in mole  $dm^{-3}$  and  $C_{ad}$  is the amount adsorbed in mole per square metre (Figure 3.1). The limiting amount of electron acceptors adsorbed, which corresponds to monolayer coverage were determined from the Langmuir plots (Figures 3.6 to 3.11).

When the electron acceptors were adsorbed on the oxide surface, the catalyst surface acquired a characteristic colouration owing to the interaction between electron acceptor adsorbed and the oxide surface [6]. Chloranil gave light to dark pink colour to the oxides and TCNQ gave dark green to bluish green colour to the oxides, the colour intensifies with increase in zirconium content.

The nature of interaction of electron acceptor with the oxide surface was studied by reflectance spectra of the solid after adsorption. The spectra of adsorbed TCNQ on solid oxide gave bands below 400 nm and near 600 nm. The first one corresponds to physically adsorbed state of neutral TCNQ which has an absorption band at 395 nm [7]. The band near 600 nm corresponds to dimeric TCNQ radical which absorbs at 643 nm [8]. In the case of chloranil the broad band extending up to 700 nm corresponds to chloranil anion radical [9]. In the case of oxides under study these assignments do not hold completely because these oxides have characteristic band in the same region.

The nature of interaction of the electron acceptor with the oxide surface was also investigated by esr spectra. The esr spectra indicated the presence of radical species. The samples after TCNQ adsorption gave unresolved esr spectra with a g

value of 2.003, due to the hindered rotational freedom of the adsorbed species which obscures the hyperfine structure of the spectrum. These spectra have been identified as being those of TCNQ anion radicals [10]. The coloured samples obtained by the adsorption chloranil gave an unresolved esr spectra with a g value of 2.011 [11]. The radical concentrations of TCNQ and chloranil adsorbed were calculated and plotted against equilibrium concentrations. The isotherms obtained were also of Langmuir type (Figures 3.4 & 3.5) and of the same shape as the plot of the amount of electron acceptor adsorbed.

The limiting amount of radical concentration of TCNQ on the surface is a measure of the total number of electron donor sites on the oxide surface. The amount adsorbed increases with increase in electron affinity of the electron acceptor. The strong electron acceptors like TCNQ are capable of forming anion radicals even from weak donor sites whereas weak acceptor like MDNB are capable of forming anion radicals only at strong donor sites. Hence the limiting radical concentration of the weak acceptor is a measure of the number of strong donor sites on the surface and that for a strong acceptor is the sum of all weak and strong donor sites on the surface. It is found that the limiting radical concentration and the limiting amount adsorbed decreases with decrease in the electron affinity of the acceptor.

### 3.1.2 Acid- Base Properties

Another property being studied is the surface acidity and basicity of the catalysts. The strength and distribution of acidic and basic sites on the oxide surface were studied using a series of Hammett indicators [12]. They are given in Table 2.

Table 2 Hammett Indicators Used

Hammett Indicator	pK <sub>a</sub>	Acid Colour	Base Colour
Crystal violet	0.8	Yellow	Blue
Dimethyl Yellow	3.3	Red	Yellow
Methyl Red	4.8	Red	Yellow
Neutral red	6.8	Red	Yellow
Bromo Thymol Blue	7.2	Yellow	Blue
4-Nitroaniline	18.4	Yellow	colourless

The oxides under study responded only to Dimethyl yellow, Methyl red and Bromothymol blue. Acidity at various acid strengths of the oxide was measured by titrating solid suspended in benzene with 0.1N n-butyl amine in benzene. Basicity was measured by titrating solid suspended in benzene with 0.1N trichloroacetic acid in benzene, using the same set of indicators as for acidity measurement. By this procedures we measured acid / base strength distribution on a common scale [13]. The acid-base strength distribution curves intersect at a point on the abscissa where acidity



= basicity = 0 [14]. The point of intersection defined as  $H_{o,max}$  value was determined for the oxides and are reported.  $H_{o,max}$  value can be regarded as a practical parameter to represent the acid-base properties of solids. A solid with a large  $H_{o,max}$  value has strong basic sites and weak acid sites. On the other hand, a solid with a small  $H_{o,max}$  value has strong acid sites and weak basic sites.

### 3.1.3. Catalytic Activity Of Oxides

The catalytic activity of the oxides were studied for three reactions *viz.*

1. Reduction of cyclohexanone in isopropanol.
2. Oxidation of cyclohexanol with benzophenone.
3. Esterification of acetic acid with butanol .

All the reactions showed a first order dependence on the concentrations of the reactants (underlined) under the experimental conditions adopted. For reduction reaction the progress of the reaction was followed by noting the change in concentrations of cyclohexanone (the absorbance at 283nm using a UV visible spectrophotometer) . The oxidation and esterification reactions are followed by a gas chromatograph using n-decane as an internal standard. The rate constants are calculated using the first order rate equation. Catalytic activity is reported as the first order rate constants per unit surface area of the catalyst. The specific surface area of the oxides were determined by BET method using Carlo Erba Strumentazion Sorptomatic series 1800.

**ACID- BASE, SURFACE ELECTRON DONATING &  
CATALYTIC PROPERTIES OF CERIUM -ZIRCONIUM  
MIXED OXIDES**

The  $\text{CeO}_2$  is found to have a normal Rutile structure in which the  $\text{Ce}^{4+}$  ion is six coordinated with no paramagnetic susceptibility [15]. In this chapter Catalytic activity, Electron donor Properties, and surface acid-base properties of Cerium-Zirconium mixed oxides were reported at three activation temperatures ( $300^\circ\text{C}$ ,  $500^\circ\text{C}$  and  $800^\circ\text{C}$ ). The effect of activation temperature and composition on acid-base properties, surface electron donor properties and surface areas were also studied. The data were correlated with their catalytic activities. The mixed oxides with various compositions, *Viz.* 20, 40, 60 and 80% of the rare earth oxide were studied. For comparison pure oxides were also incorporated in the study. The mixed oxides were prepared through the hydroxide route. The mixed oxides with various compositions, *Viz.* 20, 40, 60 and 80 % (abbreviated as 20 Ce, 40 Ce, 60 Ce and 80 Ce) of the rare earth oxide were prepared. Pure oxides were also prepared in the same fashion.

### 3.2.1 Surface Areas

$\text{CeO}_2$  and  $\text{ZrO}_2$  have comparable surface areas and their surface areas decrease with increase in activation temperature (Table 3.1, Figures 3.2 & 3.3). The rate of decrease also appears to be same for the two oxides. For the mixed oxides the surface areas are less than the pure components at the activation temperatures of  $300^\circ\text{C}$  and  $500^\circ\text{C}$ . At  $300^\circ\text{C}$  the decrease is more for the cerium rich oxides (60 Ce and 80 Ce). At  $500^\circ\text{C}$  the decrease in surface areas is more for zirconium rich samples (20 Ce and 40 Ce). At  $800^\circ\text{C}$  a different trend is observed, the surface areas of mixed

Table 3.1 Surface Areas of Cerium-Zirconium Mixed Oxides Activated at Different Temperatures

Weight % of Rare Earth oxide	Surface Areas Activated at		
	300°C	500°C	800°C
0	200.3	61.496	29.75
20	193.29	30.72	46.34
40	173.32	11.36	45.15
60	124.30	45.92	33.39
80	99.44	66.54	32.90
100	200.35	66.42	29.00

Table 3. 2 Limiting Amounts of Electron Acceptors  
 Adsorbed on Cerium -Zirconium Mixed Oxides  
 Activated at Different Temperatures

Weight %of CeO <sub>2</sub>	Activat. Temp. °C	Limiting amount Adsorbed 10 <sup>-6</sup> mol /sq.m	
		TCNQ	Chloranil
0	300	0.9656	0.6933
20	300	0.6833	0.4861
40	300	0.4964	0.2603
60	300	0.3133	0.2454
80	300	1.4137	0.8401
100	300	1.1910	0.5201
0	500	2.0814	1.0613
20	500	2.4141	0.8984
40	500	3.0810	0.5282
60	500	0.2450	0
80	500	1.7399	0.8452
100	500	0.3372	0.2050
0	800	2.2064	0.6835
20	800	0.5243	0
40	800	0.2182	0.0974
60	800	0.4306	0.3078
80	800	1.0358	0
100	800	0.2323	0.0301

oxides are found to have higher values than the pure component oxides. The increment is very small and is more for the zirconium rich samples. In general surface areas are found to be improved by mixing of the oxides only at higher temperatures even though the increment is small.

### **3.2.2. Electron Donor properties.**

The electron donor properties of Ce - Zr mixed oxides depend both on activation temperature and composition of the mixed oxides as well as on the electron affinity of the electron acceptor (See Table 3.2, Figures 3.12 to 3.15). In the case of pure  $ZrO_2$ , the limiting amount of TCNQ adsorbed increase with activation temperature and the rate of increase is more in between  $300^\circ C$  to  $500^\circ C$  than between  $500^\circ C$  to  $800^\circ C$ . In the case of ceria the trend is just reversed. The limiting amount decreased with increase in activation temperature. The decrease is more steep between 300 to  $500^\circ C$  than between 500 to  $800^\circ C$ . In the case of 60 Ce the limiting amount first decreased from 300 to  $500^\circ C$  and then increased, however, the increase is very small. For all other mixed oxides (20 Ce, 40 Ce, 80 Ce), the limiting amount is maximum at  $500^\circ C$ . In the case of 20 Ce and 40 Ce they have high electron donor properties than the pure component oxides at  $500^\circ C$ . For 80 Ce the limiting amount of TCNQ adsorbed is large at  $300^\circ C$  and is greater than both the pure oxides. At  $800^\circ C$  pure  $ZrO_2$  is having the highest value for limiting amount of TCNQ adsorbed,  $CeO_2$  having the lowest value and the mixed oxides having intermediate values.

For chloranil adsorption all the limiting amounts are found to be less than that for TCNQ. The limiting amounts adsorbed on  $ZrO_2$  increased first from 300 to 500°C and then decreased. In the case of ceria the limiting amount adsorbed gradually decreased with increase in activation temperature. For 80 Ce the limiting amount adsorbed at 300°C is greater than the pure component oxides. All the remaining compositions have lower values than the component oxides, 60 Ce having the lowest value. At 500°C  $ZrO_2$  is having the highest value for limiting amount adsorbed. 80 Ce, 40 Ce and 20 Ce have intermediate values between the component oxides. For 60 Ce it does not give chloranil adsorption. At 800°C, 20 Ce and 80 Ce do not give chloranil adsorption, 40 Ce and 60 Ce having values in between those of component oxides. For 20 Ce and 40 Ce the limiting amount adsorbed is maximum at 500°C. For 60 Ce the maximum value is at 800°C. For 80 Ce the value does not differ much from 300 to 500°C. At 800°C it does not give chloranil adsorption.

Two possible electron sources exist on the metal oxide surface responsible for electron transfer. One of these has electrons trapped in intrinsic defect and other has hydroxyl ions [16]. At lower temperatures electron donor sites are associated with unsolvated hydroxyl ions and at higher activation temperatures an electron defect centre is produced. It is reported that free electron defect site on metal oxide surface is created at activation temperatures above 500°C. It has been suggested that at higher activation temperatures the donor site consists of a co-ordinatively unsaturated doubly charged oxygen ion ( $O_{cus}^{2-}$ ) associated with a nearby  $OH^-$  group

and the concentration of this donor site is related to the base strength of the surface [17]. The more basic the surface, the higher is the number of oxygen ions which can transfer the electron to the acceptor molecule.

### 3.2.3 Acid - Base Properties

ZrO<sub>2</sub> and CeO<sub>2</sub> have acidic and basic sites on the surface (See Table 3.3, Figures 3.16 to 3.30). For pure ZrO<sub>2</sub> at  $H_0 \geq 3.3$ , the base amount increased from 300°C to 500°C and then decreased at the activation temperature of 800°C. For pure CeO<sub>2</sub> at  $H_0 \geq 3.3$ , basicity is maximum for sample activated at 800°C. At  $H_0 \geq 3.3$  all mixed oxides at all activation temperatures have basicity less than ZrO<sub>2</sub>. It is found that acidity is being generated on mixing CeO<sub>2</sub> and ZrO<sub>2</sub>. Acidity cannot be expressed as the sum of the acidities of the component oxides. At  $H_0 \geq 3.3$  acidity generated is maximum at an activation temperature of 800°C.

At the acid strength of  $H_0 \geq 4.8$ , ZrO<sub>2</sub> is more basic than CeO<sub>2</sub>. 20 Ce is found to have more basic sites at activation temperatures of 300°C and 800°C. Acidity is generated for all mixed oxides at all activation temperatures. The basicity is found to depend on activation temperature, basicity being decreased with increase in activation temperature. Samples activated at 800°C are the most acidic for 40 Ce and 60 Ce. For 20 Ce and 80 Ce, they have maximum acidity at 500°C.



Table 3.3 Acid-Base strength Distribution on Cerium-Zirconium Mixed Oxides  
Activated at different Temperatures

Weight % of CeO <sub>2</sub>	Activat. Temp.	Basicity H <sub>0</sub> ≥3.3	Acidity H <sub>0</sub> ≤3.3	Basicity H <sub>0</sub> ≥4.8	Acidity H <sub>0</sub> ≤4.8	Basicit H <sub>0</sub> ≥7.2	Acidity H <sub>0</sub> ≤7.2	H <sub>0,max</sub>
	°C	10 <sup>-3</sup> m mol m <sup>-2</sup>						
0	300	0.966	-	0.236	-	-	0.168	5.6
20	300	0.352	-	0.305	-	-	0.538	5.9
40	300	-	0.715	-	0.139	-	0.030	4.5
60	300	0.105	-	-	0.965	-	0.129	3.8
80	300	0.191	-	0.064	-	-	0.016	6.5
100	300	0.549	-	0.125	-	-	0.374	5.3
0	500	2.738	-	0.107	-	-	2.745	4.9
20	500	1.400	-	-	4.492	-	9.993	3.6
40	500	2.113	-	-	8.363	-	14.080	3.55
60	500	0.740	-	-	1.851	-	5.226	3.7
80	500	0.346	-	-	0.842	-	0.255	3.7
100	500	0.557	-	0.271	-	-	5.063	5.1
0	800	2.450	-	0.400	-	-	3.079	5.0
20	800	2.395	-	7.552	-	-	9.278	3.65
40	800	-	5.537	-	16.830	-	17.500	2.7
60	800	-	7.187	-	20.360	-	26.502	2.6
80	800	1.945	-	0	-	0.6686	-	4.8
100	800	1.966	-	0.586	-	-	2.069	5.4

At an acid strength of  $H_0 \leq 7.2$ ,  $CeO_2$  and  $ZrO_2$  are both acidic and the amount of acid sites depend on the activation temperature. For  $ZrO_2$ , the acid amount increased with activation temperature and has the maximum value at  $800^\circ C$ . In the case of  $CeO_2$  the acid amount first increased with activation temperature and then decreased. It has the maximum value at  $500^\circ C$ . All the mixed oxides except 80 Ce show acidity, by activation at  $800^\circ C$ . The acid amount is maximum in the case of 60 Ce followed by 40 Ce at  $800^\circ C$ . At  $500^\circ C$ , 40 Ce is having the highest acid amount. At  $300^\circ C$ , acidity is generated only to a small extent.

As the covalency (charge to radius ratio) of the oxide is greater, the oxide will be more acidic [18]. Ce is having +4 charge and the ionic radius will be less than the trivalent ions and so the covalency of the metal ion in the oxide will be higher and  $CeO_2$  is found to be more acidic than the other two rare earth oxides.

According to Tanabe's hypothesis [19], acidity generation is by an excess of a positive or negative charge in the model structure of a binary oxide. The model structure is pictured according to the following two postulates.

1. The coordination number of the positive element of a metal oxide,  $C_1$ , and that of the second metal oxide,  $C_2$ , are maintained even when mixed.
2. The coordination number of the negative element (oxygen) of the major component oxide is retained for all oxygens in the binary oxide.

The coordination numbers of Ce is six and oxygen is three in pure CeO<sub>2</sub>. The coordination numbers of Zr is eight and oxygen is four in pure ZrO<sub>2</sub>. When the two oxides are mixed with ZrO<sub>2</sub> as the major component, coordination numbers of the cations will remain as such but that of the anion will be 4 as by postulate 1 & 2. In its structure the positive charge of the Ce ( the added cation ) will be distributed along six bonds ( $+4/6$  for each bond). The negative charge of the oxygen will be distributed along four bonds ( $-2/4$  for each bond). The charge imbalance produced at one Ce-O bond is ( $+4/6 - 2/4 = +1/6$ )  $+1/6$ , and the total charge difference produced by one Ce cation is ( $6 \times +1/6$ )  $+1$ . In this case Lewis acidity is assumed to appear upon the presence of an excess positive charge.

When the two oxides are mixed with CeO<sub>2</sub> as the major component, the coordination number of cation will remain as such and that of the anion will be three (as in CeO<sub>2</sub>). In its structure the positive charge of the Zr ( the added cation) will be distributed along eight bonds ( $+4/8$  for each bond). The negative charge of the oxygen will be distributed along three bonds ( $-2/3$  for each bond ). The charge imbalance produced at one Zr-O bond is ( $+4/8 - 2/3 = -1/6$ )  $-1/6$ , and the total charge difference produced by one Zr cation is ( $8 \times -1/6$ )  $-8/6$ . In this case Bronsted acidity is assumed to appear, because eight protons are considered to associate with six oxygens to keep electrical neutrality. In all cases of Ce- Zr mixed oxides acidity is generated and it agrees well with our studies.

### 3.2.4 Catalytic activity

(See Table 3.4, Figures 3.31 to 3.35)

#### Reduction reaction

CeO<sub>2</sub> activated at 500°C and 800°C does not show catalytic activity. It exhibits maximum activity for samples activated at 300°C. Pure zirconia also show high catalytic activity at an activation temperature of 300°C. The reduction activity for zirconia first increased with activation temperature and then decreased to zero value. At the activation temperature of 300°C all the mixed oxide have reduction activity less than that of the component oxide. Among the mixed oxides 40 Ce is having the largest value for rate constant. For samples activated at 500°C, the mixed oxides exhibit more activity than the pure component oxides, 40 Ce exhibiting the highest value. All the samples activated at 800°C do not have any reduction activity. For all the mixed oxides, highest activity is exhibited when the samples are preheated at 500°C. Activation at 500°C generates many active sites for this particular reaction for the Ce-Zr mixed oxides. But all of them are found to be deactivated when the sample is preheated at 800°C.

The active sites for the reduction reaction is still uncertain. The proposed mechanism involves the following steps (Scheme 1) [20].

1. The attachment of the isopropanol (hydrogen source), as an alkoxide on an acid site, with the proton abstracted on a base site on the catalyst surface (both

acid and base sites involved in it) .

2. A hydride ion abstraction by the carbonyl carbon
3. Subsequent bond rearrangement
4. Desorption of the alkoxide formed as the alcohol by accepting a proton either from  
a Bronsted acid site or from the medium.

It is an acid- base bifunctional catalysis. The activity depends on the amount of acid / base sites. If they are very small in number, the availability of the particular type of site determine the rate of the reaction. For a sufficiently basic oxide, the rate of reaction may depend on the amount of acid sites coexisting with the basic sites and vice-versa.

#### Oxidation reaction

Oxidation reaction is 100 times faster than reduction reaction catalysed by these oxides. Pure zirconia shows the highest activity when it is activated at 300°C. The activity increases with activation temperature. The catalytic activity for ceria is less than that for zirconia. All the mixed oxides have activities intermediate between those of the component oxides. All samples activated at 500°C have more oxidation activity than those activated at 300°C. 40 Ce is having the highest value for catalytic activity at 500°C. On going from 500°C to 800°C, the oxidation activity decreased in the case of 20 Ce, 40 Ce and 60 Ce. But in the case of  $ZrO_2$ , 80Ce and  $CeO_2$ , the

Table 3. 4  
Catalytic activity of Cerium-Zirconium mixed oxides Activated at Different  
Temperatures

Wt % of CeO <sub>2</sub>	Act. Temp ° C	Reduction of Cyclohexanone		Oxidation of Cyclohexanol		Esterification Reaction	
		% conver sion	Rate Constant (10 <sup>-7</sup> s <sup>-1</sup> m <sup>-2</sup> )	% convers ion	Rate Constant (10 <sup>-5</sup> s <sup>-1</sup> m <sup>-2</sup> )	% conve rsion	Rate Constant (10 <sup>-7</sup> s <sup>-1</sup> m <sup>-2</sup> )
0	300	25.19	1.006	95.97	0.445		
20	300	5.75	0.213	88.20	0.307		
40	300	19.50	0.869	82.01	0.275		
60	300	2.10	0.118	84.58	0.418		
80	300	1.80	0.127	84.95	0.529		
100	300	25.23	1.065	68.75	0.161		
0	500	11.05	1.320	87.24	0.930	10.53	2.513
20	500	6.26	1.462	84.94	1.712	30.99	16.773
40	500	12.96	8.487	84.63	4.580	26.46	37.583
60	500	2.59	0.397	83.08	1.075	38.86	14.884
80	500	8.42	0.918	77.92	0.631	55.19	16.759
100	500	0	0	60.20	0.385	0	0
0	800	0	0	83.90	1.706		
20	800	0	0	89.29	1.339		
40	800	0	0	77.43	0.916		
60	800	0	0	41.02	0.439		
80	800	0	0	68.05	0.963		
100	800	0	0	58.22	0.836		

oxidation activity increased at 800°C. The oxidation activity is found to depend on activation temperature and composition of the oxides.

Several types of mechanisms are proposed for oxidation reactions.

a. The Mars-van-Krevelen [21] mechanism in which the addition of a lattice oxygen is involved.

In heterogeneous oxidation reactions in which catalytically active oxides are used, lattice oxygen is used by the reaction. Lattice oxygen then appears in the oxidation products, while oxygen vacancy in the catalyst is replenished by the gaseous molecular oxygen.

Here the activity and selectivity of the oxidation reaction depend on

the metal-oxygen bond strength (the valency of the metal ion),

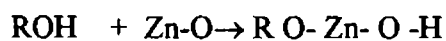
the co-ordination of the metal in the lattice,

the stability and the properties of the defects, and

the morphology of the material.

b. Oxidation takes place by dehydrogenation.

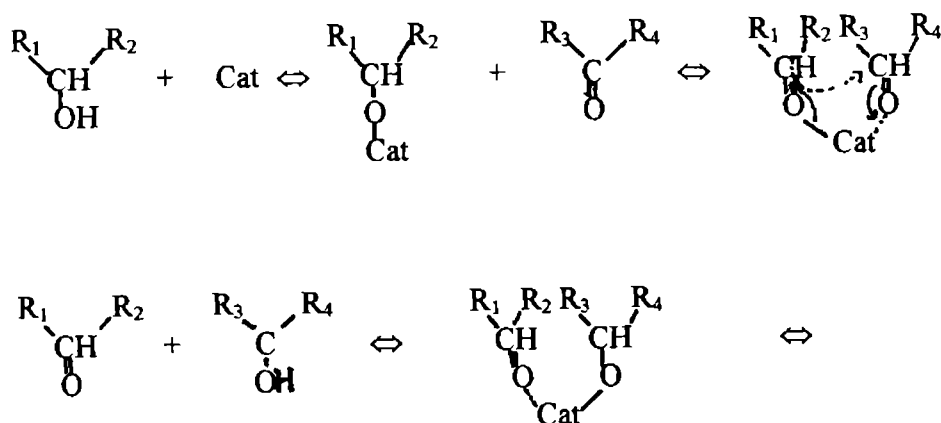
Alcohols are adsorbed by heterolytic dissociation at room temperature on a dehydroxylated surface with a proton going to a surface lattice oxygen and the alkoxide to a surface cation.



For example methoxide has been detected when methanol is adsorbed on ZnO[22] and MoO<sub>3</sub> [23]. Similarly ethoxide is found to be formed on MoO<sub>3</sub> [24] and ZnO [25]. 1-Propoxide is formed from 1-propanol [25] and 2-Propoxide is formed from 2-propanol [26]. 2-propoxide is oxidised to a surface enolate which eventually is desorbed as acetone.

The dehydrogenation of the alcohol hydroxyl group may proceed (Scheme 1) on hydrogen accepting sites with base character oxygen atoms from the oxide lattice. The dehydrogenation of the ring seems to be related rather to the transition metal. Most of the metal oxides have acid sites and hydrogen accepting sites, not only the metal ions but also the basic oxygen atoms have a hydrogen accepting ability.

Scheme1.





## Esterification Reaction

Pure  $\text{CeO}_2$  does not catalyse the esterification reaction of acetic acid with n-butanol. But  $\text{ZrO}_2$  catalyses the esterification reaction to a certain extent. The mixed oxides show very high activity for the esterification reaction, 40Ce exhibiting the highest value. The mixing of  $\text{CeO}_2$  and  $\text{ZrO}_2$  generates a number of sites which are active in the esterification reaction.

Industrially important esterifications are the reactions of alcohol with saturated and unsaturated aliphatic carboxylic acids, eg: acetic acid, fatty acids and acrylic acid and aromatic dicarboxylic acids such as terephthalic acid. These reactions may be carried out in both liquid and vapour phases. Esterification reactions are usually limited by equilibrium particularly in liquid phase. Continuous removal of water produced and/or operation with an excess of one of the reactants are necessary to obtain higher yields of ester. Vapour phase esterification is favoured from this stand point, and numerous studies have been directed toward the use of solid acid catalyst. Typical catalyst for homogeneous liquid phase reaction are mineral acids and metal alkoxide.

Ion exchange resins are representative solid catalysts. Several esterification reactions using fluorinated ion exchange resins such as Nafion have also been attempted, since they have higher thermal and chemical stability. Various inorganic solid acids such as Silica, alumina, Zeolites, layered clays,  $(\text{SO}_4^{2-})$  treated

TiO<sub>2</sub>, Niobic acid and heteropoly acids have also been applied to vapour phase and liquid phase esterifications with good results [27].

Side reactions are usually dehydration of alcohol to form olefin and ethers and some times polymerisation. Dissolution of catalytic active sites on the surface and thermal stability, which shorten the life of catalyst are other important consideration in the use of solid acids. The reaction of acetic acid and n-butanol in the liquid phase catalysed by HZSM-5 proceeds according to a rate equation which is of the first order with respect to acetic acid and of the zeroth order with respect to n-butanol [28, 29].

A plausible mechanism in which Bronsted acid sites are involved in the reaction is as follows.



Esterification can also be catalysed by Lewis acid sites (Metal ions in low coordination) [30]. In this case esterification proceeds by combination of strongly adsorbed carboxylate ion and alkoxide ion on adjacent Lewis acid sites. This type of mechanism [31] is more prominent in vapour phase esterification.

Figure 3.1  
Linear form of Langmuir adsorption isotherm  
of chloranil on  $\text{CeO}_2$  activated at  $300^\circ\text{C}$

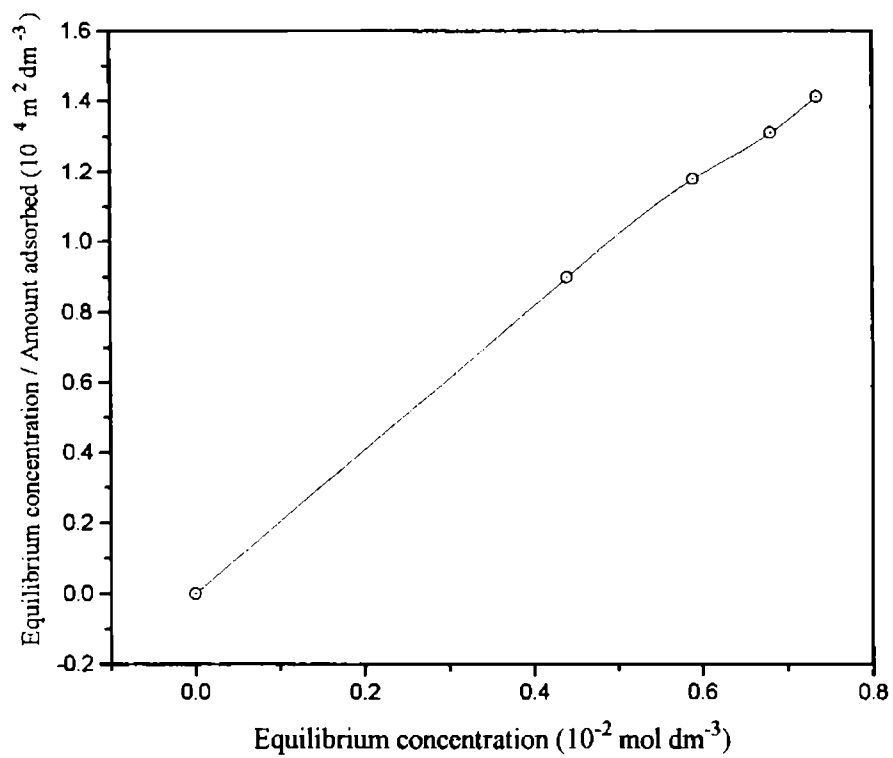


Figure 3.2  
Surface areas of Ce-Zr mixed  
Oxides as a function of  
activation temperature

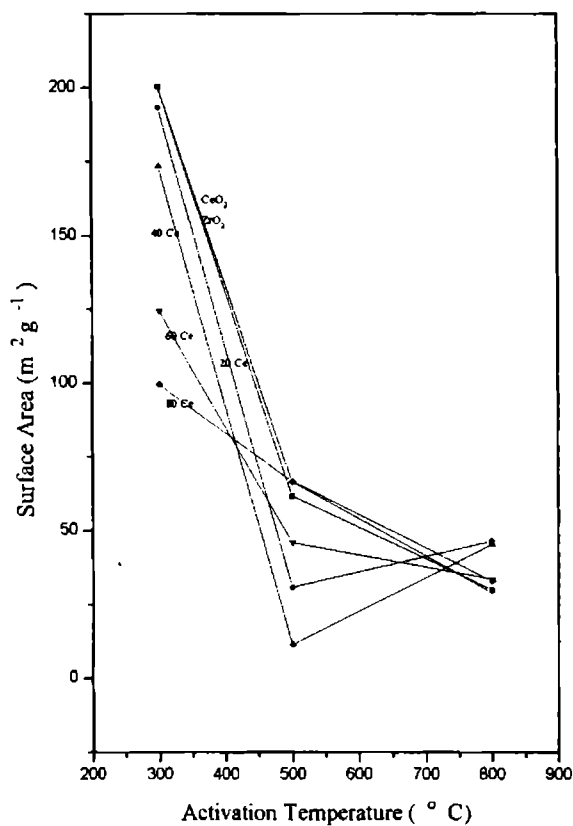


Figure 3.3  
Surface areas of Ce-Zr Mixed Oxides  
at Different activation temperatures  
as a function of composition.

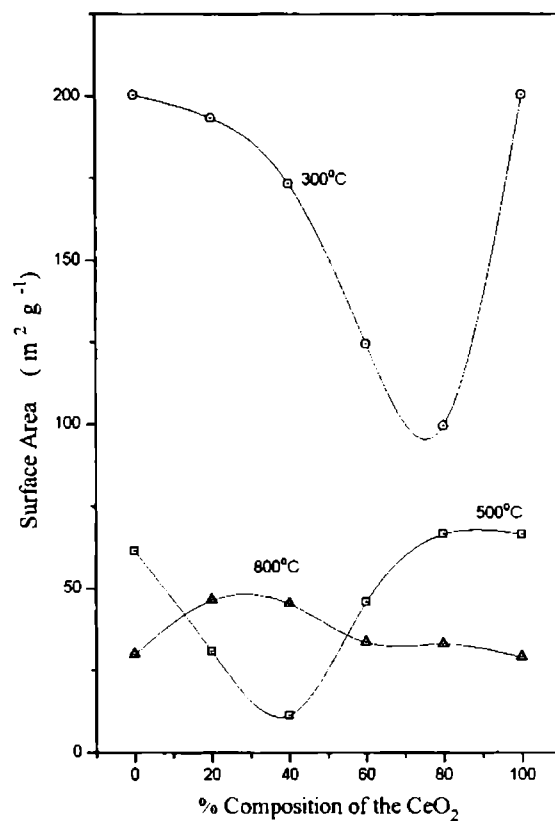


Figure 3.4  
Plot of radical concentration of TCNQ on  
CeO<sub>2</sub> activated at 300° C

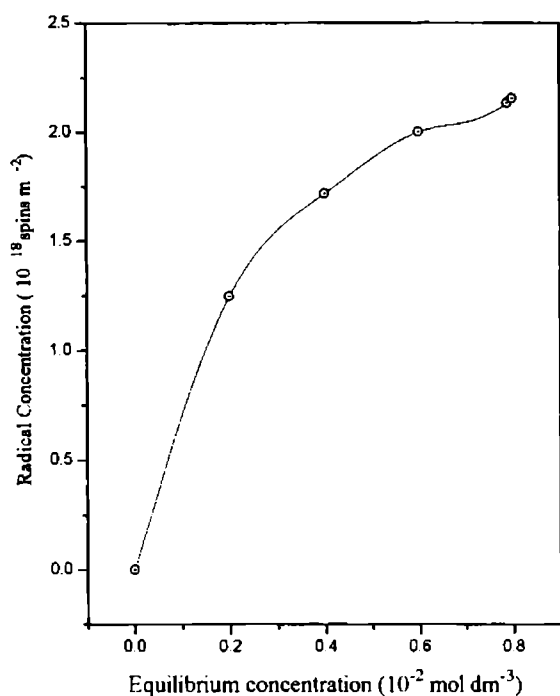


Figure 3.5  
Plot of radical concentration of chloranil  
on CeO<sub>2</sub> activated at 300° C

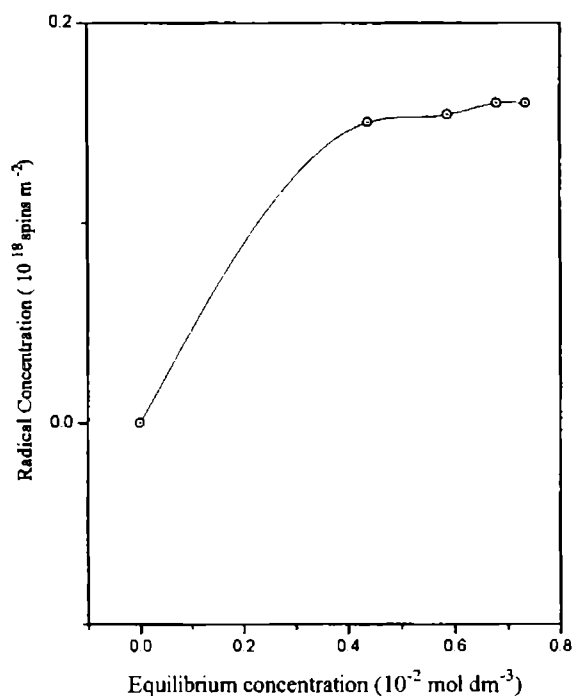


Figure 3.6  
Adsorption isotherms of electron acceptors  
on ZrO<sub>2</sub> activated at different temperature

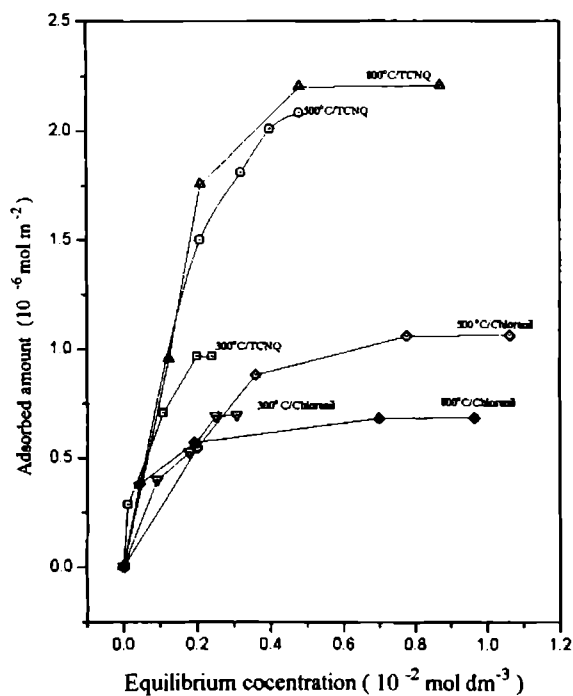


Figure 3.7  
Adsorption isotherms of electron acceptors  
on CeO<sub>2</sub> at different activation temperatures

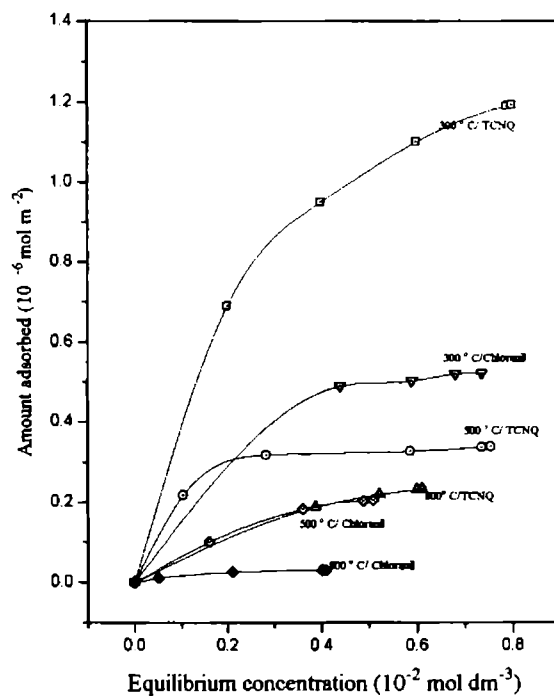


Figure 3.8

Adsorption isotherms of electron acceptors on 20 Ce activated at different temperatures

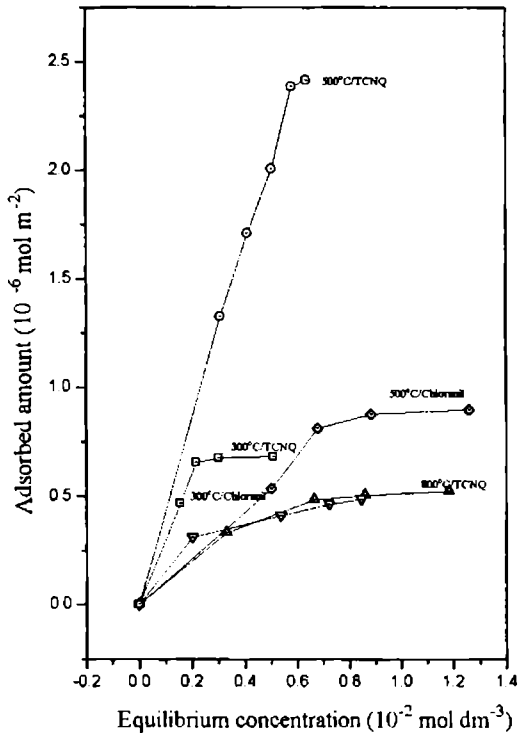


Figure 3.10

Adsorption isotherms of electron acceptors on 60 Ce activated at different temperatures

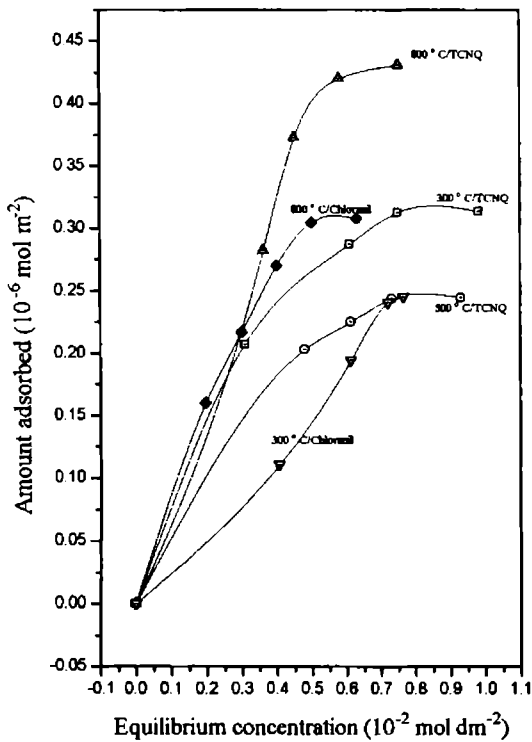


Figure 3.9

Adsorption isotherms of electron acceptors on 40 Ce activated at different temperatures

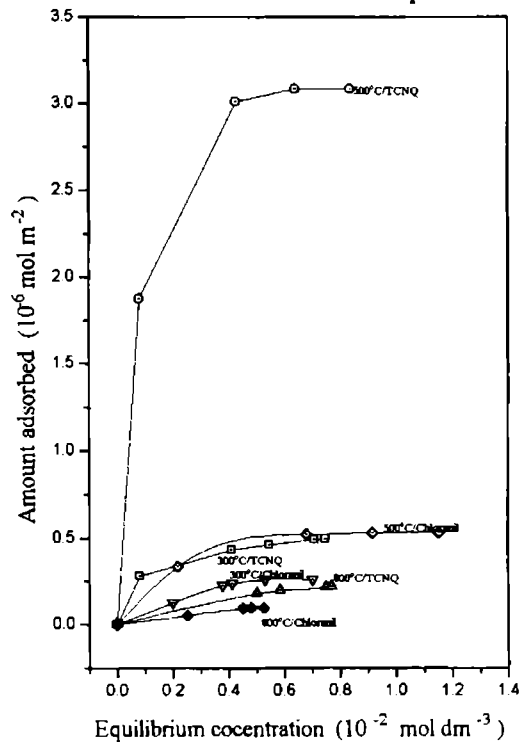


Figure 3.11

Adsorption isotherms of electron acceptors on 80 Ce activated at different temperatures

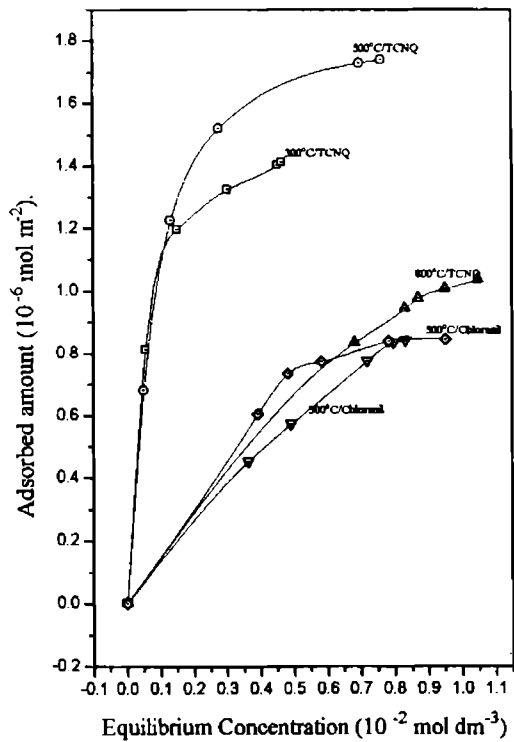


Figure 3.12  
Limiting Amount of TCNQ adsorbed  
on Ce -Zr mixed oxides as a  
function of Composition

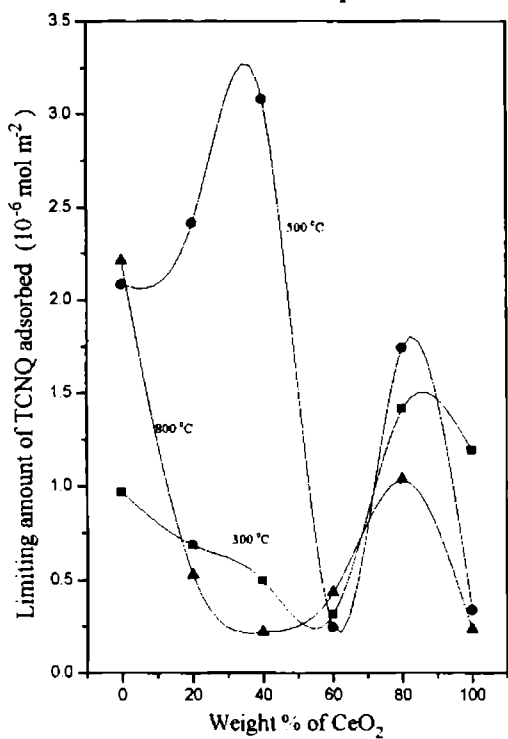


Figure 3.14  
Limiting Amount of TCNQ adsorbed  
on Ce -Zr mixed oxides as a  
function of activation temperature

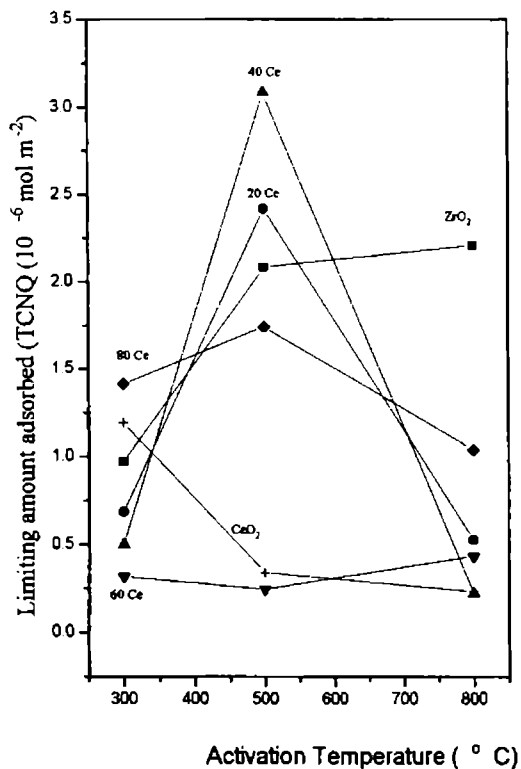


Figure 3.13  
Limiting Amount of Chloranil adsorbed  
on Ce -Zr mixed oxides as  
a function of Composition

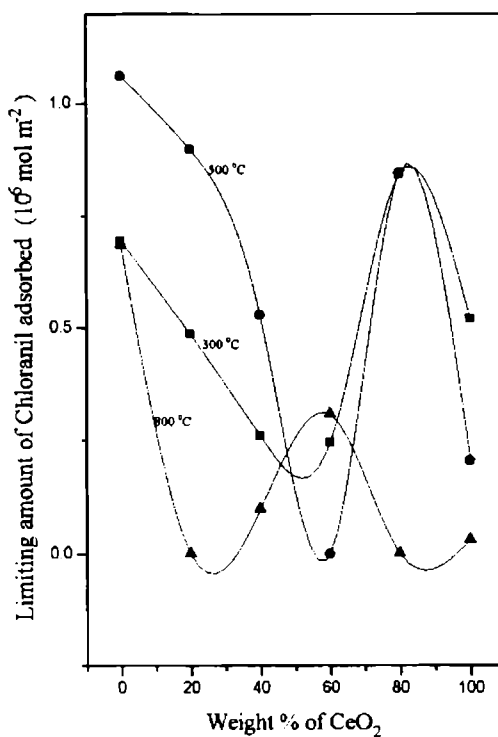


Figure 3.15  
Limiting Amount of Chloranil adsorbed  
on Ce -Zr mixed oxides as a  
function of activation temperature

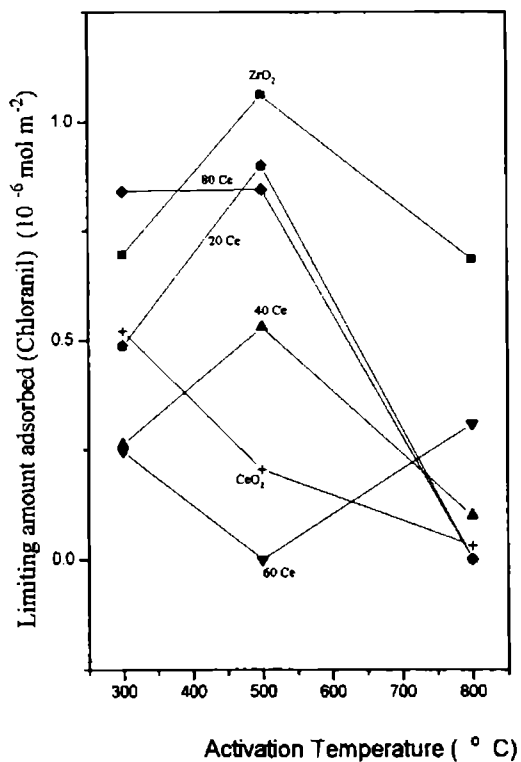


Figure 3.16  
Acid-Base Strength distribution curves on  
 $ZrO_2$  at different activation temperatures

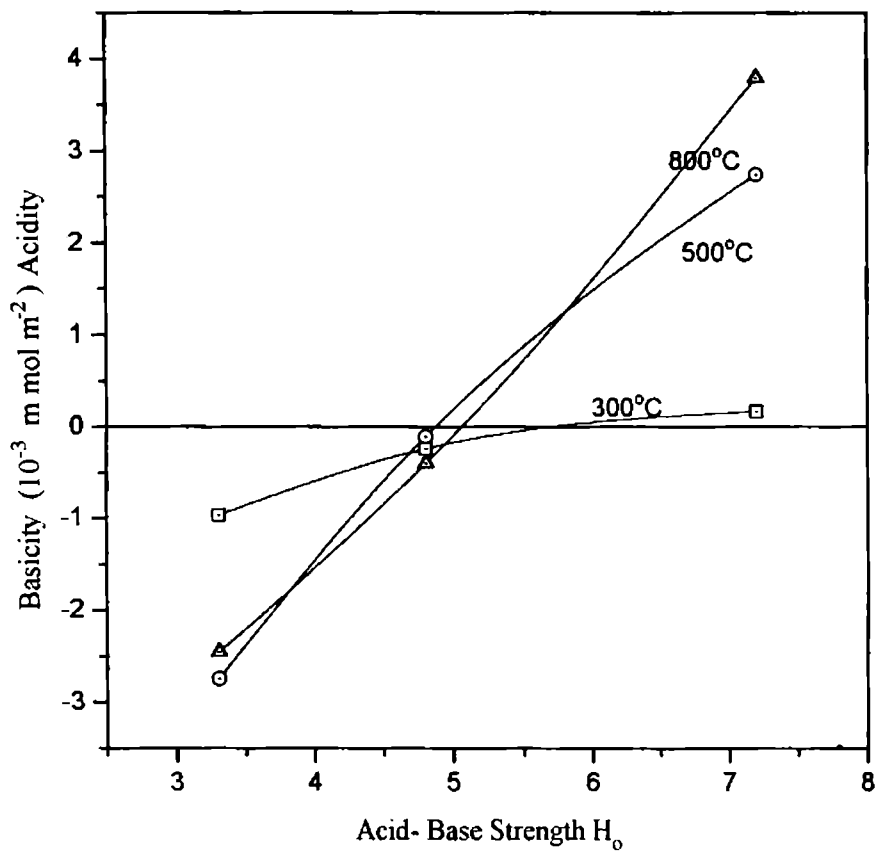




Figure 3.17  
Acid-Base Strength Distribution on Ce-Zr  
mixed oxides activated at 300°C

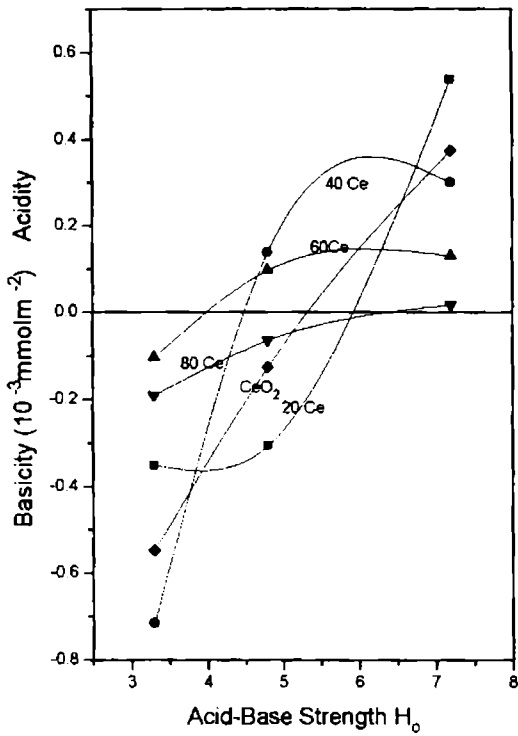


Figure 3.19  
Acid-Base Strength Distribution on Ce-Zr  
mixed oxides activated at 500°C

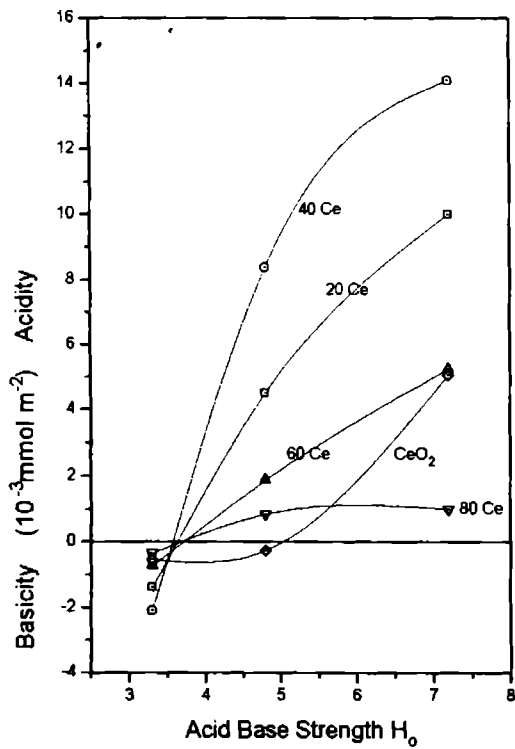


Figure 3.18  
Acid-Base Strength Distribution on Ce-Zr  
mixed oxides activated at 300°C  
as a function of composition

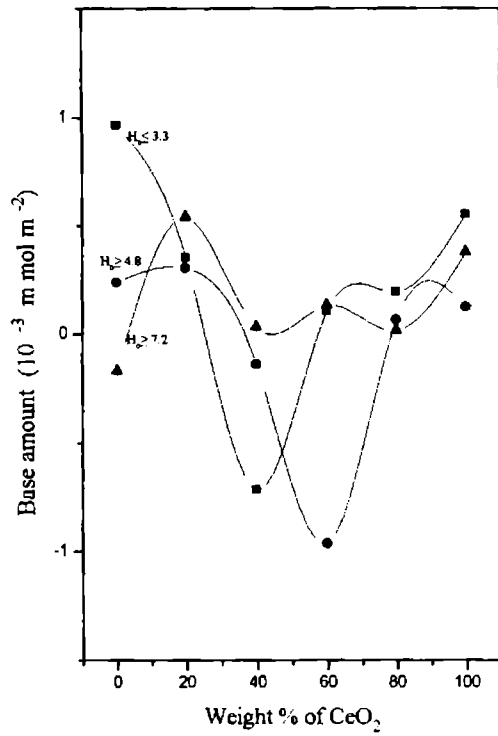


Figure 3.20  
Acid-Base Strength Distribution on Ce-Zr  
mixed oxides activated at 500°C  
as a function of composition

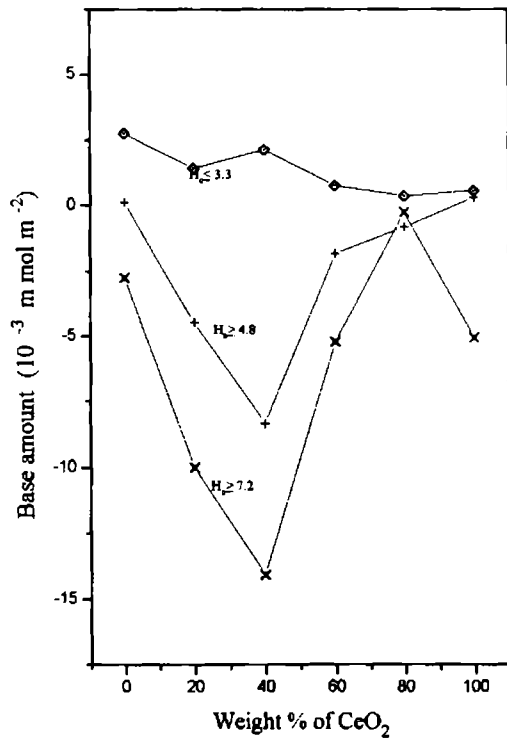


Figure 3.21  
Acid-Base Strength Distribution on Ce-Zr  
mixed oxides activated at 800°C

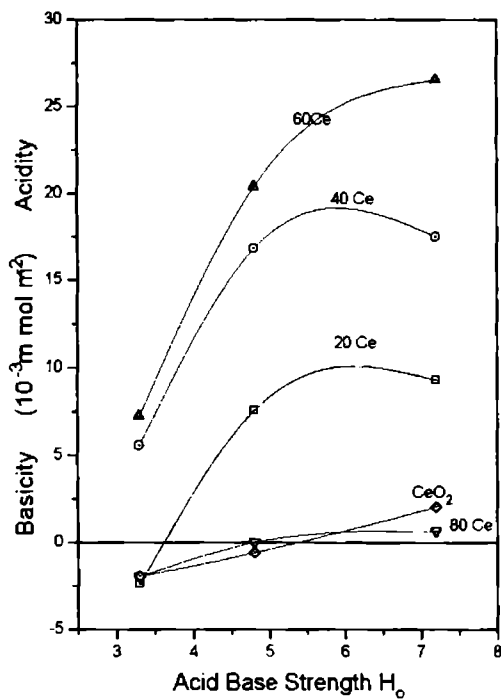


Figure 3.22  
Acid-Base Strength Distribution on Ce-Zr  
mixed oxides activated at 800°C  
as a function of composition

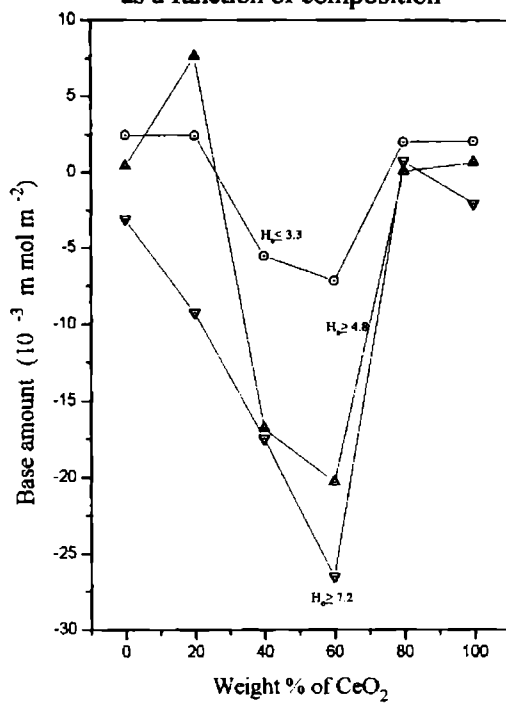


Figure 3.23  
Acid-Base Strength Distribution on Ce-Zr  
mixed oxides at H<sub>0</sub> ≥ 3.3 activated at different  
temperatures as a function of composition

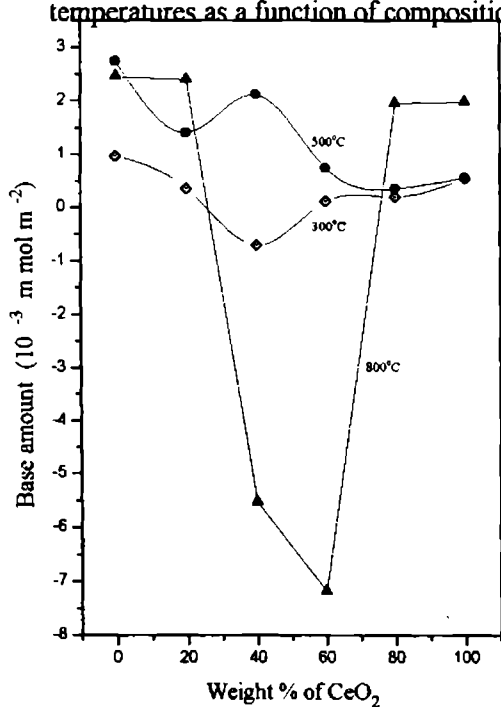
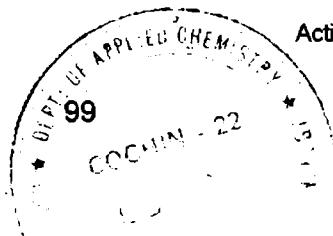
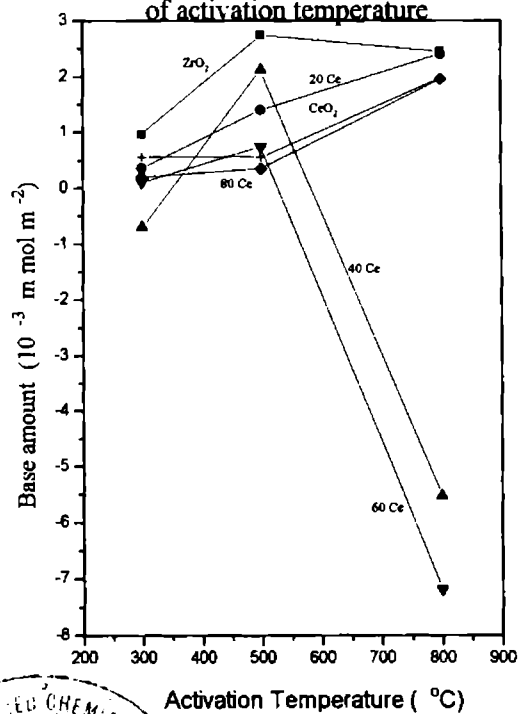


Figure 3.24  
Acid-Base Strength Distribution on Ce-Zr  
mixed oxides at H<sub>0</sub> ≥ 3.3 as a function  
of activation temperature



5723

Figure 3.25  
 Acid-Base Strength Distribution on Ce-Zr mixed oxides at  $H_0 \geq 4.8$  activated at different temperatures as a function of composition

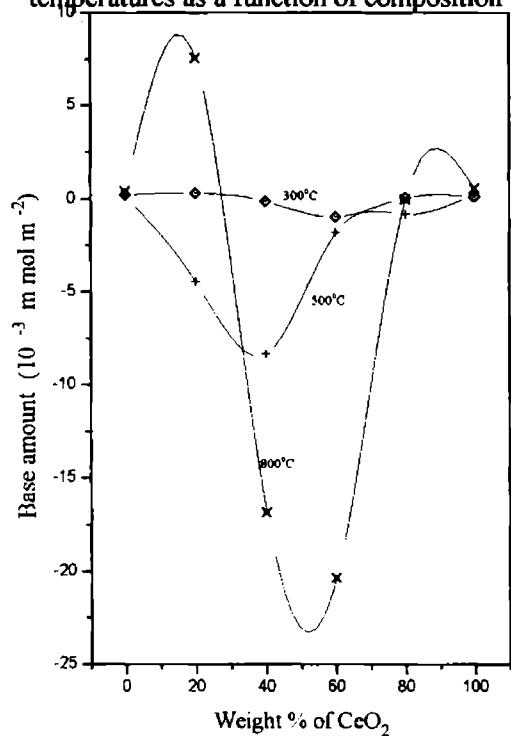


Figure 3.27

Acid-Base Strength Distribution on Ce-Zr mixed oxides at  $H_0 \geq 7.2$  activated at different temperatures as a function of composition

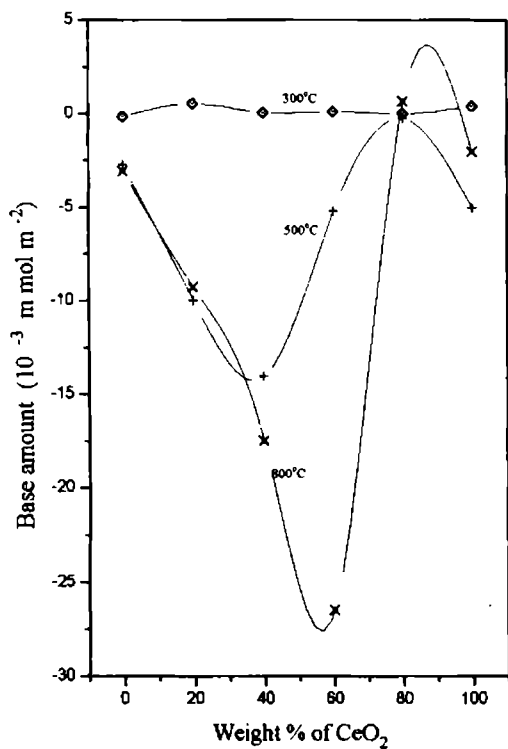


Figure 3.26  
 Acid-Base Strength Distribution on Ce-Zr mixed oxides at  $H_0 \geq 4.8$  as a function of activation temperature

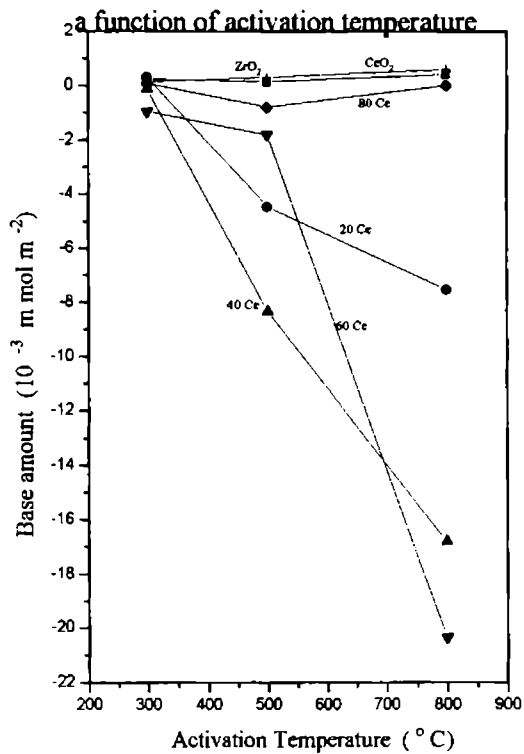


Figure 3.28

Acid-Base Strength Distribution on Ce-Zr mixed oxides at  $H_0 \geq 7.2$  as a function of activation temperature

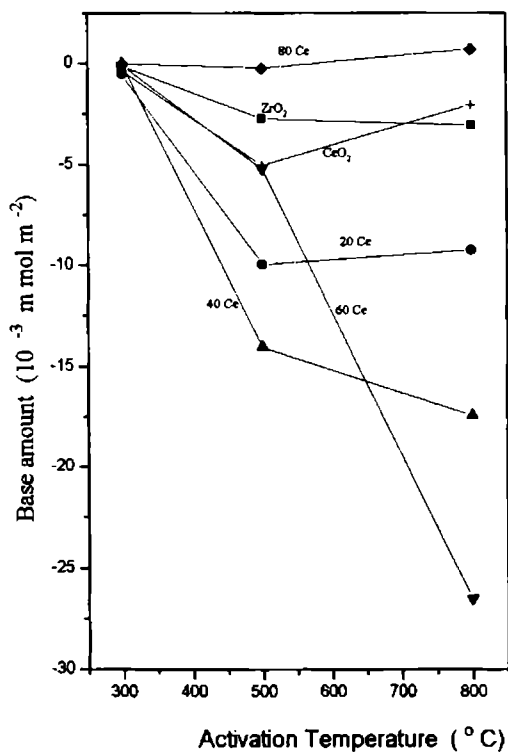


Figure 3.29

$H_{O,MAX}$  values of Ce-Zr mixed oxides at different activation temperatures as a function of composition

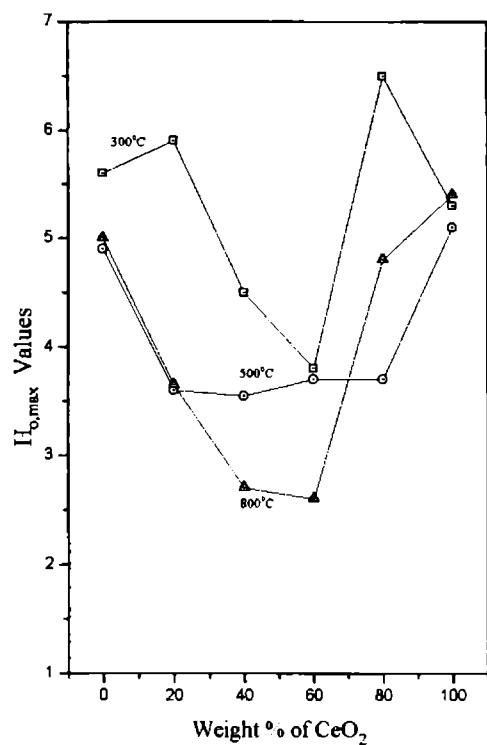


Figure 3.30

$H_{O,MAX}$  Values of Ce-Zr mixed oxides as a function of activation temperature

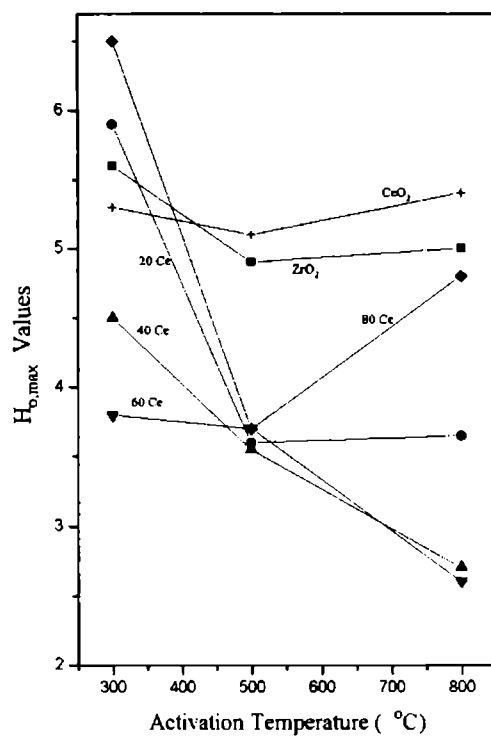


Figure 3.31

Activity- Reduction Reaction as a function of composition of Ce-Zr Mixed oxides

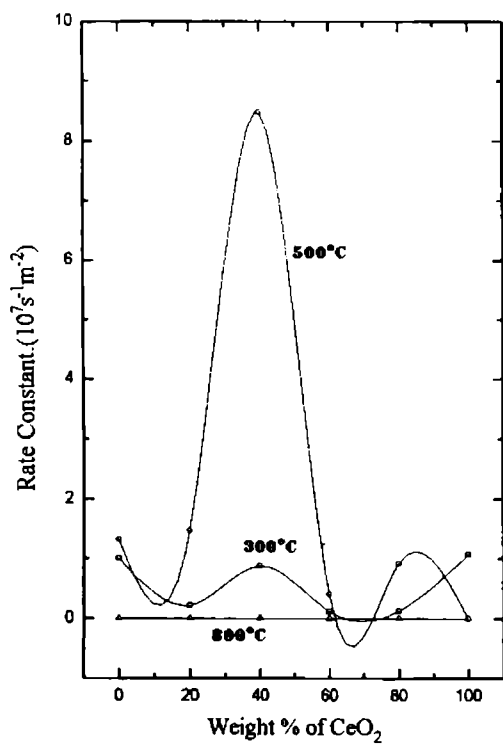


Figure 3.32

Catalytic Activity for reduction reaction of Ce-Zr mixed oxides as a function of activation temperature

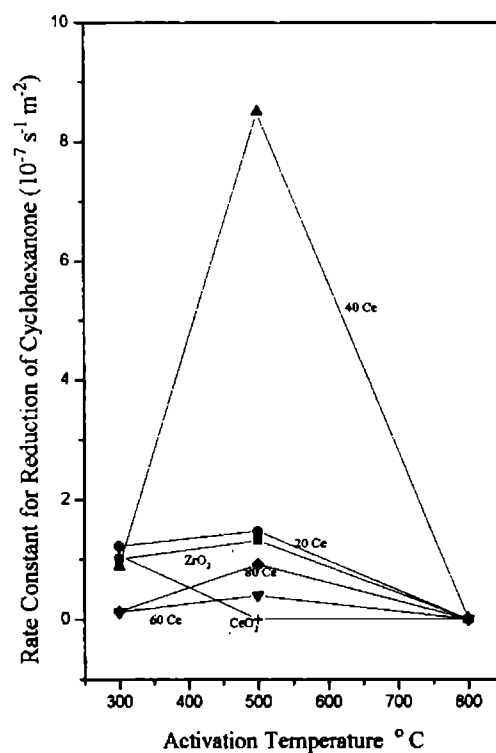


Figure 3.33  
Catalytic Activity for oxidation reaction  
of Ce-Zr mixed oxides as a function of  
activation temperature

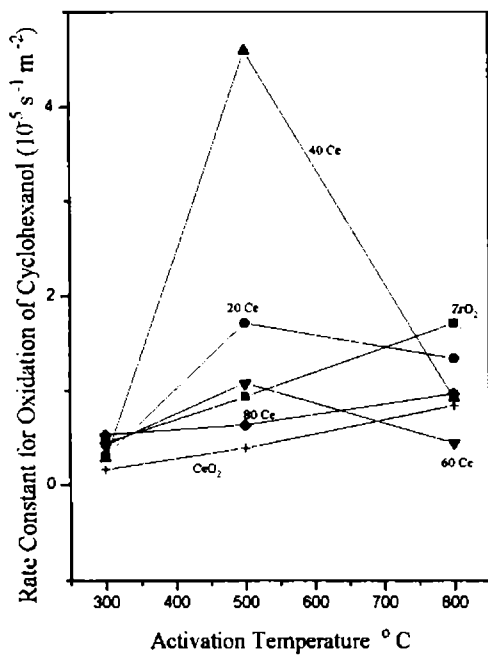


Figure 3.34  
Activity- Oxidation Reaction as a  
function of composition of  
Ce-Zr Mixed oxides

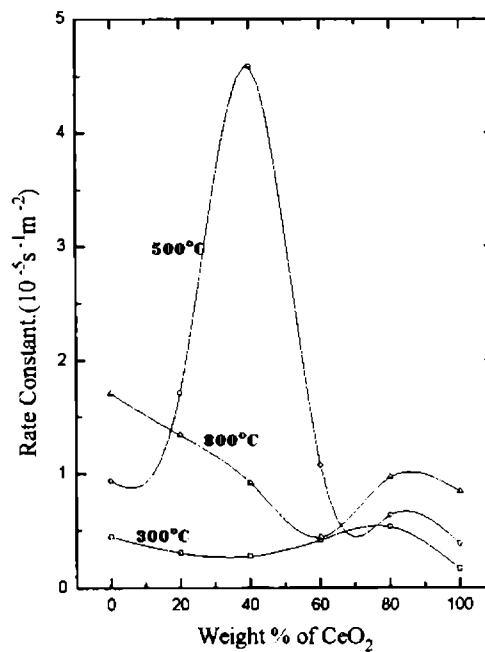
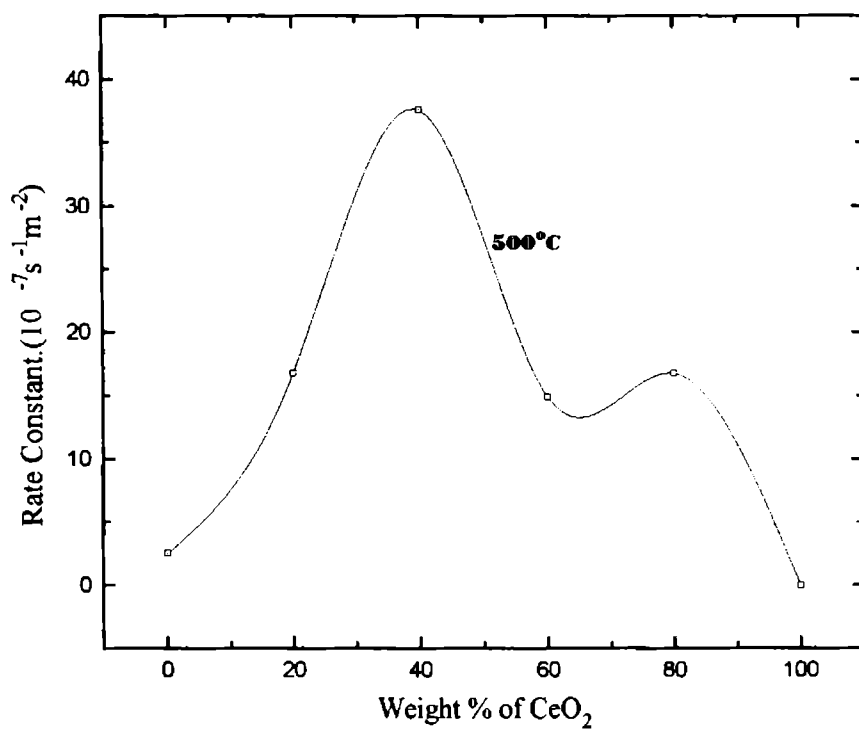


Figure 3.35  
Activity- Esterification Reaction as a function  
of composition of Ce-Zr Mixed oxides



## **REFERENCES**

1. Y. Sun and P.A. Sermon: *J. Mater. Chem.*, 6, proceeding paper (1996)
2. R. Stevens, *Catal. Today*, 20, 1 (1994)
3. K. M. Minachev, Y. S. Khodakov and V. S. Nakshunov : *J. Catal.*, 49, 207 (1977)
4. S. Sugunan , G. D. Rani and P. A. Unnikrishnan: *J. Mater. Sci. Technol.*,10, 425 (1994).
5. K. Esumi, K. Miyata, F. Waki and K. Meguro : *Colloid and Surfaces*, 20, 8 (1986)
6. M. Che, N. Naccache and B. Imelik : *J. Catal.*, 76, 61 (1982).
7. K. Meguro, K. Esumi: *J. Adhesion Sci. Technol.*, 4, 393 (1990).
8. F. H. Boyd, W. D. Philips : *J. Chem. Phys.*, 43, 2927 (1965).
9. R. Foster, T. J. Thomson : *Trans. Faraday Soc.*, 58, 860 (1962).
10. H. Hosaka, T. Fujiwara and K. meguro : *Bull. Chem. Soc. of Jpn.*, 44, 2616 (1971)
11. K. Esumi and K. Meguro : *Jpn. Soc. of Colour Mater.*, 48, 539 ((1975)
12. O. Johnson : *J. Phys. Chem .*, 827 (1955).
13. T. Yamanaka and K. Tanabe: *J. Phys. Chem.*, 79, 2407 (1975)
14. T. Yamanaka and K. Tanabe: *J. Phys. Chem.*, 80, 1723 (1976)

15. R. W. G Wyckoff: "Crystal Structures" Vol 2, Part 5, Inter Science Publishers. Inc, New york, (1951)
16. B. D. Flockhart, I. R. Leigh and R. C. Pink : Trans. Faraday Society, 65, 542 (1969)
17. V. R. Choudhary and V. H. Rane : J. Catal., 130, 411 (1911)
18. Tanabe K., Sumiyoshi T., Sibata K., kiyoyura T., Kitagawa J. : Bull. Chem. Soc. Jpn., 47, 1064 (1974)
19. Aline Auroux and Antonella Gervasini: J.Phys. Chem., 94,6371, (1990).
20. M. Shibagaki, T. Takahashi and H. Matsushita : Bull. Chem. Soc. Jpn., 61, 328 (1988).
21. Mars P and Van-Krevelen D W: Chem. Eng. Sci., 3, 41, (1994)
22. A. Ueno, T. Onishi and K. Tamaru: Trans. Faraday Soc., 67, 3585 (1971)
23. R. P. Groff : J. Catal., 86, 215 (1984).
24. K. Aika and J. H. LunsFord : J. Phys. Chem., 81, 1393 (1977)
25. M. Nagao and T. Morimoto: J. Phys. Chem., 84, 2054 (1984)
26. O. Koga, T. Onishi and K. Tamaru: J. Chem. Soc. Faraday Trans., 1, 76, 19 (1980)
27. Y. Izumi, Shokubai Kouza, 8, 285, Kodansha, Tokyo, (1985)), in Japanese



28. S. Namba, Y. Wakushima, T. Shimizu, H. Masumoto and T. Yashima, *Catalysis by acids and bases*, Elsevier, Amsterdam, 205, 1985
29. K. Tanabe, M. Misono, Y. Ono and H. Hattori, *New solid acids and bases and their catalytic properties*, Elsevier Amsterdam, Kodansha, Tokyo (1989)
30. T. Takahashi, M. Shibagaki and H. matsushita : *Bull. Chem. Soc. Jpn.*, 62, 2353 (1989).
31. E. Santacesaria, D. Gelosa, p. Danise and S. Carra : *J. Catal.*, 80, 427 (1983).

## **CHAPTER 4.**

**ACID- BASE, SURFACE ELECTRON DONATING &  
CATALYTIC PROPERTIES OF PRASEODYMIUM -  
ZIRCONIUM MIXED OXIDES.**

Zirconia is reported as an excellent catalyst [1,2], and very good supporting material [3], for many reactions. It shows both acidic and basic properties, the addition of basic oxides (La) suppress the acidic behaviour whereas addition of an acidic oxide promotes acidic property [4]. Sulfated zirconia is known as a superacid and it is shown [5] to be a better acid catalyst than Amberlyst-15. Rare earth oxides, are basic and can act as effective catalysts for a number of reactions [6]. Praseodymia, one among the rare earth oxides is a nonstoichiometric, paramagnetic oxide having Pr in +3 and +4 oxidation states in the ratio 1:2. Due to its nonstoichiometric nature it has intrinsic oxygen vacancies [7] and a higher amount of chemisorbed oxygen on its surface. The lattice oxygen atoms in  $\text{Pr}_6\text{O}_{11}$  play a major role in its catalytic activity [8]. So far no attempt has been made to study the effect of mixing of  $\text{ZrO}_2$  with  $\text{Pr}_6\text{O}_{11}$  on their surface properties. In this chapter the acid/base properties, surface electron donor properties and the catalytic activity of Praseodymium - Zirconium mixed oxides are reported at various compositions at an activation temperature of  $500^\circ\text{C}$ .

The acid/ base and surface electron donating properties and the catalytic activity of Praseodymium - Zirconium mixed oxides at various compositions at an activation temperature of  $500^\circ\text{C}$  were studied. The mixed oxides with various compositions, viz 20, 40, 60 and 80% of the rare earth oxide were studied. For comparison pure oxides were also incorporated in the study. The mixed oxides were

prepared through the hydroxide route. The hydroxides were precipitated by adding 1:1 ammonia to a solution containing calculated quantities of praseodymium nitrate and zirconyl nitrate. The precipitate is then thoroughly washed free from nitrate ions and dried at 120° C, then calcined at 300° C for two hours to get the oxide. The calcined samples were then sieved to get oxides with 100- 200 mesh size. The mixed oxides with various compositions, viz 20, 40, 60 and 80 % (abbreviated as 20 Pr, 40 Pr, 60 Pr and 80 Pr) of the rare earth oxide were prepared. Pure oxides were also prepared in the same fashion. All the oxides were heat treated at a particular temperature, namely 500°C for two hours prior to each experiment. All the reagents were purified by standard methods (Ref. chapter 2) before use. The catalytic activities have been correlated with electron donating properties and surface acidity/basicity of the oxides.

#### 4.1 Surface areas

Surface areas of  $\text{Pr}_6\text{O}_{11}$  is very small compared to that of  $\text{ZrO}_2$  (Table 4.1 and Figure 4.1). On mixing the oxides the surface areas are increased. The surface area of  $\text{ZrO}_2$  is almost doubled by addition of 20 %  $\text{Pr}_6\text{O}_{11}$  to it. For all the mixed oxides, the surface areas are more than the pure component oxides, it is maximum for 20 Pr.

## 4.2 Electron Donor Properties

The strength and distribution of electron donor sites are determined from the studies on the adsorption of electron acceptors (EA) of various electron affinity in acetonitrile, a solvent with low basicity. The following electron acceptors used are given in chapter 3, table 1.

The adsorption studies were carried out by a procedure reported earlier [9]. The amount of electron acceptor adsorbed was determined by noting the concentration of the electron acceptor before and after adsorption by means of a UV-Visible spectrophotometer at the  $\lambda_{\max}$  of the EA in acetonitrile, ie. at 393.5, 288, 262 and 237 nm for TCNQ, Chloranil, PDNB and MDNB respectively.

The adsorption of EA on the oxides were of Langmuir type. From the Langmuir plots (Figure 4.2 & 4.3) the limiting amount of EA adsorbed were determined (Table 4.1). In the case of PDNB and MDNB, adsorption was so negligible that the amount could not be detected by spectrophotometric method. When EA were adsorbed, the surface of the oxides showed characteristic coloration owing to the interaction between the EA adsorbed and the oxide surface, [9] (for dark colored oxides the coloration was not detectable by visual method). The electron donor property of pure praseodymia is less than that of zirconia. Highest value for electron donating capacity is shown by 80 Pr followed by 60 Pr and then 20 Pr, which are higher than that of the pure oxides. 40 Pr is having lower electron donating power than

the pure component oxides. In the case of chloranil adsorption also the same trend is followed, all the values being less than that for TCNQ. The extent of electron acceptor adsorption depends on the electron affinity of the electron acceptor and on the composition of the mixed oxide. The nature of the adsorbed species was studied by ESR and Reflectance spectra of the adsorbed samples.

The limiting amount of TCNQ adsorbed is a measure of the total number of electron donor sites on the surface. The extent of electron transfer depends on the electron affinity of the acceptor. Two possible electron sources exist on the oxide surface capable of electron transfer, namely electrons trapped in intrinsic defects and surface hydroxyl ions [10]. It has been reported at higher activation temperatures the donor sites consists of a co-ordinatively unsaturated  $O^{2-}$  associated with a nearby  $OH^-$  group and the concentration of these sites is related to the base strength of the surface [11]. The more basic the surface the higher is the number of  $O^{2-}$  which can transfer electrons to the EA.

#### **4.3 Acid- Base Properties**

The surface acidity/ basicity of the oxides were determined by titration method using the same set of Hammett indicators [12] given in chapter 3, table 2. The oxides under study responded only to dimethyl yellow, methyl red and bromothymol blue. The surface acidity/ basicity of the dark colored oxides were determined by a

modified procedure [13] . It was done by comparing the acidity/ basicity of the combination of the oxide with a white standard oxide material with the standard oxide.

The acid/ base strength distribution of the oxides were measured on a common  $H_0$  scale [14] (Table 4.2). The acid-base properties of Pr-Zr mixed oxides change with composition of the mixed oxide. Pure  $ZrO_2$  is having both acidic and basic sites . Praseodymia is having only basic sites . The acidity and basicity of the mixed oxides are intermediate between those of the pure component oxides. The acid/base strength distribution curves ( Figure 4.5) intersect at a point on the abscissa where acidity = basicity = 0 [14] . The point of intersection is defined as  $H_{0,max}$  . It can be regarded as a practical parameter to represent acid /base properties on solids. A solid with a large positive  $H_{0,max}$  value has strong basic sites and weak acid sites and a solid with a large negative  $H_{0,max}$  value has strong acid sites and weak basic sites.

$Pr_6O_{11}$  is a mixture of two crystalline forms , the C (body centered cubic, coordination number of cation 6 ) and A ( distorted hexagonal, coordination number of cation 7) forms which are prominent in the rare earth oxides, the amount of each form being varying [15] . According to Tanabe's model [16] ,  $Pr^{+3}$  in cubic form when mixed with zirconia will not generate acidity, but in the A form it can generate acidity on mixing. The A form is prominent at higher temperatures. Praseodymia itself is a mixture of  $Pr^{+3}$  and  $Pr^{+4}$  , and there will be a small amount of intrinsic acidity

in it , which will not be much affected by the addition of  $Zr^{+4}$ . Acidities present in the mixed oxides are only the sum of their components or slightly more.

#### 4.4 Catalytic activity measurements.

The catalytic activity of the mixed oxides for three reactions *Viz.* reduction of cyclohexanone, oxidation of cyclohexanol and esterification of acetic acid with n-butanol were studied ( See Table 4.3). The catalytic activity is expressed as the first order rate constant per  $m^2$  of the oxide surface.

The rate constant for the reduction is very small when catalysed by praseodymia. Zirconia is having a higher value for activity than praseodymia. All the mixed oxides are having higher activities than the pure oxides. The activity is the highest for 40 Pr. The active sites for the reduction reaction is still uncertain. Shibagaki et al proposed a mechanism involving the adsorption of ketone and alcohol on the oxide surface [17] (See section 3.2.4).

It is an acid- base bifunctional catalysis. The activity can depend on the amount of acid / base sites, if they are very small in number the availability of the particular type of site determine the rate of the reaction. For a sufficiently basic oxide, the rate of reaction may depend on the amount of acid sites coexisting with the basic sites and vice-versa. The active sites for the reaction may be surface  $OH^-$ ,  $O^{2-}$  or lattice disorders such as trapped electrons formed in the system. The latter two increase in concentration at high activation temperatures. Surface  $O^{2-}$  are formed by



sintering of surface OH<sup>-</sup>. The catalytic activity showed dependence on both the surface acidity and basicity, however the relationship is not straight forward. The lack of a linear relationship between activity and basicity implies the involvement of acid sites also in the reaction, the exact nature being unknown [11].

Praseodymia is having a very high value of rate constant for the oxidation of cyclohexanol. This can be due to the availability of lattice oxygens [7] (high mobility through the intrinsic oxygen vacancies) to take part in the reaction or due to the presence of chemisorbed oxygen [8] on its surface. The activity is more for Pr<sub>6</sub>O<sub>11</sub> than that for zirconia. The mixed oxides are having lower values of catalytic activity than pure praseodymia and zirconia. Sites which catalyse the oxidation reactions are not generated on mixing the two oxides.

Praseodymium oxide does not catalyse the esterification reaction while zirconia catalyses the same reaction. Esterification reaction is a typical acid catalysed reaction, zirconia having a polyfunctional behaviour, have acid sites on it. All the mixed oxides catalyse the esterification reaction but the activity is less than that for zirconia. Among the mixed oxides 40 Pr and 60 Pr are having higher activity than 20 Pr and 80 Pr. In 40 Pr and 60 Pr (both having the higher amount of Pr-O-Zr bonds than 20 Pr and 80 Pr) have higher amount of acidity associated with them and will catalyse the esterification reaction more effectively.

Table 4.1. Surface areas & Limiting Amounts of Electron Acceptors Adsorbed on Praseodymium -Zirconium Mixed Oxides activated at 500°C

Weight % of Pr <sub>6</sub> O <sub>11</sub>	Surface Areas m <sup>2</sup> g <sup>-1</sup>	Limiting amount Adsorbed 10 <sup>-6</sup> mol /sq.m	
		TCNQ	Chloranil
0	61.50	2.081	1.061
20	127.56	2.138	1.129
40	101.59	1.961	0.951
60	90.17	2.145	0.855
80	69.90	3.311	1.251
100	11.40	0.744	0.339

Table 4. 2 .Acid-Base strength Distribution on Praseodymium-Zirconium Mixed Oxides activated at 500 °C

Weight % of Pr <sub>6</sub> O <sub>11</sub>	Basicity 10 <sup>-3</sup> m mol m <sup>-2</sup>			Acidity	H <sub>0,max</sub>
	H <sub>0</sub> ≥3.3	H <sub>0</sub> ≥4.8	H <sub>0</sub> ≥7.2	H <sub>0</sub> ≤7.2	
0	2.738	0.107	-	2.745	4.89
20	2.512	2.000	-	2.431	6.05
40	2.074	1.693	-	2.012	6.09
60	2.814	1.704	-	1.231	6.26
80	3.274	1.813	-	0.081	7.04
100	4.210	2.880	0.082	-	7.22

Table 4.3. Catalytic activity of Praseodymium-Zirconium mixed oxides Activated at 500°C

Weight % of Pr <sub>6</sub> O <sub>11</sub>	Reduction of Cyclohexanone		Oxidation of Cyclohexanol		Esterification Reaction	
	% conversion	Rate Constant (10 <sup>-7</sup> s <sup>-1</sup> m <sup>-2</sup> )	% conversion	Rate Constant (10 <sup>-5</sup> s <sup>-1</sup> m <sup>-2</sup> )	% conversion	Rate Constant (10 <sup>-7</sup> s <sup>-1</sup> m <sup>-2</sup> )
0	11.05	1.320	87.24	0.930	10.53	2.513
20	34.71	2.321	89.20	0.485	0.74	0.081
40	34.25	2.867	91.75	0.682	6.70	0.948
60	19.31	1.653	95.02	0.924	6.38	1.015
80	11.00	1.158	88.79	0.870	1.19	0.238
100	1.10	0.612	95.59	7.607	0.00	-

Figure 4.1  
Surface areas of Pr-Zr Mixed Oxides  
Activated at 500°C

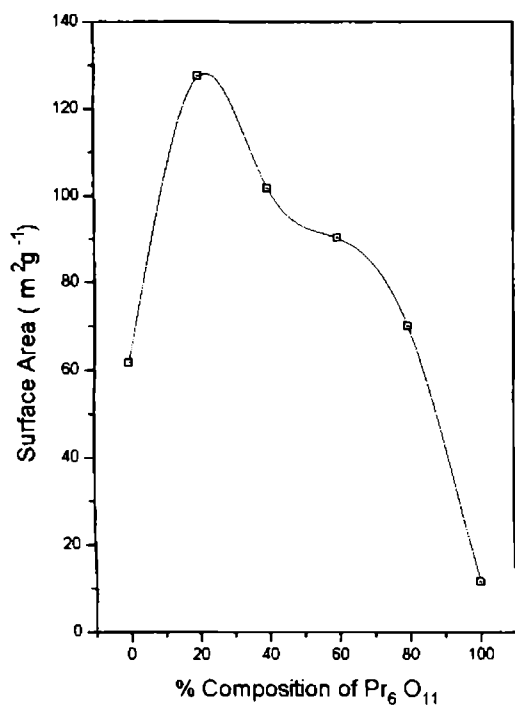


Figure 4.3

Limiting Amounts of Electron acceptors adsorbed on Pr-Zr mixed oxides activated at 500°C as a function of composition

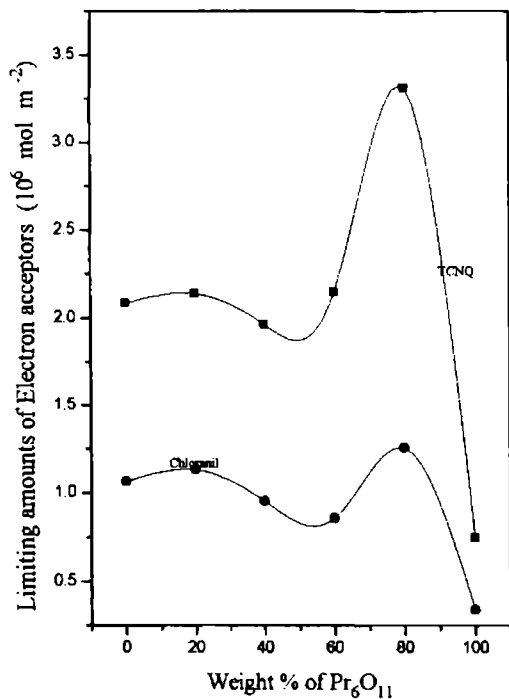


Figure 4.2  
Adsorption isotherms of TCNQ on Pr-Zr  
Mixed oxides activated at 500°C

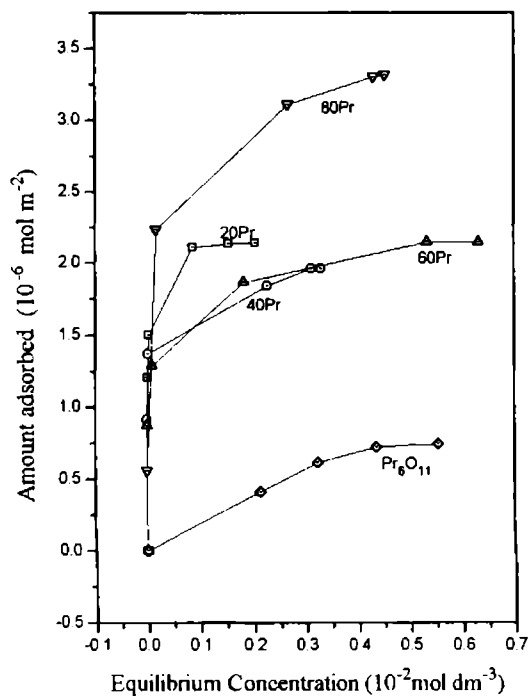


Figure 4.4

Adsorption isotherms of Chloranil on Pr-Zr  
Mixed oxides activated at 500°C

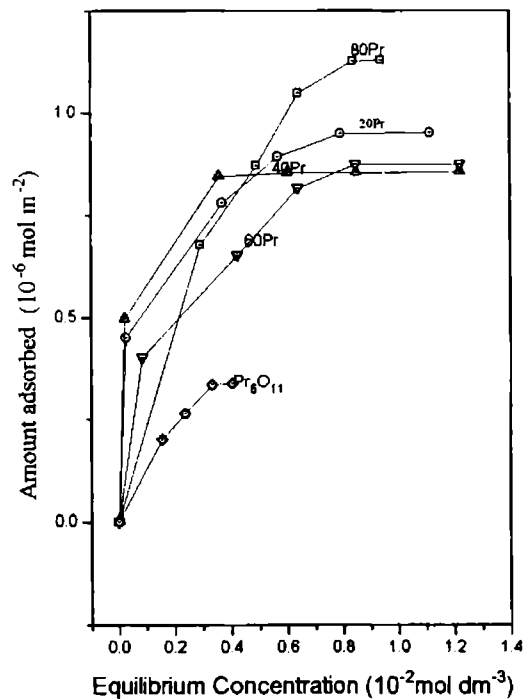


Figure 4.5  
Acid-Base Strength Distribution on Pr-Zr  
mixed oxides activated at 500°C as  
a function of composition

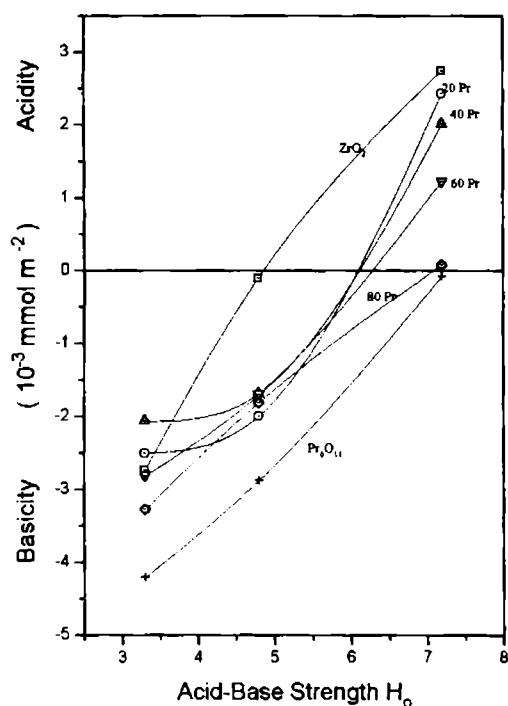


Figure 4.7  
 $H_{0,max}$  Values of Pr-Zr mixed  
oxides activated at 500°C as  
a function of composition

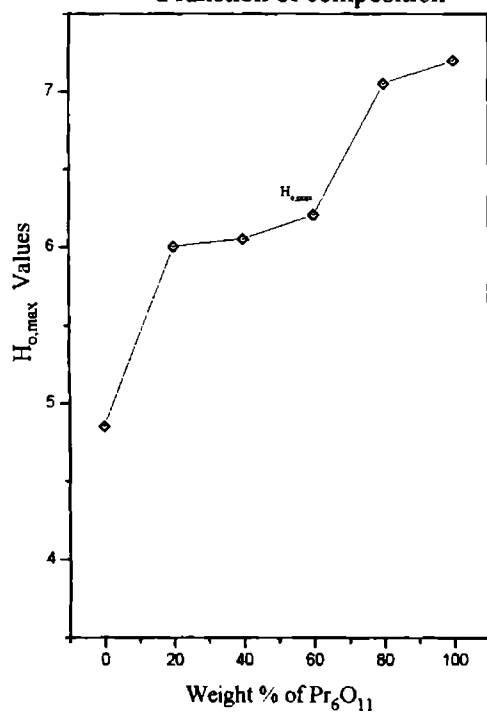


Figure 4.6  
Acid-base strength distribution on Pr-Zr  
Mixed Oxides Activated at 500°C  
as a function of composition

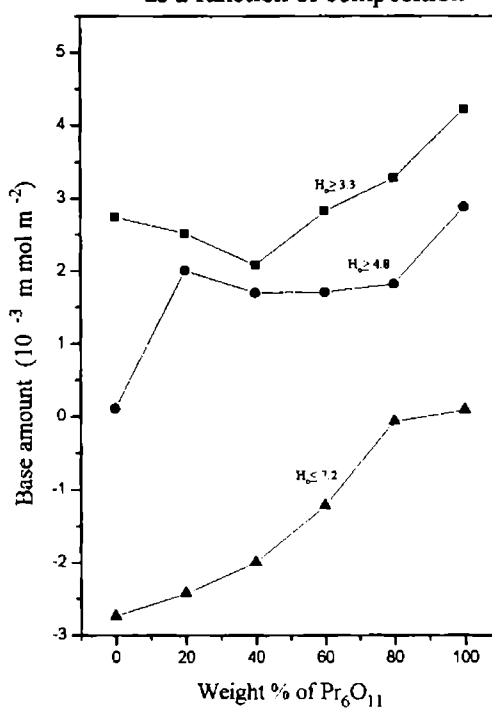


Figure 4.8  
Catalytic activity for Reduction of  
cyclohexanone on Pr-Zr mixed oxides  
activated at 500°C as a function of composition

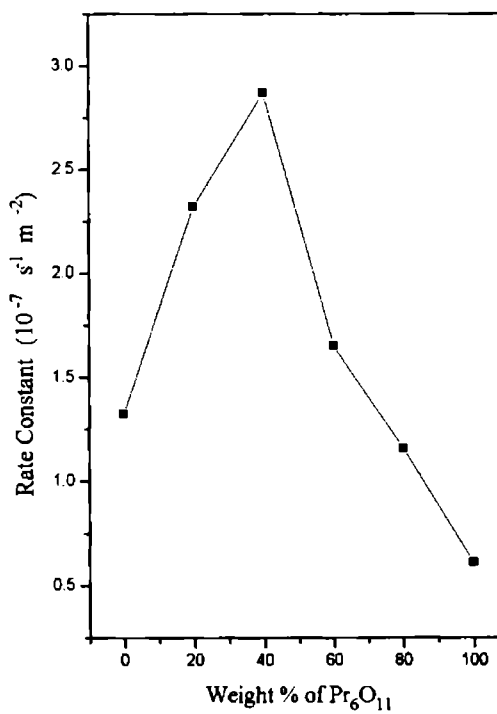


Figure 4.9  
Catalytic activity for Oxidation of  
cyclohexanol on Pr -Zr mixed oxides  
activated at 500°C  
as a function of composition

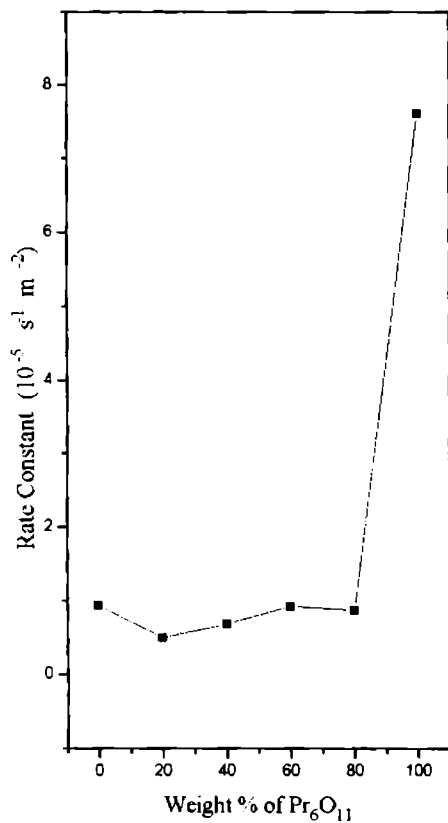
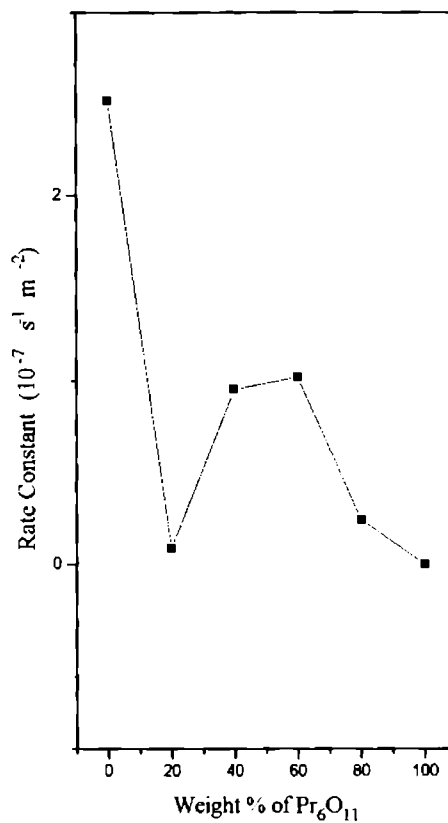


Figure 4.10  
Catalytic activity for Esterification  
of n-Butanol on Pr -Zr mixed oxides  
activated at 500°C  
as a function of composition



## REFERENCES

1. M. Shibagaki, K. Takahashi and H. Matsushita : Bull. Chem. Soc. Jpn, 61, 3283 (1988)
2. M. Shibagaki, H. Kuno K. Takahashi and H. Matsushita : Bull. Chem. Soc. Jpn, 61, 4153 (1988)
3. T. Lizuaka, M. Itoh, H. Hattori and K. Tanabe : J. Chem. Soc. Faraday Trans. 1, 78, 501 (1982)
4. R. Franklin, P. Goulding, J. Haviland, R. W. Joyner, I. McAlpine, P. Moles, C. Norman and T. Nowell : Catalysis Today, 10, 405 (1991)
5. J. A. Navio, G. Colon, M. Macias, J. M. Campelo, A. A. Romero and J. M. Marinas : J. Catal., 161, 605 (1996)
6. K. M. Minachev, Y. S. Khodakov and V. S. Nakshunov : J. Catal. 49, 207 (1977)
7. F. L. Normand, J. Barrault, R. Breault, L. Hilaire, A. Kinnemann: J. Phys. Chem. 95, 257 (1991)
8. Y. Takasu, M. Matsui and Y. Matsuda : J. Catal. 76, 61 (1982)
9. M. Che, C. Naccache, B. Imelik : J. Catal., 24, 328 (1972).



10. K.Esumi, K.Meguro: J. Colloid Interface Sci., 59, 43(1977).
11. V.R.Choudhary , V.H.Rane : J.Catal.,130, 411 (1911).
12. O.Johnson: J. Phys. Chem ., 827(1955).
13. S.E. Voltz, A. E. Hirsthler and A. Smith : J. Phy. Chem. 64, 1594, (1960)
14. T.Yamanaka, K.Tanabe : J. Phys.Chem., 80, 1723(1976).
15. M. P. Rosynek and D. T. Magnuson : J. Catal. 46, 402 (1977)
16. K. Tanabe, T. Sumiyoshi, K. Sibata, T. kiyoyura and J. Kitagawa : Bull.  
Chem. Soc. Jpn. 47, 1064 (1974)
- 17 M. Shibagaki, T. Takahashi and H. Matsushita : Bull. Chem. Soc. Jpn., 61, 328  
(1988).

## **CHAPTER 5.**

**ACID- BASE, SURFACE ELECTRON DONATING &**

**CATALYTIC PROPERTIES OF NEODYMIUM -**

**ZIRCONIUM MIXED OXIDES.**

Fluorite structure is the structure of the high temperature form of  $ZrO_2$  and of the so called stabilized Zirconias. At room temperature  $ZrO_2$  has a deformed structure, derived from the fluorite structure. Pure  $ZrO_2$ , when cooled from high temperatures, undergoes several phase transitions which are accompanied by relatively large volume changes. Due to the volume changes caused by the phase transitions, sintered compacts of pure  $ZrO_2$  are pulverised on cooling. By doping  $ZrO_2$  with lower valent ions the cubic structure is stabilized and remains viable down to room temperature, even though it is metastable at that temperature.

In the stabilized Zirconias the oxygen vacancies, which are present as the ionic majority defects, are randomly distributed over the crystallographic oxygen positions. In particular, ordering effects may occur at high dopant concentrations, depending on the ratio of the radii of the  $Zr^{4+}$  to dopant ion. When an equimolar amount of trivalent ions has been added the formula of the mixed oxide is  $A_2B_2O_7$  and, depending on the type of A and B ion an ordered super structure of the fluorite structure, the pyrochlore structure is formed. Pyrochlore has a unit cell, consisting of 8 fluorite cells with an ordered arrangement of oxygen vacancies. Six of the remaining oxygen are of the same crystallographic type the seventh has a different crystallographic type. There is also cation ordering and the lattice is distorted in such a

way that the smaller of the cations is surrounded by a distorted octahedron of oxygen, the larger by a distorted cube of oxygens.

When comparing the phase diagrams of the different  $ZrO_2 - Ln_2O_3$  systems, it is clear that the pyrochlore structure becomes less stable as the radius ratio  $r(Ln^{3+})/r(Zr^{4+})$  decreases. As a consequence of the lanthanide contraction, from Gadolinium onwards the pyrochlore structure is no longer formed. Around the corresponding composition the stable phase is then the cubic fluorite structure with a random distribution of the metal cations over the accessible sites in the structure [1].

In this chapter Catalytic activity, Electron donor Properties, and surface acid-base properties of Neodymium-Zirconium mixed oxides are reported at three activation temperatures (300°C, 500°C and 800°C). The effect of activation temperature on acid-base properties, surface electron donor properties and surface areas were studied. The data obtained were correlated with their catalytic activities.

The mixed oxides with various compositions, *Viz* 20, 40, 60 and 80% of the rare earth oxide were studied. For comparison pure oxides were also incorporated in the study. The mixed oxides were prepared through the hydroxide route. The mixed oxides with various compositions, *Viz* 20, 40, 60 and 80 % (abbreviated as 20 Nd, 40 Nd, 60 Nd and 80 Nd) of the rare earth oxide were prepared. Pure oxides were also prepared in the same fashion.

### 5.1.1 Surface Area

ZrO<sub>2</sub> is having very high surface area when activated at 300°C, surface area decreased with activation temperature, the decrease is steep (table 5.1). In the case of Nd<sub>2</sub>O<sub>3</sub> the surface area is less compared to ZrO<sub>2</sub>. The surface area of Nd<sub>2</sub>O<sub>3</sub> increases from 300°C up to 500°C and then decreases. At 300°C and 500°C, surface areas of all mixed oxides are greater than that of neodymia. At all activation temperature 20 Nd have larger surface areas than zirconia. At 800°C surface areas of 60 Nd and 40 Nd were less than the component oxides. However, surface areas can be considered to be improved by the mixing of oxides especially at lower activation temperatures.

### 5.1.2 Electron Donating Properties.

The strength and distribution of electron donor sites are determined from the studies on the adsorption of electron acceptors (EA) of various electron affinity in acetonitrile, a solvent with low basicity. The electron acceptors used are given in chapter 3, table 1.

The adsorption studies were carried out by a procedure reported earlier [2]. The amount of electron acceptor adsorbed was determined by noting the concentration of the electron acceptor before and after adsorption by means of a UV-Visible spectrophotometer at the  $\lambda_{\text{max}}$  of the EA in acetonitrile, ie. at 393.5, 288, 262 and 237 nm for TCNQ, Chloranil, PDNB and MDNB respectively.

The adsorption of EA on the oxides were of Langmuir type. From the Langmuir plots (Figure 5.3 to 5.7) the limiting amount of EA adsorbed were determined (Table 5.2). In the case of PDNB and MDNB, adsorption was so negligible that the amount could not be detected by spectrophotometric method. When EA were adsorbed, the surface of the oxides showed characteristic coloration owing to the interaction between the EA adsorbed and the oxide surface [3].

The limiting amount of electron acceptor adsorbed depends on the electron affinity of the electron acceptor. For  $ZrO_2$  the limiting amount of TCNQ adsorbed increased with activation temperature having its maximum value for the sample activated at  $800^\circ C$ . For pure  $Nd_2O_3$  the limiting amount adsorbed is less than that on  $ZrO_2$  having the same trend as for  $ZrO_2$  with the activation temperature, having its maximum value at  $800^\circ C$ . At  $300^\circ C$  all the mixed oxides have large values for limiting amount adsorbed than the component oxides. At  $500^\circ C$  the limiting amount of TCNQ adsorbed on the mixed oxides is intermediate between those of the component oxides, except in the case of 80 Nd which is having a higher value than the component oxides. At  $800^\circ C$  the limiting amount of TCNQ adsorbed on 20 Nd and 80 Nd is intermediate between those at  $300^\circ C$  and  $500^\circ C$ . That is for these two mixed oxides the limiting amount of TCNQ adsorbed first increases with activation temperature and then decreases. For 40 Nd and 60 Nd the limiting amount of TCNQ adsorbed increased with activation temperature as in the case of pure oxides. For 40 Nd the increase is very steep from 500 to  $800^\circ C$ .

The limiting amount of chloranil adsorbed on  $ZrO_2$  increased from 300°C to 500°C and then decreased. In the case of neodymia the limiting amount increased with activation temperature. Neodymia is having a very low EA adsorption compared to zirconia. At 300°C the mixed oxides have higher value for the limiting amount of chloranil adsorbed than pure component oxides. At 500°C all the mixed oxides except 40 Nd are having higher values for limiting amount of chloranil adsorbed than the component oxides. For 40 Nd activated at 500°C the limiting amount adsorbed is intermediate between those of component oxides. 80 Nd is having the highest value for samples activated at 300°C and 500°C. At 800°C 40 Nd is having a lower value than the component oxides, all others have higher values than the component oxides. 60 Nd has the highest value at 800°C.

### 5.1.3 Acid-Base properties

The surface acidity/ basicity of the oxides were determined by titration method using the same set of Hammett indicators [4] ; given in chapter 3, table 2. Of these the oxides under study responded only to dimethyl yellow, methyl red and bromothymol blue the acidity/ basicity. The acid/ base strength distribution of the oxides were measured on a common  $H_0$  scale [5] (Table 5.3, Figures 5.12 to 5.15 ).

Pure zirconia is more acidic than neodymia. The base amount of zirconia increases first with activation temperature up to 500°C and then decreases. For neodymia the base amount increases with activation temperature having its maximum at 800°C. At the acid strength of  $H_0 \geq 3.3$ , base amount is less in the mixed

oxides than the pure oxides. Acidity is being created on mixing the oxides. At activation temperature 500°C, the base amount of all the mixed oxides is greater than that activated at 300°C. For most of the mixed oxides the base amount for the samples activated at 800°C is less than that at 500°C. For most of the mixed oxides the maximum value of the base amounts are for samples activated at 500°C.

At the acid strength of  $H_0 \geq 4.8$  the base amount of zirconia decreased first up to 500°C and then increased, the maximum exhibited at 800°C. For neodymia, the base amount increased with activation temperature, showing its maximum at 800°C. For all the mixed oxides activated at 300°C the base amount is less than the pure component oxide. For samples activated at 500°C except 40 Nd have base amounts greater than the pure component oxides. For samples activated at 800°C, all the mixed oxides have less basicity than the component oxides, 40 Nd being the lowest.

At the acid strength of  $H_0 \geq 7.2$  the pure oxides activated at 300°C and 500°C and  $ZrO_2$  activated at 800°C are acidic. For samples activated at 300°C all the mixed oxides except 40 Nd show basicity. At 500°C all the mixed oxides exhibit basicity even though the pure oxides are acidic. For samples activated at 800°C all the zirconium rich samples are acidic and then neodymium rich samples are basic.

The coordination numbers of Nd is six and oxygen is four in pure  $Nd_2O_3$ . The coordination numbers of Zr is eight and oxygen is four in pure  $ZrO_2$ . When the two oxides are mixed with  $ZrO_2$  as the major component, coordination numbers of the cations will remain as such but that of the anion will be 4 as by



postulate 1 & 2 (refer section 3.2.3). In its structure the positive charge of the Nd (the added cation) will be distributed along six bonds ( $+3/6$  for each bond). The negative charge of the oxygen will be distributed along four bonds ( $-2/4$  for each bond). The charge imbalance produced at one Nd-O bond is ( $+3/6 - 2/4 = 0$ ) zero, and the total charge difference produced by one Nd cation is again zero. In this case no acidity is assumed to appear upon the mixing of two oxides.

When the two oxides are mixed with  $\text{Nd}_2\text{O}_3$  as the major component, the coordination number of cation will remain as such and that of the anion will be four (as in  $\text{Nd}_2\text{O}_3$ ). In its structure the positive charge of the Zr (the added cation) will be distributed along eight bonds ( $+4/8$  for each bond). The negative charge of the oxygen will be distributed along four bonds ( $-2/4$  for each bond). The charge imbalance produced at one Zr-O bond is ( $+4/8 - 2/4 = 0$ ) zero, and the total charge difference produced by one Zr cation is again zero. In this case also no acidity is assumed to appear, because no charge imbalance is created on mixing the oxides. In any case of Nd - Zr mixed oxide acidity will not be generated according to Tanabe's hypothesis and it agrees well with our studies [6].

#### 5.1.4 Catalytic activity

The catalytic activity of the mixed oxides for three reactions *Viz.* reduction of cyclohexanone, oxidation of cyclohexanol and esterification of acetic acid with n-butanol were studied (table 5.4).

### Reduction Reaction (figures 5.24, 5.25)

Pure  $ZrO_2$  have maximum activity at  $300^\circ C$ . Activity decreases with increase in activation temperature, lowest value is at  $800^\circ C$ . Pure  $Nd_2O_3$  also shows maximum activity at  $300^\circ C$ , and has the same trend with the activation temperature as in the case of  $ZrO_2$ .  $Nd_2O_3$  has very low activity compared to  $ZrO_2$ . For the samples activated at  $800^\circ C$ , pure oxides and all the mixed oxides except 20 Nd have no activity. At  $300^\circ C$  all the mixed oxides are active for the reduction reaction, the activity is intermediate between the component oxides. At  $500^\circ C$  all the mixed oxides have their maximum activity. 40Nd and 60Nd have the highest activity at the activation temperature of  $500^\circ C$ . A mechanism [7] has been proposed which involves both the acid and the base sites in the reaction (refer section 3.2.4).

### Oxidation reaction (figures 5.26, 5.27)

Pure  $Nd_2O_3$  catalyses the oxidation of cyclohexanol to cyclohexanone, the rate constants found to decrease with increase in activation temperature. In the case of  $ZrO_2$ , the catalytic activity is increasing with activation temperature, the maximum being at  $800^\circ C$ . Among the samples activated at  $300^\circ C$ ,  $Nd_2O_3$  is having the highest activity. All the mixed oxides except 80Nd are having rate constants intermediate between the component oxides, 60 Nd having the lowest value. At the activation temperature of  $500^\circ C$ , the catalytic activity of all the mixed oxides increased except for 20 Nd. The largest value of the rate constant is for 80 Nd and the lowest value is for 20 Nd.

At an activation temperature of 800°C, all the mixed oxides have their highest activities for the oxidation of cyclohexanol, 60 Nd having the largest value.

The DTA curve of Nd(OH)<sub>3</sub> shows three endothermic effects. The first two peaks are due to dehydration, and the third is caused by two simultaneous processes, namely, dehydration and decomposition of nitrate ions captured by the hydroxide upon precipitation.

The DTA curve of commercial neodymia which had been kept in air also shows three endothermic effects. The first two are caused by dehydration and the last peak has been shown by mass spectrometric analysis to be due to the evolution of carbon dioxide at 702-820 °C. The results of the thermogravimetric study on commercial neodymia indicate abilities to rehydrate in air and to adsorb CO<sub>2</sub>. The thermal curves of Zirconium and Hafnium hydroxides, in an inert gas unlike those of rare earth hydroxides show only one endo and one exothermal effects. The first peak is caused by dehydration, the other by transition of the amorphous dioxide to a crystalline dioxide. They do not form surface nitrates or surface carbonates.

Neodymia and lanthana have the ability to undergo polymorphic transformation in the range of 600-900 °C from the cubic body centered (C form) into the hexagonal (A form). Among the remaining rare earth oxides the C form is stable under the conditions studied. Thus one may suggest that an increase in the coordination number of the cation from 6 in the C form to 7 in the A form would decrease the catalytic activity [8].

In heterogeneous oxidation reactions in which catalytically active oxides are used, lattice oxygen is used by the reaction. Lattice oxygen then appears in the oxidation products, while oxygen vacancy in the catalyst is replenished by the gaseous molecular oxygen [9].

#### Esterification reaction

ZrO<sub>2</sub> catalyses the esterification of acetic acid with n-butanol, while Nd<sub>2</sub>O<sub>3</sub> does not (figure 5.28). 80 Nd also does not catalyse the esterification reaction, 40 Nd and 60 Nd are having rate constants almost equal to that of ZrO<sub>2</sub>. The rate constant for the esterification of acetic acid with n-butanol catalysed by 20Nd is very small.

#### 5.2 Comparison of the three rare earths

In the case of CeO<sub>2</sub> the surface area decreases with activation temperature (figure 5.29). For Nd<sub>2</sub>O<sub>3</sub> the surface area first increased and then decreased with activation temperature. Samples activated at 500°C, the Ce-Zr mixed oxides are having lower surface areas than the component oxides, while for Pr-Zr mixed oxides and Nd-Zr mixed oxides are having higher surface areas than the component oxides.

The limit of electron transfer remain the same (between 1.77eV and 2.40eV in terms of the electron affinities of the electron acceptor), except in the case of 60 Ce (500°C), 20 Ce 80 Ce (800°C). In these three cases the limit of electron transfer

is between 2.40eV and 2.84eV in terms of the electron affinity of the electron acceptor. On comparing the limiting amounts of electron acceptors adsorbed on the mixed oxides, there is not much difference in the values (figures 5.30, 5.31).

Reduction reaction : ( figure 5.32) (Oxides activated at 500°C are compared) Pure CeO<sub>2</sub> does not catalyse the reduction reaction. All other pure oxides under study catalyse the reduction reaction. All the mixed oxides catalyse the reduction reaction more effectively than the pure component oxides. Acid or base sites can be created on mixing the oxides. Sites which can catalyse the reduction reaction are generated on mixing the oxides.

Oxidation reaction: (figure 5.34) On comparing the pure oxides Pr<sub>6</sub>O<sub>11</sub> is having the highest activity followed by Nd<sub>2</sub>O<sub>3</sub> and then CeO<sub>2</sub>. Weak acid sites and ability to undergo oxidation and reduction (coexistence of different valence states ) are the factors which contribute to the oxidation activity. Praseodymia is having +3 and +4 oxidation states coexisting and have a very high value for the rate constant. In the case of Nd<sub>2</sub>O<sub>3</sub> a small amount of +4 state is also contained in it, which is not so stable. Also there is a small amount of acidity ( $H_0 \leq 7.2$ ) on its surface. So neodymia is having activity for oxidation reaction, eventhough it is small compared to that of praseodymia. CeO<sub>2</sub> is having only +4 oxidation state (very stable) in it but it is sufficiently acidic. So CeO<sub>2</sub> also catalyses the oxidation reaction to a small extent.

The Ce-Zr mixed oxides show high catalytic activity, due to the generation of acid sites on mixing the oxides. It is due to the coordinative

unsaturation created on mixing the oxides. Nd-Zr and Pr-Zr mixed oxides also catalyse oxidation reaction but to a lesser extent than Ce-Zr mixed oxides.

Esterification reaction is known to be catalysed by strong acid sites on the solid surface. Pure rare earth oxides do not possess strong acid sites on their surface to catalyse the esterification reaction. But  $ZrO_2$  having a polyfunctional behaviour can catalyse esterification reaction. On mixing  $ZrO_2$  with rare earth oxides, strong acid sites are generated in the case of Ce-Zr mixed oxides which can catalyse the esterification reaction. So Ce-Zr (figure 5.33) mixed oxides have very high values for rate constant for the esterification reaction. Nd-Zr mixed oxides and Pr-Zr mixed oxides also catalyse esterification reaction, the rate constants are less than that for  $ZrO_2$ . They have activities intermediate between the component oxides. Nd-Zr mixed oxides are having a slightly higher value than the other. Strong acid sites are not generated on mixing  $Nd_2O_3$  and  $Pr_6O_{11}$  with  $ZrO_2$ .

#### Effect of activation temperature

For Nd-Zr and Ce-Zr mixed oxides higher activity is observed at  $500^\circ C$  both for oxidation and for reduction. In the case of reduction reaction all oxides (pure and mixed) are inactive or show very low activity, when preheated at  $800^\circ C$ . It can be concluded from the results that active sites for the reduction reaction are absent at the activation temperature of  $800^\circ C$ . The decrease in activity observed in all cases for pretreatment temperature higher than  $650^\circ C$  may be due to a decrease in surface

disorder that results from a relatively high mobility of  $O^{2-}$  in lanthanide sesqui oxides [8]. The  $O^{2-}$  may not be available for proton abstraction.

But in the oxidation reaction, the activity is not much affected, it may be due to the fact that the hydrogen acceptor (benzophenone) is in the reaction mixture which will abstract the proton and thus adsorption of the alkoxide on the acid site will be possible and then the subsequent dehydrogenation.

At 300°C the activity for the reduction reaction is greater than at 800°C, because of the presence of more basic sites on the surface which can abstract the proton in the first step. The activity at 500°C is more than that at 300°C because at 500°C there will be sufficient acid sites to adsorb the alkoxide species.

In oxidation reaction the rate constants for the samples activated at 300°C and 500°C are comparable because the diminution in the number of the proton abstracting sites are not prominent in the presence of the hydrogen acceptor (benzophenone).

At 500°C it is assumed that there will be the coexistence of optimum levels of acid and base sites on the oxide surface, which promotes both the oxidation and reduction reactions.

Table 5.1 Surface Areas of Neodymium-Zirconium Mixed Oxides

Activated at Different Temperatures

Weight % of Rare Earth Oxide	<u>Surface areas</u> activated at		
	300°C	500°C	800°C
0	200.30	61.50	29.75
20	223.55	115.28	60.29
40	183.78	120.57	21.45
60	158.90	89.10	26.33
80	84.35	59.59	34.88
100	39.70	42.40	37.90



Table 5.2 Limiting Amounts of Electron Acceptors Adsorbed on Neodymium-Zirconium Mixed Oxides Activated at Different Temperatures

Weight %of Nd <sub>2</sub> O <sub>3</sub>	Activation Temp. °C	Limiting amount Adsorbed	
		TCNQ $10^{-6}$ mol /sq.m	Chloranil
0	300	0.9656	0.6933
20	300	1.3733	0.9036
40	300	1.1653	0.9517
60	300	1.1498	0.9978
80	300	1.8045	1.6089
100	300	0.6008	0.2030
0	500	2.0814	1.0613
20	500	1.8840	1.3391
40	500	1.2585	0.9421
60	500	1.6319	1.2429
80	500	2.2291	1.8995
100	500	0.7358	0.294
0	800	2.2064	0.6835
20	800	1.5241	0.6878
40	800	4.4756	0.3608
60	800	2.5526	1.6708
80	800	1.8163	1.2484
100	800	0.9338	0.4348

Table 5.3 Acid-Base strength Distribution on Neodymium-Zirconium Mixed Oxides Activated at different Temperatures

Weight % of Nd <sub>2</sub> O <sub>3</sub>	Activat. Temp. °C	Basicity H <sub>0</sub> ≥3.3	Basicity H <sub>0</sub> ≥4.8	Acidity H <sub>0</sub> ≤4.8	Basicity H <sub>0</sub> ≥7.2	Acidity H <sub>0</sub> ≤7.2
		10 <sup>-3</sup> m mol m <sup>-2</sup>				
0	300	0.9655	0.2361	-	-	0.1679
20	300	0.0671	0.0447	-	0.0224	-
40	300	0.0544	-	0.0263	-	0.0394
60	300	0.0786	0.0157	-	0.0157	-
80	300	0.1481	0.0296	-	0.0296	-
100	300	0.3270	0.1051	-	-	0.2510
0	500	2.7380	0.1072	-	-	2.7448
20	500	0.1725	0.1300	-	0.0217	-
40	500	0.1036	0.0414	-	0.0257	-
60	500	0.3646	0.1402	-	0.1122	-
80	500	4.1930	0.2935	-	0.2516	-
100	500	0.4000	0.2350	-	-	0.1650
0	800	2.4500	0.4000	-	-	3.0794
20	800	0.1659	0.0415	-	-	0.0401
40	800	0.1165	-	0.1125	-	0.2250
60	800	0.759	0.0949	-	0.0949	-
80	800	2.86	0.1043	-	0.0716	-
100	800	0.421	0.382	-	0.0250	-

**Table 5.4 Catalytic activity of Neodymium-Zirconium mixed oxides Activated at Different Temperatures**

Wt% Nd <sub>2</sub> O <sub>3</sub>	Act. Temp	Reduction of Cyclohexanone		Oxidation of Cyclohexanol		Esterification Reaction	
		% conversion	Rate Constant (10 <sup>-7</sup> s <sup>-1</sup> m <sup>-2</sup> )	% conversion	Rate Constant (10 <sup>-5</sup> s <sup>-1</sup> m <sup>-2</sup> )	% conversion	Rate Constant (10 <sup>-7</sup> s <sup>-1</sup> m <sup>-2</sup> )

0	300	25.19	1.006	95.97	0.445		
20	300	10.27	0.337	86.70	0.251		
40	300	6.60	0.258	85.65	0.293		
60	300	8.22	0.375	55.85	0.143		
80	300	3.18	0.266	84.89	0.622		
100	300	5.70	1.027	86.52	1.402		

0	500	11.05	1.320	87.24	0.930	10.53	2.513
20	500	43.43	3.433	64.07	0.247	2.40	0.293
40	500	43.77	3.317	83.91	0.421	16.09	2.021
60	500	16.36	1.393	83.98	0.571	11.55	1.913
80	500	17.92	2.302	79.58	0.741	0	0
100	500	2.80	0.465	86.65	1.319	0	0

0	800	0	0	83.90	1.706		
20	800	1.8	0.209	87.63	0.964		
40	800	0	0	60.26	1.195		
60	800	0	0	87.17	2.166		
80	800	0	0	88.52	1.724		
100	800	0	0	63.21	0.733		

Figure 5.1  
Surface areas of Nd-Zr mixed oxides  
as a function of composition

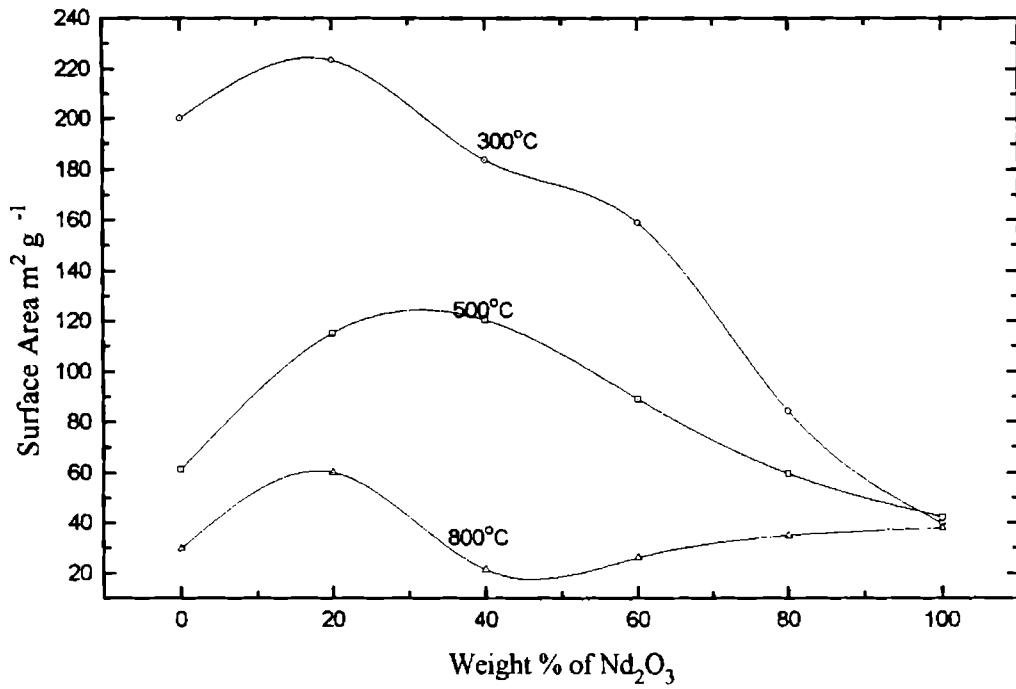


Figure 5.2  
Surface areas of Nd-Zr mixed oxides  
as a function of activation temperature

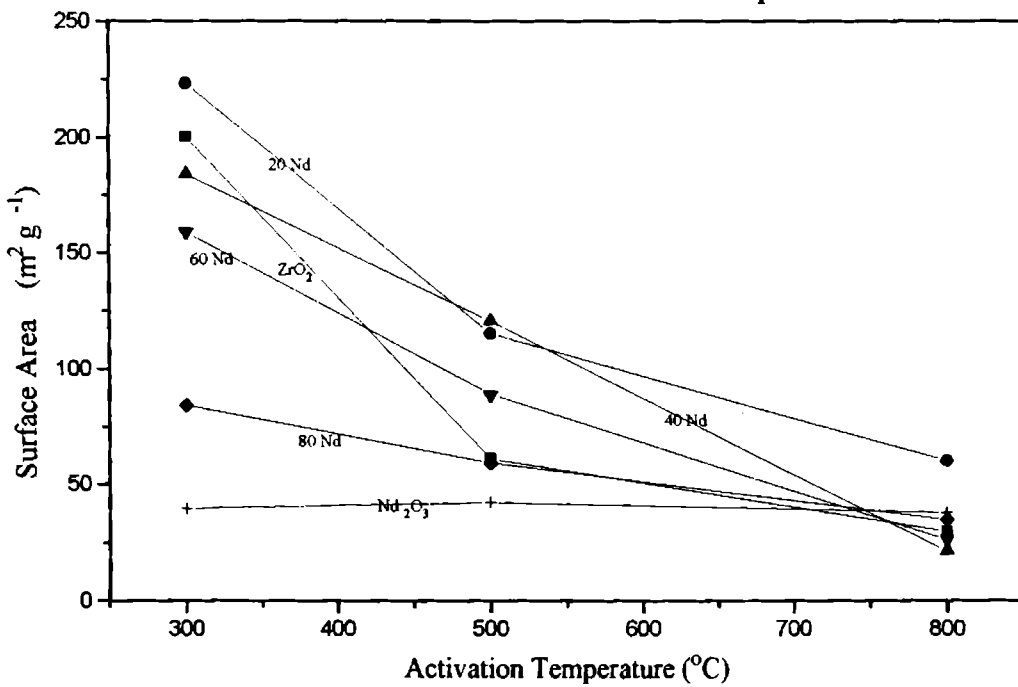


Figure 5.3  
Adsorption isotherms of electron acceptors  
on  $\text{Nd}_2\text{O}_3$  activated at different temperatures

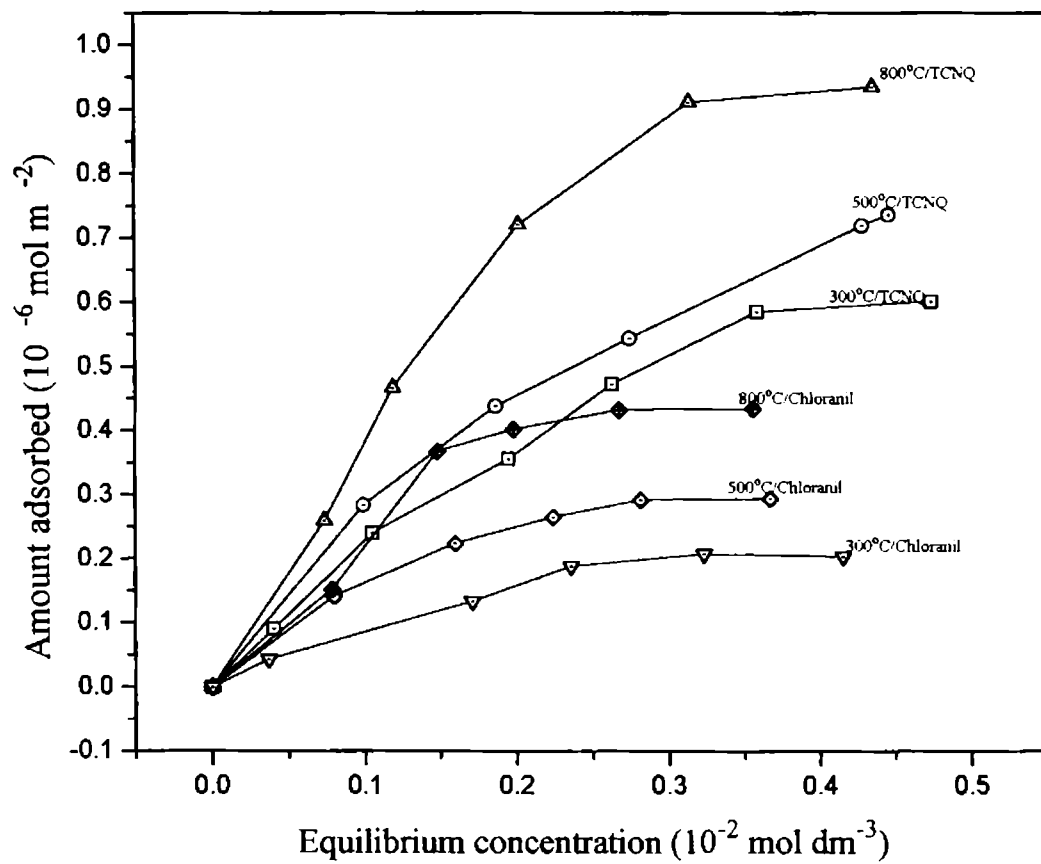


Figure 5.4

Adsorption isotherms of electron acceptors on 20Nd activated at different temperatures

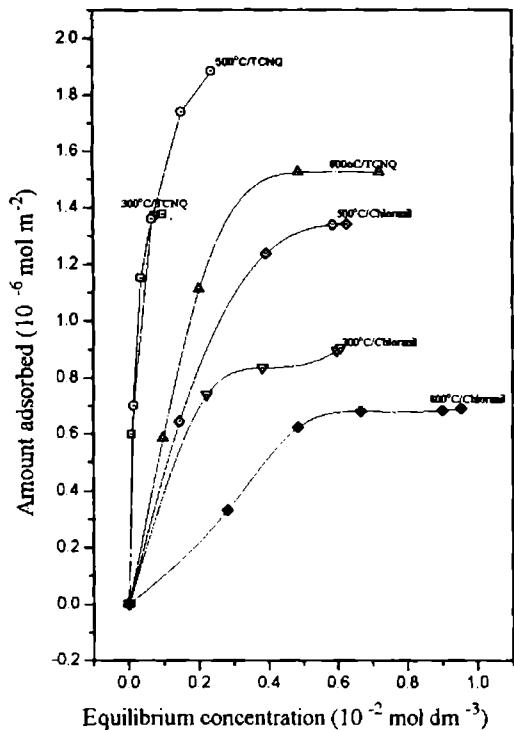


Figure 5.5

Adsorption isotherms of electron acceptors on 40Nd activated at different temperatures

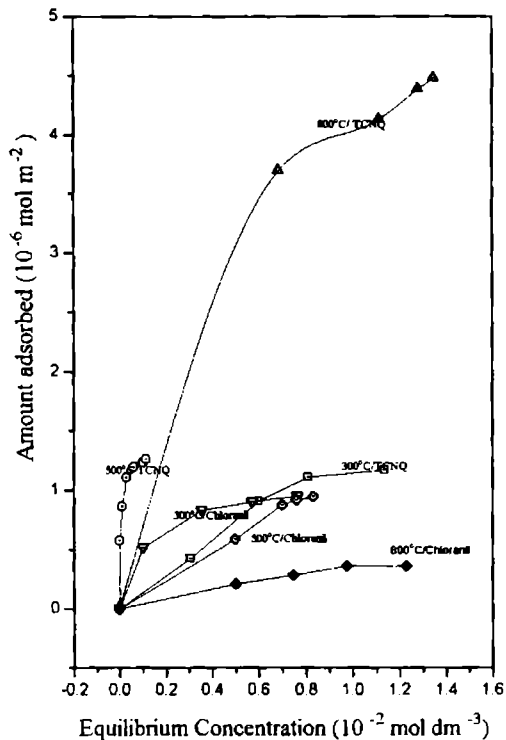


Figure 5.6

Adsorption isotherms of electron acceptors on 60Nd activated at different temperatures

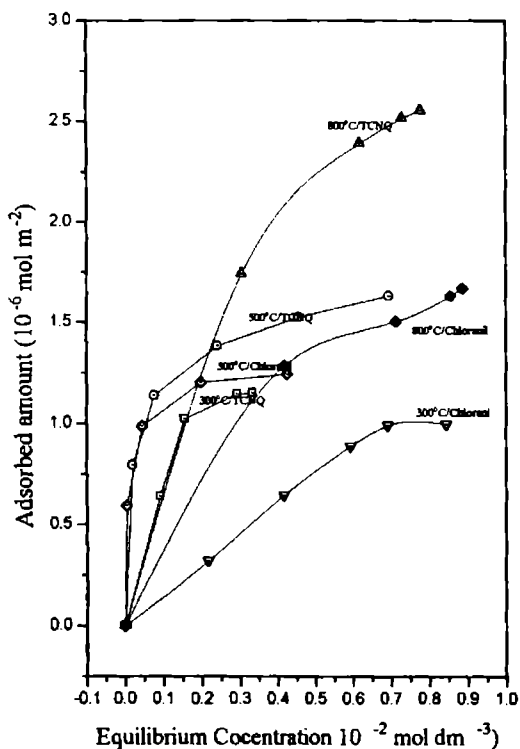


Figure 5.7

Adsorption isotherms of electron acceptors on 80Nd activated at different temperatures

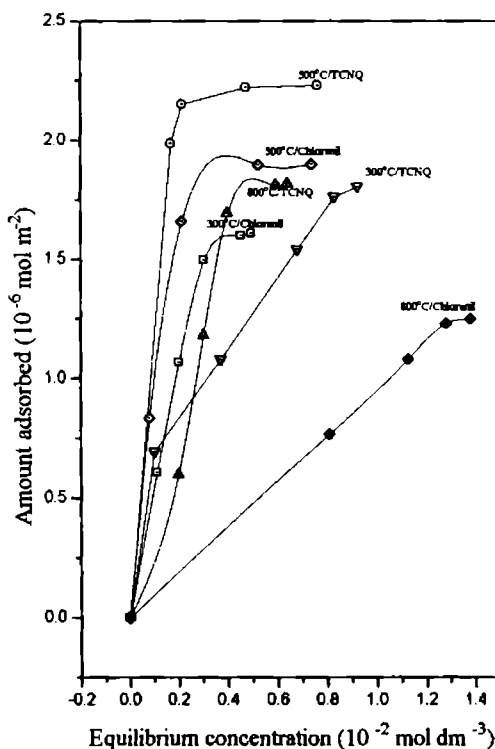


Figure 5.8  
Limiting Amount of TCNQ adsorbed on Nd-Zr mixed oxides as a function of Composition

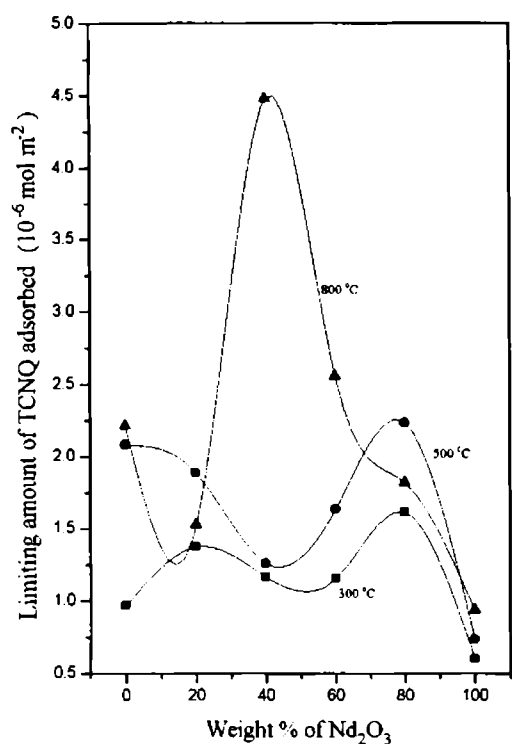


Figure 5.10  
Limiting Amount of Chloranil adsorbed on Nd-Zr mixed oxides as a function of Composition

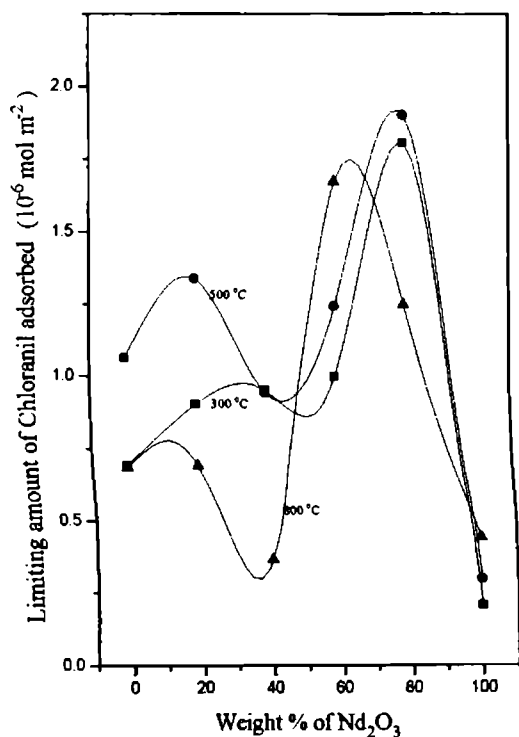


Figure 5.9  
Limiting Amount of TCNQ adsorbed on Nd-Zr mixed oxides as a function of activation temperature

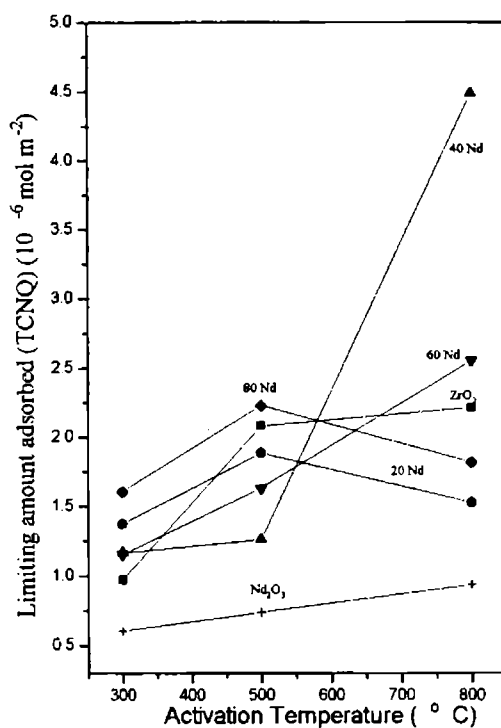


Figure 5.11  
Limiting Amount of TCNQ adsorbed on Nd-Zr mixed oxides as a function of activation temperature

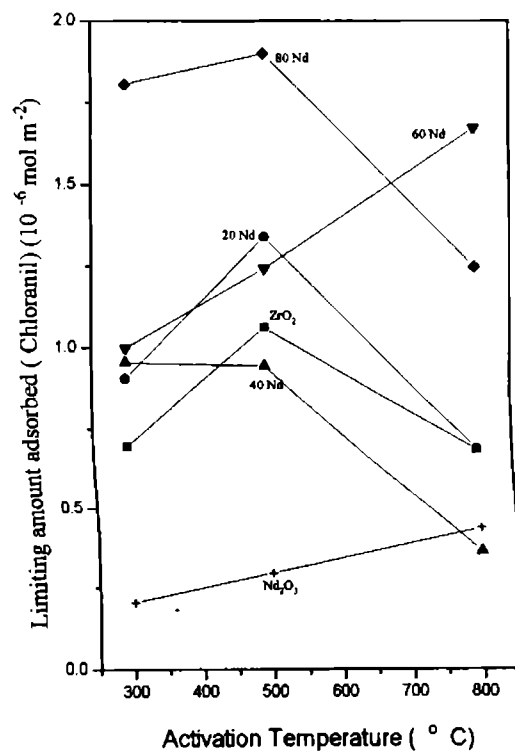


Figure 5.12  
Acid-Base Strength distribution curves on  
Nd<sub>2</sub>O<sub>3</sub> activated at different temperatures

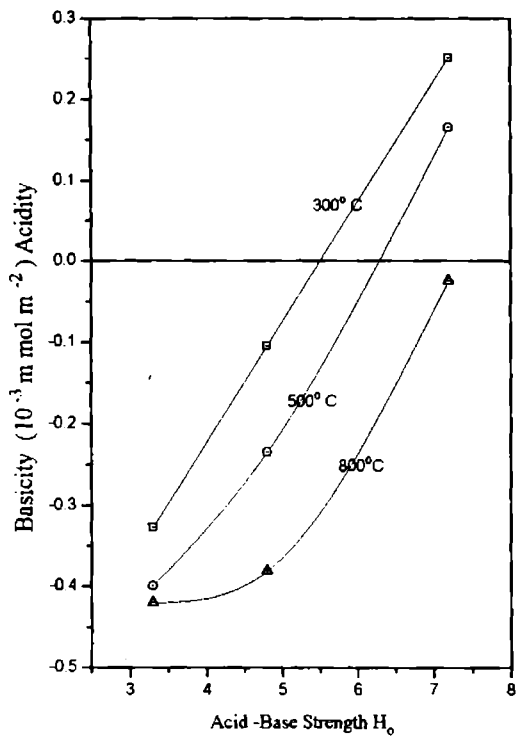


Figure 5.13  
Acid-base strength distribution on Nd-Zr  
mixed oxides activated at 300° C

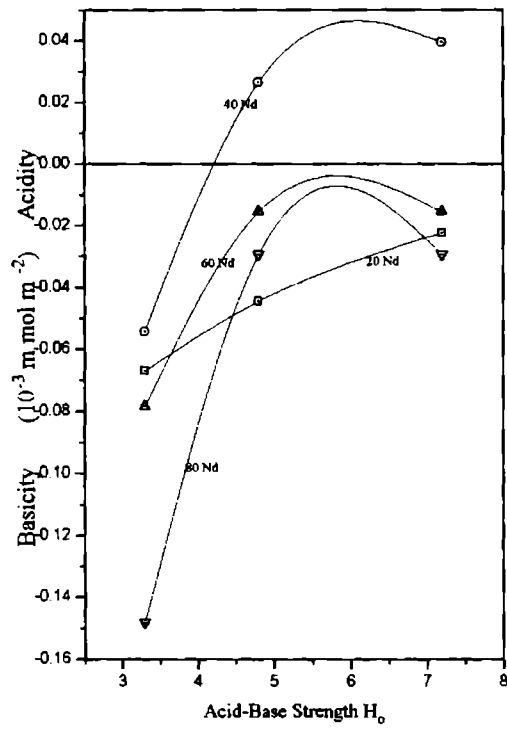


Figure 5.14  
Acid-base strength distribution on Nd-Zr  
mixed oxides activated at 500° C

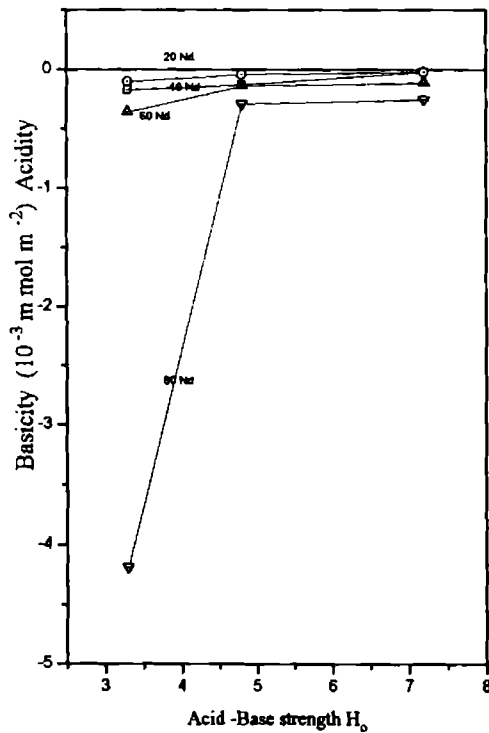


Figure 5.15  
Acid-base strength distribution on Nd-Zr  
mixed oxides activated at 800° C

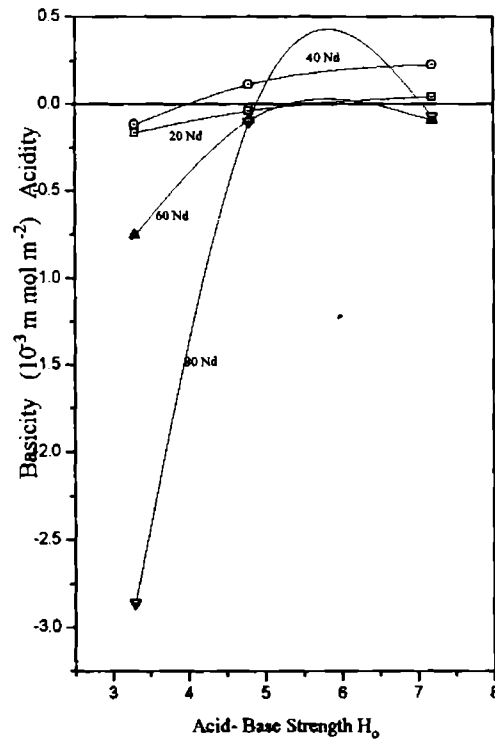




Figure 5.16  
Acid-Base Strength Distribution on  
Nd-Zr mixed oxides at  $H_0 \geq 3.3$  as  
a function of composition

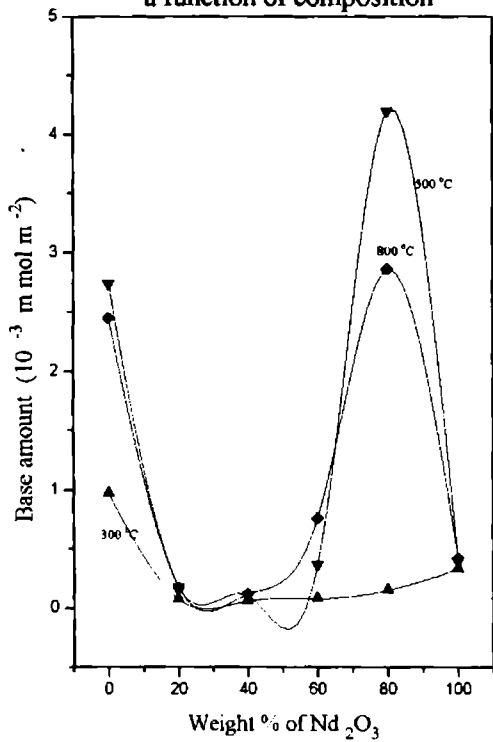


Figure 5.18  
Acid-Base Strength Distribution on  
Nd-Zr mixed oxides at  $H_0 \geq 4.8$  as  
a function of composition

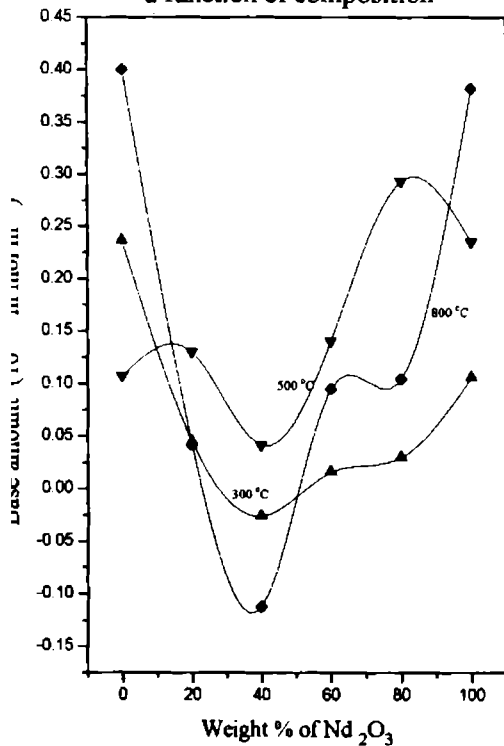


Figure 5.17  
Acid-Base Strength Distribution on  
Nd-Zr mixed oxides at  $H_0 \geq 3.3$  as  
a function of activation temperature

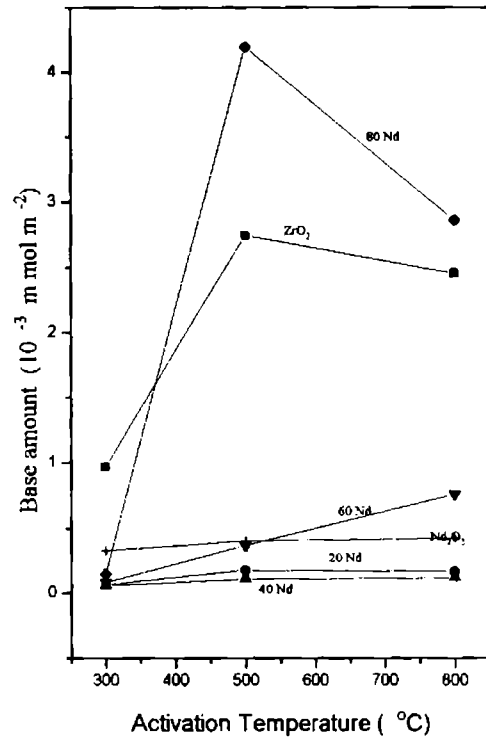


Figure 5.19  
Acid-Base Strength Distribution on  
Nd-Zr mixed oxides at  $H_0 \geq 4.8$  as  
a function of activation temperature

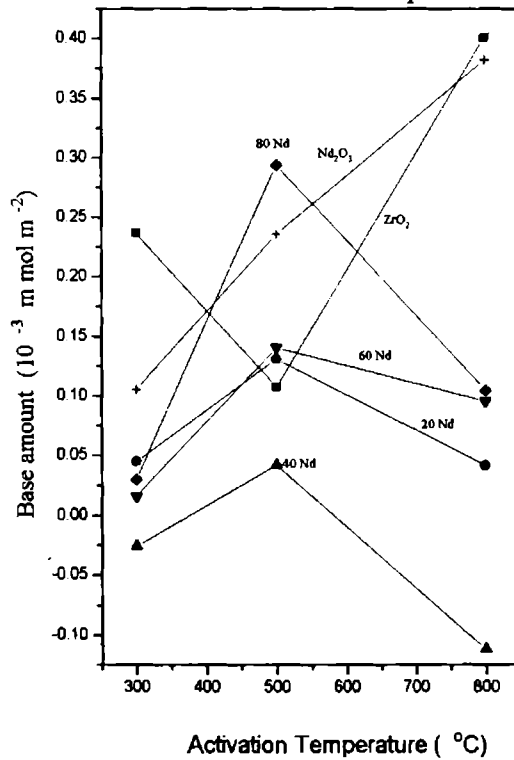


Figure 5.20

Acid-Base Strength Distribution on Nd-Zr mixed oxides at  $H_o \geq 7.2$  activated at different temperatures as a function of composition

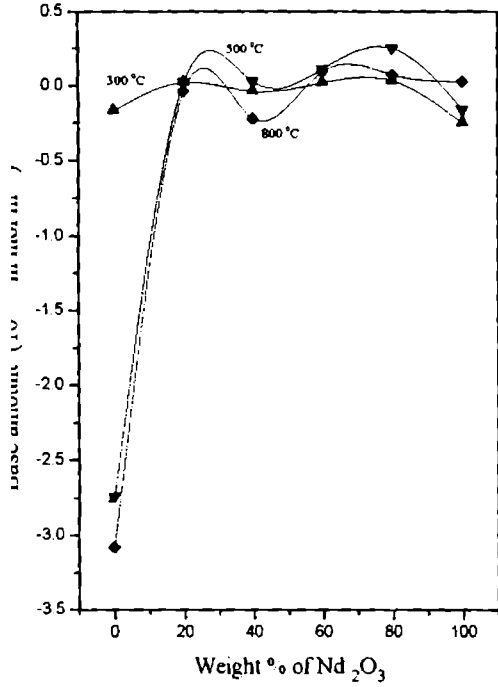


Figure 5.22

Acid-Base Strength Distribution on Nd-Zr mixed oxides activated at 300 °C as a function of composition

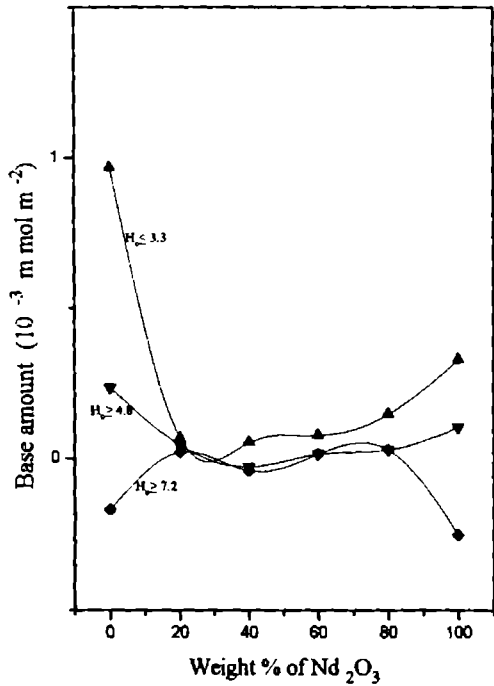


Figure 5.21

Acid-Base Strength Distribution on Nd-Zr mixed oxides at  $H_o \geq 7.2$  as a function of activation Temperature

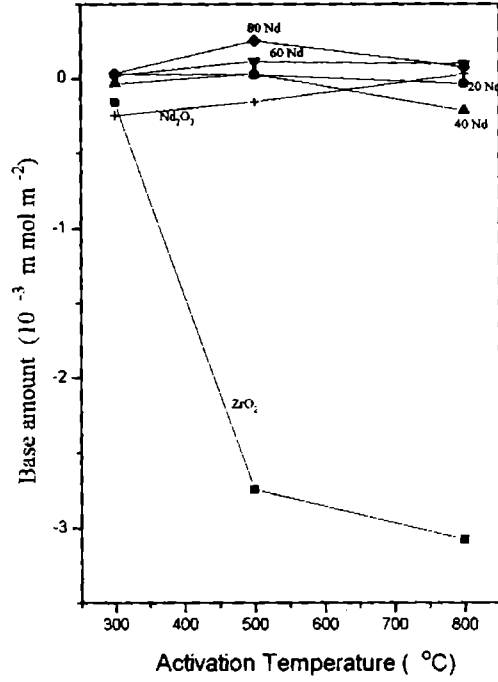


Figure 5.23

Acid-Base Strength Distribution on Nd-Zr mixed oxides activated at 500 °C as a function of composition

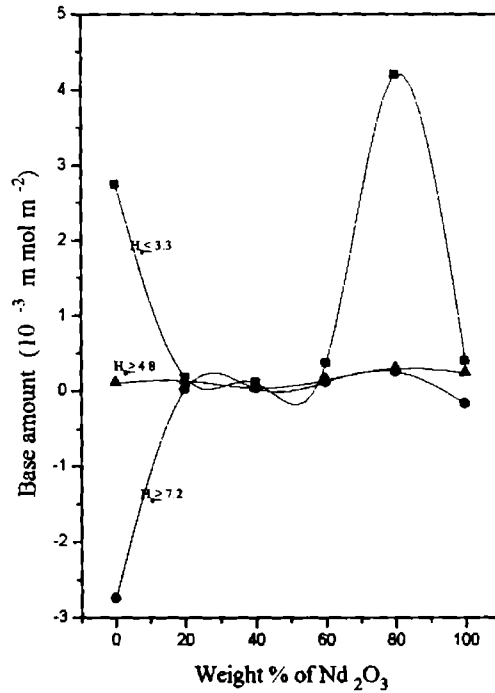


Figure 5.24  
Activity- Reduction Reaction Nd-Zr Mixed  
oxides as a function of composition

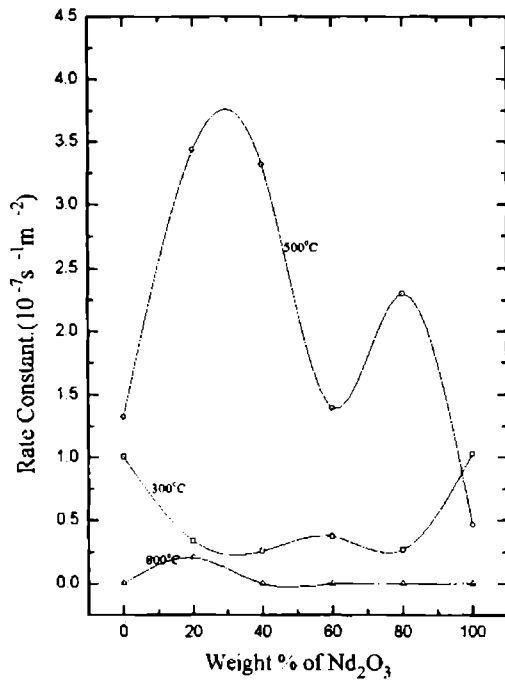


Figure 5.25  
Catalytic Activity for reduction reaction  
Nd-Zr mixed Oxides as a function of  
activation temperature

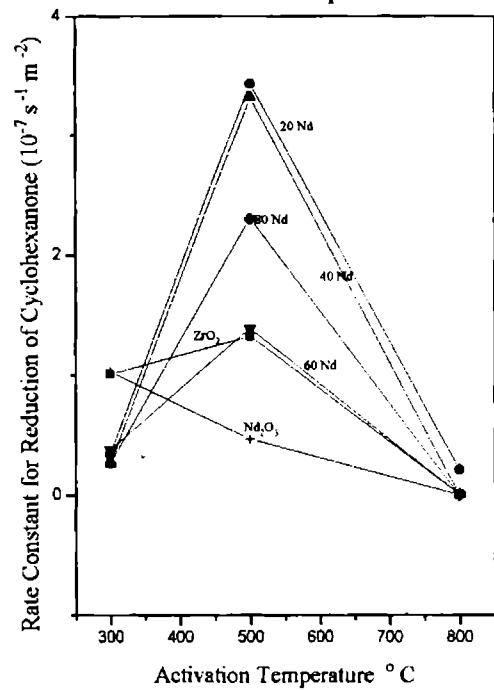


Figure 5.26  
Activity Oxidation Reaction Nd-Zr Mixed  
oxides as a function of composition

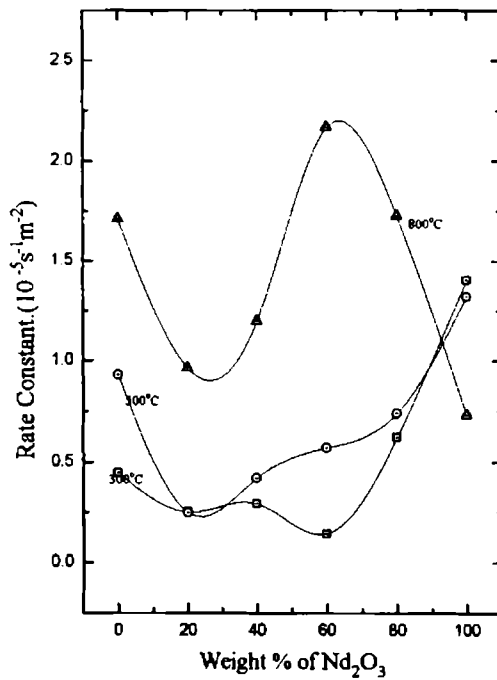


Figure 5.27  
Catalytic Activity for Oxidation reaction  
of Nd -Zr mixed as a function o  
activation temperature

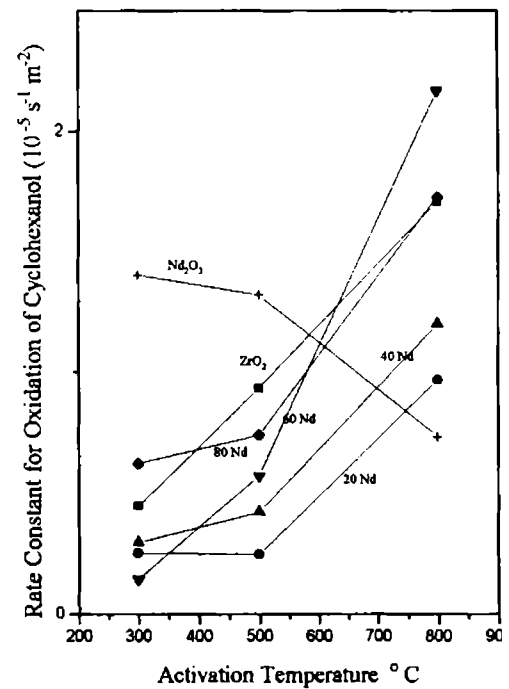


Figure 5.28  
Activity For Esterification Reaction Nd-Zr Mixed  
oxides as a function of composition

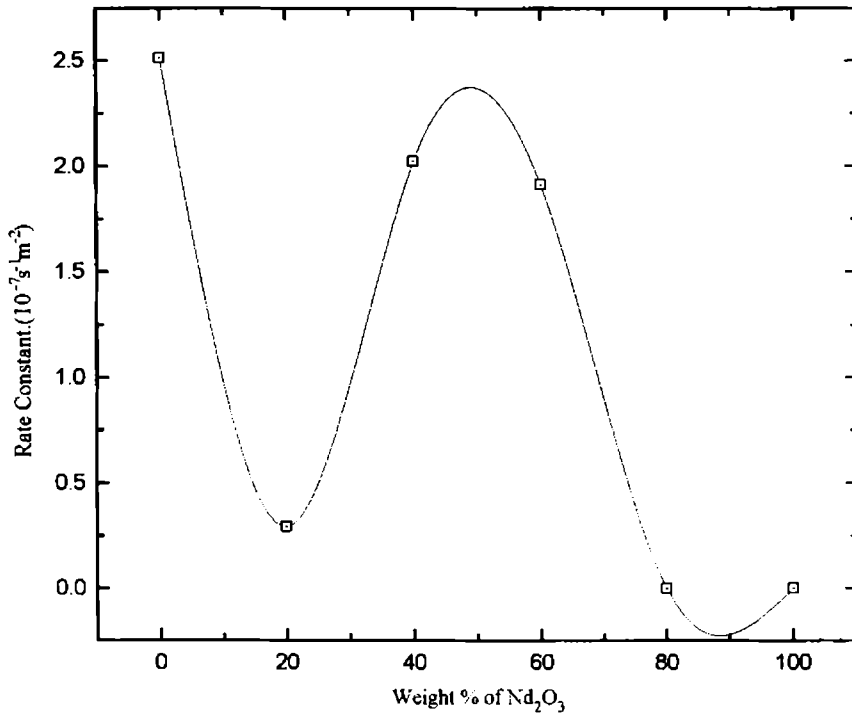


Figure 5.29  
Surface Areas of Mixed Oxides  
Activated at 500°C

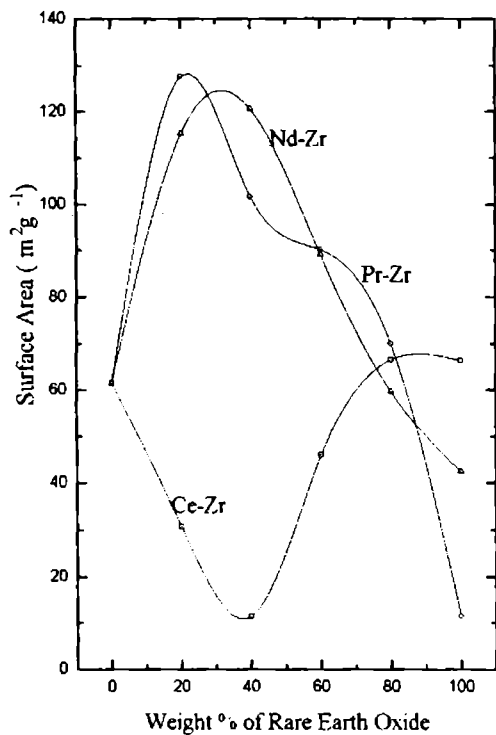


Figure 5.31  
Limiting Amount of Chloranil adsorbed  
mixed oxides activated at 500°C

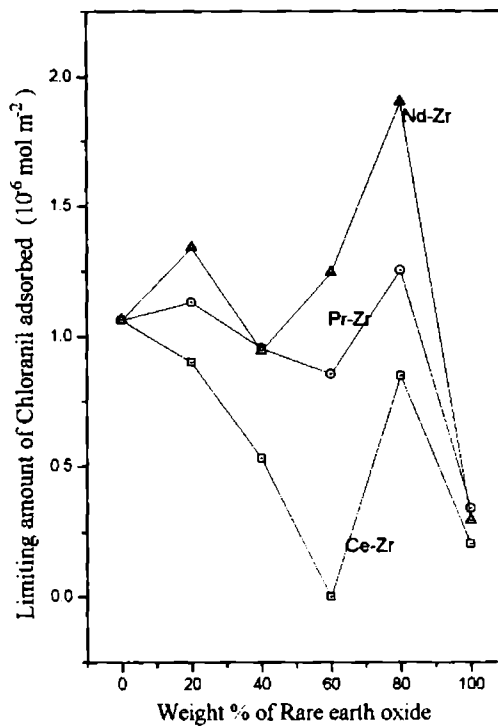


Figure 5.30  
Limiting Amount of TCNQ adsorbed on  
mixed oxides activated at 500°C

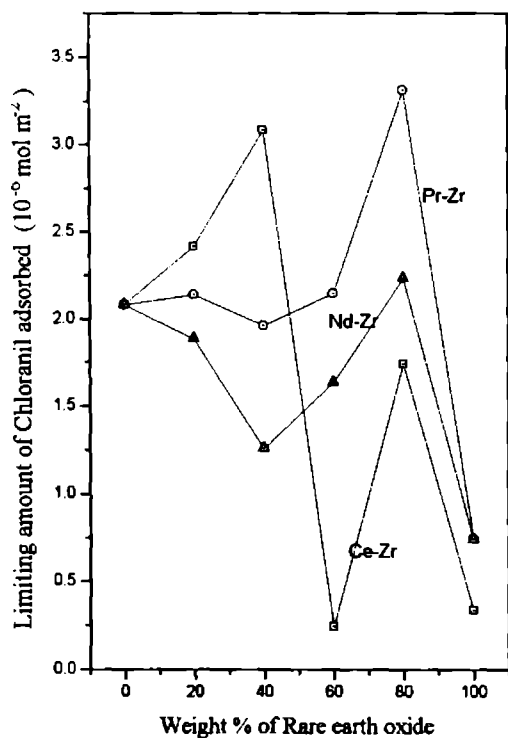


Figure 5.32  
Catalytic activity for Reduction reaction  
of mixed oxides activated at 500°C

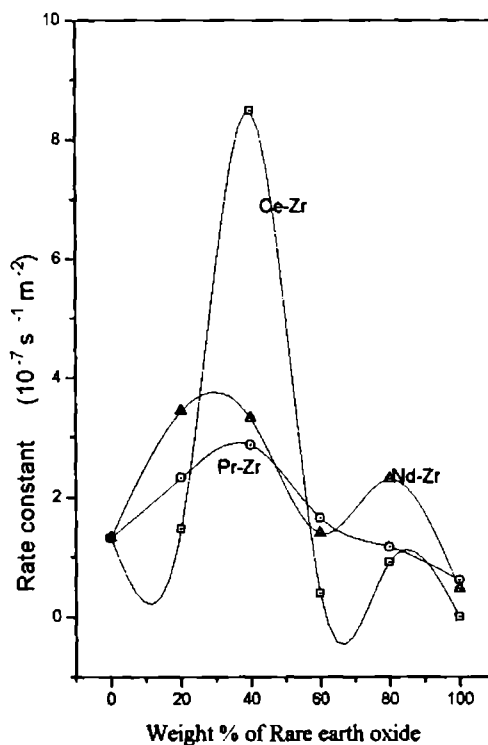


Figure 5.33  
Catalytic activity of mixed oxides  
activated at  
500°C for esterification reaction

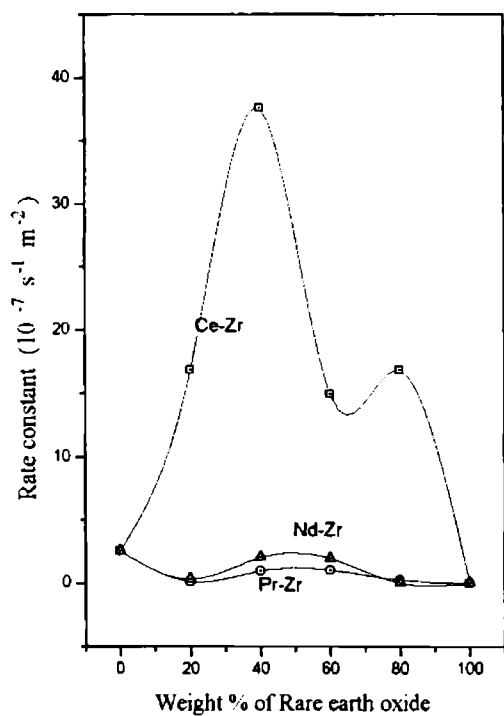
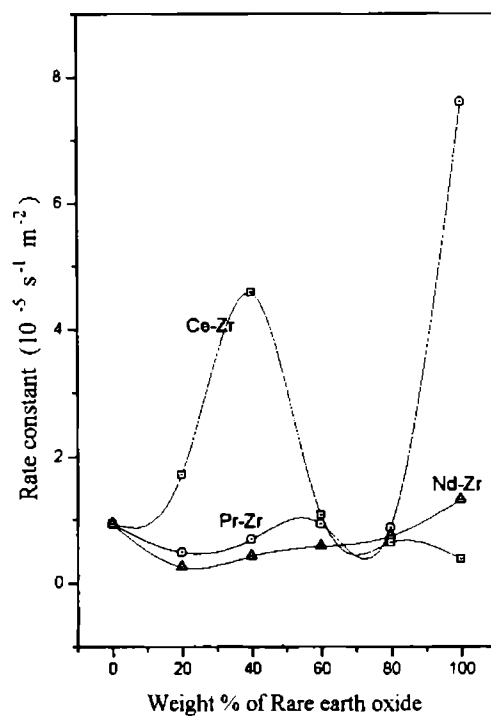


Figure 5.34  
Catalytic activity of mixed oxides  
activated at  
500°C for oxidation reaction



## REFERENCES

1. P. J. Gellings and H.J.M. Bouwmeester : *Catalysis today*, 12, 19 (1992)
2. K.Esumi, K.Meguro: *J. Colloid Interface Sci.*, 59, 43(1977).
3. M.Che, C.Naccache, B.Imelik : *J.Catal.*, 24,328(1972).
4. O.Johnson: *J. Phys. Chem .*, 827(1955).
5. T.Yamanaka, K.Tanabe : *J. Phys.Chem.*, 80, 1723(1976).
6. K. Tanabe, T. Sumiyoshi, K. Sibata, T. kiyoyura and J. Kitagawa : *Bull. Chem. Soc. Jpn.* 47, 1064 (1974)
7. M. Shibagaki, T. Takahashi and H. Matsushita : *Bull. Chem. Soc. Jpn.*, 61, 328 (1988).
8. K.M.Minachev, Y.S.Khodakov and V.S.Nakshunov : *J. Catal.* 49, 207 (1977)
9. Mars P, Van-Krevelen D W, *Chem. Eng. Sci.*, 3, 41, (1994)

## **CONCLUSIONS**

1. Amount of electron acceptor adsorbed depend on the composition of the mixed oxide, activation temperature and electron affinity of the acceptor.
2. Electron donor power increases with basicity of the oxide.
3. The limit of electron transfer is between 1.77- 2.40 eV for all oxides under study except for some Ce- Zr mixed oxides.
4. CeO<sub>2</sub> and its mixed oxides with zirconium are found to be more acidic than others.
5. Acidity is generated on mixing cerium oxide with zirconium oxide.
6. Ce-Zr mixed oxides catalyse esterification reaction more effectively.
7. Mixed oxides are found to exhibit more catalytic activity.
8. Ce-Zr mixed oxides show a different trend for all the properties investigated, which may be due to the difference in oxidation state.
9. No relationship is established between surface properties of mixed oxides and the f electron configuration of the rare earths in this study.



## LIST OF PAPERS PUBLISHED/ COMMUNICATED

1. S. Sugunan and Binsy Varghese ; Surface electron properties and catalytic activity of Sr doped Lantana :React. Kinet. Catal. Lett., 57(1), 87, (1996)
2. S. Sugunan and Binsy Varghese ; Acidity basicity and Catalytic activity of La-Zn mixed oxides : React. Kinet. Catal. Lett., 62(1), 157, (1997)
3. S. Sugunan and Binsy Varghese; Surface electron properties and catalytic activity of Praseodymium- zirconium mixed oxides: Communicated to Coll. Czeck. Chem. Commun., Czeck Republic.
4. S. Sugunan and Binsy Varghese; Surface electron properties and catalytic activity of Cerium - zirconium mixed oxides (under preparation).
5. S. Sugunan and Binsy Varghese; Surface electron properties and acid- base properties of Neodymium- zirconium mixed oxides (under preparation).